Novel Control Algorithms for Hierarchical Control of Power Systems

Submitted in partial fulfillment of the requirements for

the degree of

Doctor of Philosophy

in

Electrical and Computer Engineering

Irfan Ahmad Khan

B.Sc., Electrical Engineering, University of Engineering & Technology, Lahore
M.Sc., Electrical Power Engineering, University of Greenwich, London
M.S., Electrical and Computer Engineering, Carnegie Mellon University

Carnegie Mellon University
Pittsburgh, PA

June, 2018

Acknowledgment:

The pursuit of Ph.D. has been a period of fruitful learning experience for me, not only in the academic arena, but also on a personal level. I would like to reflect on the many people who have supported and helped me to become who I am today.

I am indebted to Dr. Soummya Kar, the chair of my committee, who has taught me how to think critically, speak clearly, and write thoroughly. Dr. Kar generously provided the resources and the open environment that enabled me to carry out my research. As my teacher and mentor, he has taught me more than I could ever give him credit for here. He has shown me, by his example, what a good scientist (and person) should be.

In addition, I would especially like to thank Dr. Yinliang Xu, who has been supportive of my career goals and who worked actively to provide me with the protected academic time to pursue those goals.

I am grateful to each of the members of my Dissertation Committee: Dr. Mao, Dr. Ilic, Dr. Liu and Dr. Mohammadi for serving on my defense. They provided me valuable comments and helped make the final stretch of my Ph.D. very smooth. They have provided me extensive personal and professional guidance and taught me a great deal about both scientific research and life in general.

During graduate school, I have met many wonderful fellow graduate students and friends whom I am grateful to. Vikram Bhattacharjee was my great cubic mate who supported and tolerated me for many years. Hadi Amini was my collaborator and colleague who assisted me in many ways.

Dedication:

I would like to thank my family for their enormous support and sacrifices that they made. Most importantly, I wish to thank my loving and supportive wife, Rabia, and my three wonderful children, Hareem, Ahmed and Hoorain, who provide me an unending inspiration. Rabia is the epitome of love, strength, and sacrifice. I am grateful to her strong belief in education.

My mother, Shahnaz, has been a pillar of support throughout my life. My brother, Imran, has always been there kindly supporting me with unwavering love. I would like to thank my late father, Muhammad Asghar Khan, for his love and full support. My childhood was full of joy because of him. I am sorry that he has not lived to see me finish my Ph.D. I also thank my uncle, Muhammad Akhter Khan, for his support. Lastly, I thank my Grandfather, Khuda Bakhsh Khan and grandmother, Ghulam Jannat for all their love and support throughout my life.

Abstract:

With the recent large scale integration of Distributed Generation (DG), the power system has changed drastically. Due to the intermittent nature of DG, real-time control of power generating units has become much more challenging. Consequently, voltage abnormalities and power loss problems are more frequent now in power systems. Load frequency stability is another serious concern in this changing paradigm of power systems. Also, large scale integration of DGs would require massive amounts of real-time data to be communicated from local systems to the controller to achieve effective regulation. However, this ever-growing data sizes may incur delays in transmission that in turn, may slow down the control algorithms.

This thesis addresses the issue of communication congestion in transmission of real-time data from local power systems to the centralized controller. It addresses this communication congestion issue in the context of three control problems in the power system: Load frequency control, secondary voltage control and optimal reactive power control. Load Frequency Control (LFC), is employed to allow an area to first meet its own load demands, then to assist in returning the steady-state frequency of the system with a response time of a few seconds. The fast LFC may be affected with the slow transmission of information from the system. To deal with this communication bottleneck, a Singular Value Decomposition (SVD) based LFC algorithm is proposed where SVD is used to significantly reduce the size of transmitted information. A second communication efficient control solution is proposed to address secondary voltage control of multi-area power systems which utilizes compressive sensing (CS) techniques to reduce the data size to deal with the limited bandwidth problem of the communication channel. It is also equipped with a technique based on Mathematical Morphology Singular Entropy (MSE) to identify faults/ abnormal disturbances locally in the system to avoid bad data/corrupt data being sent to the central controller. To further filter the sensed measurements from local sensors, it is passed through Mathematical Morphological Filters (MMF). Finally, a tertiary control algorithm for optimal reactive power generation control is proposed to minimize power loss, and voltage deviation on the tertiary level control. A consensus based gradient distributed approach is proposed to deal with potential communication delays.

Keywords:

Contents

List of Figures

List of Tables

Nomenclature

Acronyms

ρ	Compression Ratio
SNR	Signal to Noise Ratio
BA	Bus Agent
CS	Compressive Sensing
DG	Distributed Generation
KVA	Kilo Volt-Ampere
KVAR	Volt-Ampere-Reactive
LFC	Load Frequency Control
LMI	Linear Matrix Inequality
MAS	Multi-Agent Systems
MM	Mathematical Morphology
MMF	Mathematical Morphology Filter
MPC	Model Predictive Control
MSE	Mathematical Morphology Singular Entropy
ORPC	Optimal Reactive Power Control
p.f	Power Factor
PMU	Phasor Measurement Unit
QCQP	quadratic cone quadratic programming
RPCA	Reactive Power Control Agent
SE	Structuring Element
SVC	Secondary Voltage Control
SVD	Singular Value Decomposition

Chapter 1

Introduction

This chapter provides an overview of reactive power control and existing challenges in power system control. Aims and objectives of this research as well as contributions of this thesis are discussed.

1.1   Motivation

Distributed renewable energy generation (DG) is being deployed rapidly in the power system domain to reduce carbon emission, lower environmental impact and improve energy diversity. However, high penetration level of DGs pose challenging control issues in the power system due to the intermittent nature of the renewable energy sources. In addition, user loads are increasingly more dynamic, due to which, operation and control of the microgrids have become more complicated. As the number of DG units and dynamic loads are increasing every day, the amount of information flow from local area power systems to the central controller is rising rapidly[2]. Because of this system transformation, the conventional control techniques may not operate reliably and timely. Hence, it is recommended to propose new advanced control and communication techniques to deal with these challenges.

In this research, we propose a hierarchical control structure which consists of primary, secondary and tertiary level control of the power system. Primary control is the local control of a generating unit and is very fast (i.e. of the order of miliseconds). Secondary level control deals with a local control area, ranging from a single bus to few dozen buses and it is applied at a short time frame of a few seconds to 10 minutes. Tertiary control is a system level control which controls the whole system and is applied at a relatively large time scale, ranging from 30 minutes to couple of days. This research focuses on secondary and tertiary level voltage control using optimal reactive power dispatch.

Conventionally, centralized control algorithms are utilized for tertiary control. However, due to transmission of a huge amount of information between the whole system and the central controller, overburdening of the communication system may slow down the control or may even lead to inaccurate control signals [3]. To overcome this problem, distributed control and optimization techniques are implemented. They can improve the response speed effectively by allocating communication and computational burden among multiple local controllers. Distributed techniques have been shown to be suitable for online applications that require frequent control setting update. Hence, we propose distributed control algorithms for tertiary level control of optimal reactive power generation. It makes the ORPC faster with less computational burden.

As secondary level control is associated with the local control area rather than the complete system, the information data size is much less than the tertiary control which makes it viable for adopting the centralized control architecture. We employ compressive sensing techniques to further reduce the data size to deal with the communication bandwidth requirement for secondary control. Another reason for choosing a centralized control approach is that a distributed approach may converge to sub-optimal solutions for non-linear and non-convex problems which is the case in our application. By deploying CS for data size reduction, it requires less bandwidth requirement which means less communication cost and less power loss on the communication channel. In another application of secondary level control, Singular Value Decomposition based Load Frequency Control is proposed, where Singular Value Decompostion is employed to reduce the data size of the control area.

1.2 Reactive Power Generation Control

Reactive power generation control is an important control for stability, reliability and efficiency of power system. It is used to regulate the terminal voltage of the buses as well as minimize the power loss in the power system. It is a multi-level control technique, usually implemented in a hierarchical fashion to fully optimize the reactive power generation from reactive power sources. Hierarchical control consists of primary, secondary and tertiary control which are solved using centralized techniques. In centralized control, real-time power system data is monitored from all over the system, and transmitted to a central controller. This central controller then uses these real-time data to compute an optimal control input for the control sources in the system. After calculating the optimal control input, it sends it back to the local systems for the purpose of regulation.

1.3 Challenges

Although reactive power control has been extensively investigated [4, 5, 6], due to the integration of distributed generation in power systems and ever increasing complexity of the network, the current paradigm is facing many challenges that may affect the response time of control actions, reliability, efficiency and regulation. Some of these challenges which are the impeding factors in reliable and efficient operation of the network are listed below:

C1: The complexity of the power system is ever increasing to meet rising load demand, to incorporate renewable energy generation and to integrate advanced sensing and communication devices [7]. The amount of real-time data has risen significantly due to increase in the complexity of the system. This huge amount of data transmission from local systems to a central controller poses various challenges. One of the challenges is the restricted bandwidth of the given communication channel [3]. Communication channels have bandwidth limitations affecting data transfer capabilities. It may not be feasible to transfer all real-time data concurrently. Sometimes, data loss occurs during transmission of data due to limited bandwidth of the communication channel [8]. This data loss may worsen as the amount of data need to be transmitted increases.

C2: In addition to data loss in the limited bandwidth communication channel, the speed and responsiveness of the control implementation may be slower in a centralized operating framework where data needs to be transmitted to the central controller, often geographically distant from the actual power system [9]. It further consumes much time in transmitting the control input back to power system. Limited bandwidth of the communication further worsens this issue. The Shannon theory of Entropy indeed dictates the limit of reliable data transfer rate.

C3: Due to the limited speed of reliable data transfer in centralized control, it may not be possible to realize very fast control schemes and actions which is indeed required in today's complex power system [10]. The intermittent nature of distributed energy resources based power plants requires a much faster rate of control for a reliable and stable operation of the system [11]. For instance, in case of abrupt load changes, or outage of a transmission line/ a large power plant, immediate action needs to be taken to mitigate the impact. This immediate action may not be possible with centralized architectures.

C4: Furthermore, a centralized control paradigm relies on the successful operation of a single central controller. If, under any circumstances, the central

controller fails to operate, the centralized control scheme might fall apart leading to severe effects including large scale system blackouts. Such reliability issues may incur big financial as well as operational losses in the affected community. Thus, it is always recommended to come up with a new advanced control scheme that is fast enough, and free from single point of failure.

1.4   Aims and Objectives

The aim of this thesis is to investigate and design optimal reactive power control algorithms that are reliable and effective for an ever increasing complex power system, especially taking into account distributed energy resources in the system. The goal is to propose faster and single point of failure free algorithms for optimal reactive power control. Keeping in view the aforementioned challenges, the major objectives of this research work are as follows:

- The first objective of the thesis is to minimize the power loss, voltage deviation and cost of reactive power generation simultaneously while achieving effective reactive power control of the power system.

- The second objective of the thesis is to design a distributed consensus based optimal reactive power control which distributes the computation among bus agents such that each agent needs to communicate with his neighboring agents only.

- The third objective of the thesis is to design a centralized secondary voltage control of a multi-area power system. However, to deal with the limited communication bandwidth, a data compression technique needs to be employed to compress the data before sending it through the communication channels.

- The fourth objective of the thesis is to compare different compression techniques based on their achievable compression ratios and information losses in the context of speed.

- Finally, another objective of the thesis is to design a fault identification technique that can detect broad classes of faults locally in the system and can actuate the protection system to enhance the reliability of the overall power system.

1.5   Major Research Contributions

The major contributions of this thesis are summarized as follows:

- An innovative tertiary reactive power control algorithm based on a multi-agent system framework has been proposed to address a multi-objective criterion: minimize the power loss, voltage deviation and the opportunity cost of distributed generations' reactive power generation, simultaneously.

- The formulated optimization problem has been relaxed to a convex problem by posing it as a quadratically constrained quadratic program (QCQP).

- The proposed algorithm is distributed in nature as information sharing among neighboring buses only is required to optimize the objective function.

- A consensus-based algorithm is introduced, that can achieve reactive power fair utilization ratio for all DGs with different capacities.

- Real-time Secondary Voltage Control (SVCON) is proposed to minimize the worst-case voltage deviation of the control area by adopting an infinite norm minimization approach.

- Compressive Sensing (CS) is used to encode and then decode the real-time power system data to deal with the issues of data congestion and limited bandwidth.

- To deal with the noise in the signals, Mathematical Morphology Filter (MMF) is proposed to reduce the noise in the Phasor Measurement Unit (PMU) output.

- Mathematical Morphology Singular Entropy (MSE) based fault identification approach is employed for the fast identification of disturbances in the control area.

- Singular Value Decomposition (SVD) is proposed to compress the real-time data for load frequency control (LFC) application of a multi-area power system.

1.6   Publications

The work carried out in this thesis has resulted in the following publications:

- **Irfan Khan**, Soummya Kar, Yinliang Xu, "Real-time Singular Value Decomposition based Load Frequency Control of Multi-area Power System", submitted in *Power Systems Conference at Clemson University 2018.*

- **Irfan Khan**, Vikram Bhattacharjee, Yinliang Xu, Soummya Kar, "Compressive Sensing and Morphology Singular Entropy-Based Real-time Secondary Voltage Control of Multi-area Power Systems", under second review in *IEEE Trans. Industrial Informatics.*

- Vikram Bhattacharjee, **Irfan Khan**, "A Non-linear Convex Cost Model for Economic Dispatch in Microgrids",*Applied Energy* 222 (2018): 637-648.

- **Irfan Khan**, Y. Xu, S. Kar and H. Sun, "Compressive Sensing-based Optimal Reactive Power Control of a Multi-area Power System", in *IEEE Access*, vol. 5, pp. 23576-23588, 2017.

- **Irfan Khan**, Yinliang Xu, Vikram Bhattacharjee, Hongbin Sun, "Distributed optimal reactive power control of power system", in *IEEE Access*, vol. PP, Issue.99, pp. 1-1, 2017.

- **Irfan Khan**, Z. Li, W. Gu, and Y. Xu, "Distributed control algorithm for optimal reactive power control in power grids", *International Journal of Electrical Power and Energy Systems*, vol. 83, pp 505?513, Dec. 2016.(SCI, IF:2.28)

- **Irfan Khan**, Y. Xu, and B. Tahir."Design and construction of digital automatic voltage regulator for stand-alone synchronous generator", 2015 *IEEE International Conference on Cyber Technology in Automation, Control, and Intelligent Systems*, pp.217-222, 2015. (EI)

- Qiang Wan, W. Zhang, Y. Xu and **Irfan Khan**, "Distributed control for energy management in a microgrid", *2016 IEEE PES Transmission and Distribution Conference and Exposition (T & D)*, Dallas, TX, 2016, pp.1-5. (EI)

1.7   Thesis Outline

The rest of the thesis is organized as follows:

Chapter 2 gives an overview of the theory which includes fundamentals of power system operation specifically focusing on the importance of power factor, and methods of power factor improvement with some solved examples. It also explains hierarchical control and importance of reactive power generation to stabilize the frequency and voltage of the system. Moreover, it outlines the existing

methods of stabilization including centralized and distributed control methods, their advantages, disadvantages and challenges. Furthermore, it talks about various compression techniques including lossless and lossy compression techniques, specifically compressive sensing and singular value decomposition as means of compression. Finally, this chapter discusses various fault detection techniques with special emphasis on Mathematical Morphology Singular Entropy as a means to detect abnormal conditions. Overall, this chapter lays the foundation to address all the challenges.

In Chapter 3, focusing on Secondary Control, Load Frequency Control of a multi-area power system is proposed. To deal with the challenges presented in C1 and C2, Singular Value Decomposition is utilized to reduce the size of power system data before sending it to the central controller. Its achievable compression ratio is compared with other compression techniques. Settings of control variables to minimize frequency deviations are also presented.

Chapter 4, focusing on Secondary Control, addresses the challenge C1. We present secondary voltage control of a multi-area power system. To deal with the challenge C1 of restricted bandwidth, we propose compressive sensing technique to compress the size of power system data before sending it through the communication channel. At the end of communication channel, it is recovered using efficient recovery algorithms. In case of faults, if faulty data is sent to centralized controller and centralized controller decides the control input for fault, it may slow down the fault identification process. To avoid such sceneries, we also propose a fault identification technique that detects any abnormal condition locally and raises an alarm to actuate the protection system.

In Chapter 5, focusing on Tertiary Control, we address the challenge C4 by proposing a distributed optimal reactive power control to reduce power loss, voltage deviation and reactive power generation cost simultaneously. A consensus based distributed algorithm is designed that computes the control input of optimal reactive power generation. It addresses the challenge of single point of failure as it does not need a central controller as computation is distributed among local controllers on each bus.

Chapter 6 concludes the dissertation by summarizing the major results achieved in this work and highlighting important lessons learned from the research. We also discuss future work and some possible directions for new search.

Chapter 2

Theoretical Background: An Overview

This chapter provides a theoretical background for the work conducted in thesis. Different types of power generation, importance of reactive power generation and power factor are presented in Section 2.1. The hierarchical control scheme for power systems is presented in Section 2.2, while the role of reactive power generation is discussed in Section 2.3. Section 2.4 describes existing methods for reactive power control, their challenges and solutions, whereas Section 2.5 describes different data compression techniques, their advantages, disadvantages and mathematical formulations and finally, Section 2.6 presents the Mathematical Morphology Singular Entropy as a fault identification technique.

2.1   Types of Power Generation

An electrical power generator is rated by its kilo-volt-ampere ratings (KVA/MVA), referred to as apparent power, which means it can generate its rated power generation equal to its KVA ratings as shown in Fig. 2.1. Mathematically, apparent power in three phase systems can be calculated as

$$S = \sqrt{3}VI, \tag{2.1}$$

where V and I are the voltage and current magnitudes. However, not all KVA (denoted by S in the triangle of Fig. 2.1) is used in useful "working" of the power system. The real part of S, measured in kW denoted by P provides the "working" of the power system e.g. producing light, heat, motion etc. The real power can be calculated as
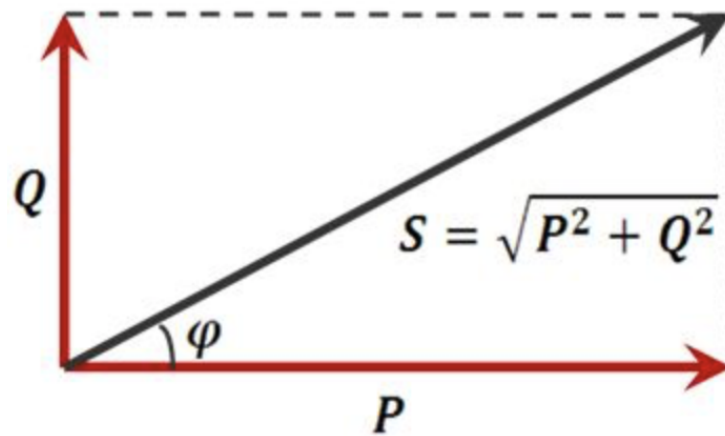
Figure 2.1: Power triangle.

$$S = \sqrt{3}VI\cos\delta, \tag{2.2}$$

where δ is the angle between voltage and current.

The perpendicular component of S, measured in Volt-Ampere-Reactive (KVAR) and denoted by Q only maintains the electromagnetic field of the electromagnetic devices present in the power system and provides no "working" part of the power system. It is interesting to note that in a purely resistive load, current and voltage are in phase and reactive power does not exist in the system. However, when current either leads or lags the voltage, the system is no longer resistive anymore and $Q \neq 0$. Furthermore, reactive power is of two types: either leading reactive power (capacitive) or lagging reactive power (inductive). Mathematically, reactive power is calculated as

$$S = \sqrt{3}VI\sin\delta. \tag{2.3}$$

As shown in Fig.2.2, in a purely resistive circuit, current and voltage are in phase and so there is no reactive power in the circuit. However, reactive power is needed to magnetize the circuit in case of inductive and capacitive circuits. In an inductive circuit, current lags the voltage, so circuit requires lagging reactive power whereas in a capacitive circuit, current leads the voltage and leading reactive power is required by the circuit. Cosine of the angle between voltage and current is referred to as power factor that has an ideal value of one in case of purely resistive circuit.

Reactive power generation is required to magnetize the inductive component in the first half cycle of the AC signal which is demagnetized in the second half of the cycle as shown in Fig.2.3. In the waveforms, 0 to t_1, V and I are both positive; so, power is positive. At $t=t_1$, V is $0V$ and therefore P is $0W$. Since,
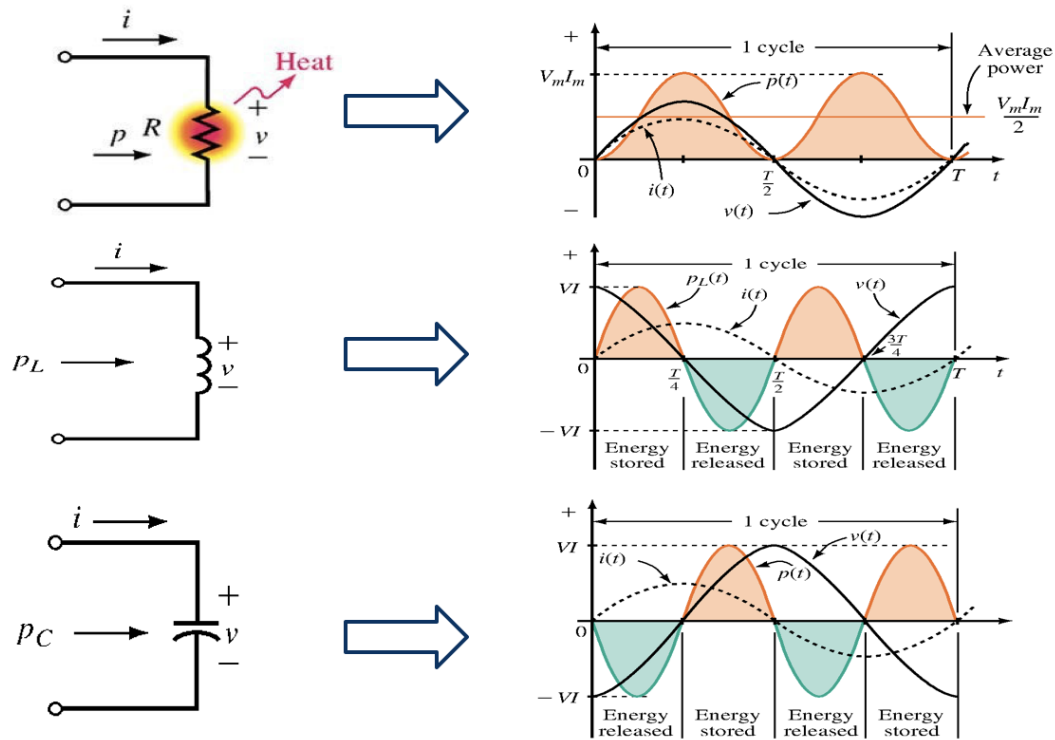
Figure 2.2: Phase difference in Resistive, Inductive and Capacitive system

from t_1 to t_2, I is positive and V is negative, P is negative. From t_2 to t_3, both V and I are negative; therefore power is positive, and so on. So, in an inductive system, reactive power generation is required to magnetize and demagnetize the inductive component all the time. In fact, this energy flows to and from the system and is not involved in any useful work.

2.1.1 Inductive Nature of the Power System

Most of the power system is inductive in nature because of the conductors carrying electrical energy from generation to distribution. Also, electrical equipments like transformers draw a magnetizing current from the supply. They draw large amount of magnetizing current at light load and thus causes low power factor. Similarly, other devices like fans, air conditioners, washing machines, blenders, induction machines, arc lamps, electric discharge lamps, pumps, compressors, welding equipment and industrial heating furnaces are operated at low lagging power factor. Due to this, overall, the behavior of power system is inductive in nature and thus current lags the voltage which makes power factor lagging from unity.
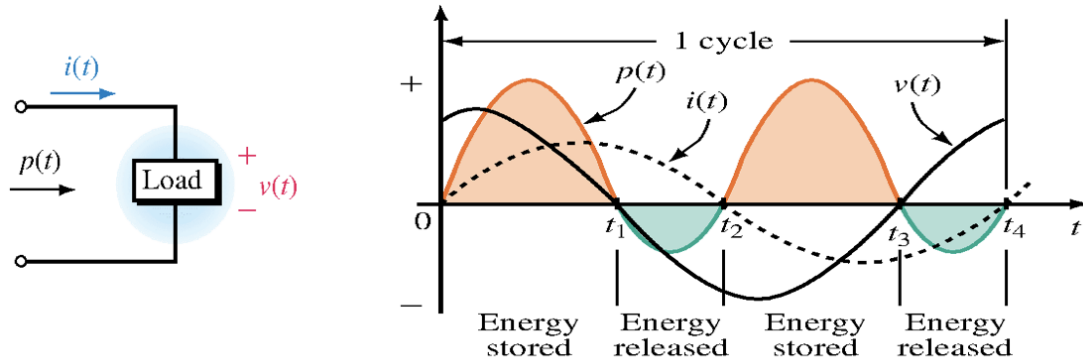
Figure 2.3: Representation of various quantities in power system load

2.1.1.1 Importance of Reactive Power Generation The operation of transformers, motors, and generators depends on the reactive power generation which is required to produce magnetic flux in these devices. In addition, several switching power supplies used in computers and televisions draw current only during certain part of the cycle, hence creating a net reactive load. Similar behavior is seen in mercury-vapor lamps. It is important to note that all of these devices present an inductive load. These devices can do useful work only if magnetic flux is generated with the help of reactive power flow. However, the irrational and big reactive power consumption presents a series of disadvantages for the power system.

Obviously, all the inductive load requires lagging reactive power generation from power generators. As the size of the inductive load increases,the generators have to generate more reactive power rather than the useful "working" power. For the same amount of real power, generator needs to generator more current to meet the reactive power demand. This high current leads to a higher real power loss in the power system as given by 2.4

$$Loss = I^2 R, \tag{2.4}$$

where R is the resistance in the system. Higher power losses means higher amount of useful power is being wasted in the form of heat which results in poor efficiency of the power system as 2.5

$$\% \, Efficiency = \frac{P_{out}}{P_{out} + Loss}, \tag{2.5}$$

where P_{out} is the useful real power used by power system. In addition, higher current means higher ratings of transmission conductors and installed equipments that result in higher overall cost of the power system. If the current, in case, increases too much, transmission lines may go off line for the sake of their pro-

tection, thus overloading other lines. It may potentially cause cascading failure in the system.

Furthermore, the volume of conductor depends on the current ratings. Higher current demands thicker and heavier conductor. The thicker conductor, in turn requires stronger and taller towers to support them during transmission of electrical power. All these equipments cause increase in the cost of the installation and potentially diminished electric energy transfer capability. Moreover, in case of higher current, electricity suppliers usually demand extra charges from consumers. It also causes overheating of generators and motors installation and increase in voltage losses.

Considering all these problems associated with the higher amount of current requirement, it is usually advised to optimally utilize other sources of reactive power generations locally in the system to regulate the local voltage of the buses and decrease the current flow from the central generator.

2.1.1.2 Importance of Voltage Regulation Reactive power flow is a very important task to ensure voltage regulation throughout the system. Generally speaking, increasing reactive power generation to the system causes voltage rise while decreasing its supply causes voltage drop. More specifically, voltage of the system may collapse in case of severe transients if sufficient reactive power reserve are not present in the system. In the past, many electrical blackouts like, that in many parts of India in 2012, northeast countries in 2003 and in France during 1978 are believed to be caused by insufficient reactive power reserve in the electrical system.

In power systems, since loads are inductive in nature, reactive power is required in the system. This reactive power is supplied by the power generators. Since reactive power does not perform any real work, the extra current is supplied by the power generator to meet the required reactive power [12]. This large current produces a large voltage drop in the alternators, transformers, transmission line conductors and distributors leading to poor voltage regulation, calculated as 2.6

$$Voltage\ Regulation = \frac{(V_{SE} - V_{RE}) \times 100\%}{V_{RE}}, \tag{2.6}$$

where V_{SE} is the sending end voltage and V_{RE} is the receiving end voltage. Due to large current flow, more voltage drop (Voltage Drop $= IR$) occurs in the system and receiving end voltage drops down. This is a serious problem, especially in feeders very far from the generation side. This may ultimately lead to shut down of various feeders and electrical devices due to low voltages. So it is very important to have sufficient amount of reactive power generation reserve in the system.

2.1.2 Power Factor Improvement

The power factor can be defined in one of the following 3 ways (2.7 - 2.9). It has been explained that reactive power is very important for the successful operation of power system. Therefore, it should be calculated accurately that how much reactive power generation is needed for power systems. As the electrical load is changing all the time, so is the reactive power generation requirement. We should come up with methods of finding reactive power generation. Power factor is one of the convenient ways to find out the required amount of reactive power generation. Measuring the power factor allows us to assess how much reactive power is required by electrical devices. Power Factor (p.f) can be calculated in three different ways as given by 2.7, 2.8 and 2.9

$$p.f = cos\delta, \tag{2.7}$$

$$p.f = cos\delta = \frac{R}{Z}, \tag{2.8}$$

$$p.f = cos\delta = \frac{P}{S}, \tag{2.9}$$

where δ, R, Z, P, and S are the angle between voltage and current, resistance, impedance, real power and apparent power (true power) in the system, respectively.

Ideally, power factor should be unity i.e. all electrical apparent power generation should be utilized towards real work. Typically homes have overall power factor in the range of 70% to 85%, depending upon the type of appliances running at home. However, newer homes equipped with the latest energy efficient appliances may have a power factor of 90%.

Electric companies take several measures to improve the power factor. They may either correct it around industrial complexes by themselves, or they may request the offending customer to correct it, or even may charge for reactive power load. Usually, residential service reactive load is not a big problem for electric utility companies because its impact on the distribution grid is not as grave as of heavily loaded industrialized areas. Thus, it is important that power factor should be improved so that electric utility companies can reduce their demand for electricity, thereby allowing them to meet service needs elsewhere.

2.1.2.1 Methods of Power Factor Improvement Correction of power factor means reducing the phase angle difference between voltage and current to make it near to unity. Several popular devices, designed to improve the p.f are capacitors, synchronous condensor and phase advancer. All of these devices generate leading reactive power to neutralize the effect of lagging reactive power
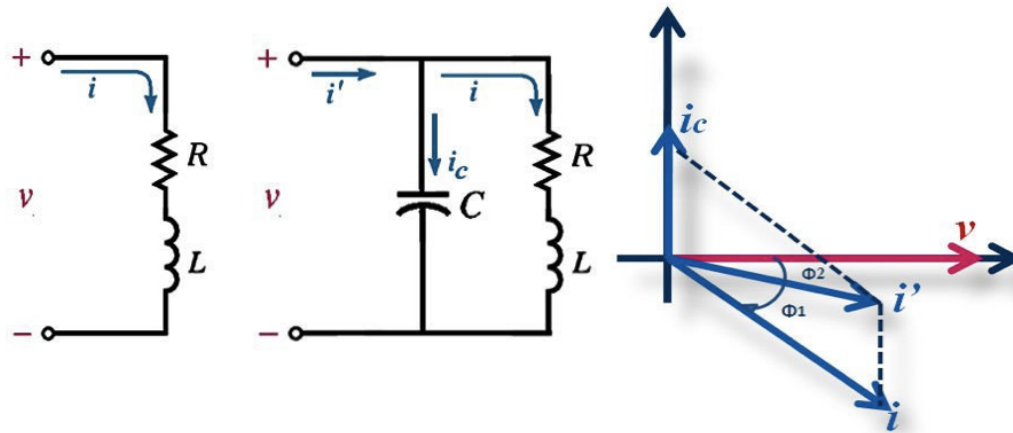
Figure 2.4: Power factor improvement with the help of capacitor bank

present in the system. This required amount of reactive power can be provided by a single capacitor or bank of capacitors when installed parallel to the inductive load. They act as a source of local reactive power generation, thereby reducing reactive power flows through the line. By doing so, they basically reduce the phase angle difference between the voltage and current as explained by Fig. 2.4 where current i flows before installing a capacitor bank that reduces to i' after connecting the capacitor bank. Thus, it improves the p.f by reducing the phase angle difference between voltage and current [13].

Similar to capacitor banks, synchronous condensors are also used as means of correcting power factor. Synchronous condensors are 3 phase synchronous motors with no load connected to their shaft. Synchronous machine has the capability of operating under any load power factor: leading, lagging or even unity depending upon the level of its excitation. For an inductive load, it is connected towards the load side and is operated under over excitation. This makes it act like a capacitor bank. During over excitation, it draws the lagging current from the supply or in other words it supplies the leading reactive power.

Phase advancer is mainly an AC exciter that is used to improve the p.f of the induction motor. It is mounted on the shaft of the induction motor and is connected to the rotor circuit of the induction motor. Induction motor needs reactive power to produce magnetic flux at slip frequency which are provided by the phase advancer to improve the power factor. It does so by providing the exciting ampere turns to the induction motor. It can be made to operate at leading power factor if ampere turns are further increased.

Other sources of automatic reactive power generation to improve p.f include static and dynamic var compensator. The former is essentially a thyristor based-controlled bank of capacitors while the latter is a more complex high-power elec-
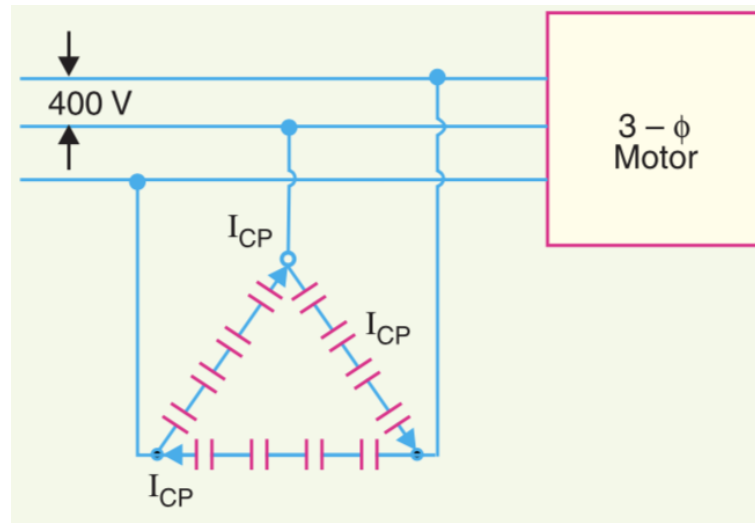
Figure 2.5: Connection of 3-phase capacitor bank with the motor [1]

tronic device. Both devices automatically detect the required amount of reactive power and electronically control the reactive power generation to improve the p.f. Recently a modern utility power grid is connected with many solar genera-tors through DC-AC inverters and wind turbines through induction generators. If correctly designed, these DC-AC inverters can also be utilized to generate or absorb reactive power as needed for p.f improvement.

2.1.2.2 Example of Power Factor Improvement In power factor correc-tion calculation, we use a voltmeter, ammeter and a wattmeter to measure the source voltage, current drawn and power flow. Here, a example is presented to improve the p.f.

In the example, let's suppose we need to improve the p.f of a 3-phase, 50 Hz, 400 V and 74.6 KW induction motor operating at an efficiency of 93% from 0.75 lagging p.f to 0.95 p.f. as shown in Fig 2.5. We need to calculate the KVAR required by the capacitor bank.

Solution:

Original p.f $= cos\delta_1 = 0.75 \implies \delta_1 = 41.41° \implies tan\delta_1 = 0.8819$

Required p.f $= cos\delta_2 = 0.95 \implies \delta_2 = 18.19° \implies tan\delta_2 = 0.3288$

Motor input, $P = \frac{output}{efficiency} = \frac{74.6}{0.93} = 80$ kW

Leading KVAR required by the capacitor bank $= P(tan\delta_1 - tan\delta_2) = 44.25$ KVAR

Capacitor bank should have capacitance $= \frac{V^2}{2\pi f * Required\ KVAR}$

Capacitor bank should have capacitance $= \frac{400^2}{2\pi 60 * 44.25} = 9.5913\ mF$

Thus, a capacitor bank of this much capacitance should be installed to improve the p.f.

2.2 Hierarchical Control of Optimal Reactive Power Generation

Hierarchical control is a type of control that is applied to achieve various control objectives in different time scales, physical levels and regional areas. The hierarchical control architecture contains three main levels: primary, secondary, and tertiary control levels as shown in Fig.2.6.

The primary control generates the control signals based on reference signals that are fed to it from secondary and tertiary control. Droop control is one of the popular types of primary control that regulates the frequency and voltage of the system depending on any change in active and reactive power load requirement. It is a very fast control technique that aims to meet the load demand within milliseconds. It is a local controller for generator and controls the active power, reactive power, terminal voltage, and speed of the generator [14].

The second level of control, the secondary control restores the frequency and voltage deviation caused by the primary control of the local generator. It is slower than the primary control and takes $20s$-15 minutes to compute the deviation caused by droop control and send this error signal to the primary control to

change the reference signal. Furthermore, it is a regional control and deal with a zone of an electrical system. In other words, it is responsible for regulating a local control area only. To regulate the frequency and voltage deviation, it can utilize up to 20% of the generation capacity of the generator. One of the popular example of secondary control is Secondary Voltage Control (SVCON).

The third level of control, the tertiary control deals with the economic related issues i.e. optimal economic dispatching, operation scheduling and other optimization problems for different objectives [15]. It is the slowest control of all the given control levels and only activates at the start of operation or every half an hour or so. It is a system level control technique which takes into account the whole system while optimizing. It generates the reference control signals for primary control based on the minimum operational cost. Popular examples of tertiary control are economic dispatch [16, 17] and unit commitment. The differences of secondary and tertiary control schemes have been tabulated in the form of table and shown in Table. 2.1

2.3 Role of Reactive Power Generation in Stabilization

The stability of an electrical power system is its capability to regain an operating equilibrium state after being subjected to a physical disturbance [18]. This physical disturbance could be breaking of a line, outage of a power generator, sudden rise/fall of power demand or malfunction of a controller. To counteract the effect of these disturbances, active and reactive power generation control is usually used to minimize the effect of any such disturbance. All these distur-

Table 2.1: Difference between secondary and tertiary control

Secondary Control	Tertiary Control
1. It is a control technique which usually focuses on the regulation of power system.	It is an optimization algorithm which takes into account the economics of the power system.
2. Local area-wide approach: It is responsible for regulating a local control area only.	System-wide approach: it considers the whole system while optimizing.
3. It helps primary control to achieve this reference value after any disturbance, just like an integrator.	It determines the reference value for primary control of each generator.
4. It can consume remaining 20% capacity to restore the reference value.	It utilizes 80% of the generator available capacity to determine its reference value.
5. Its timescale ranges from 20s-15 minutes after disturbance.	Operating timescale is 20-30 minutes or in the beginning of operation.
6. Its example is secondary voltage control (SVCON)	Example of tertiary control are economic dispatch problem or unit commitment.
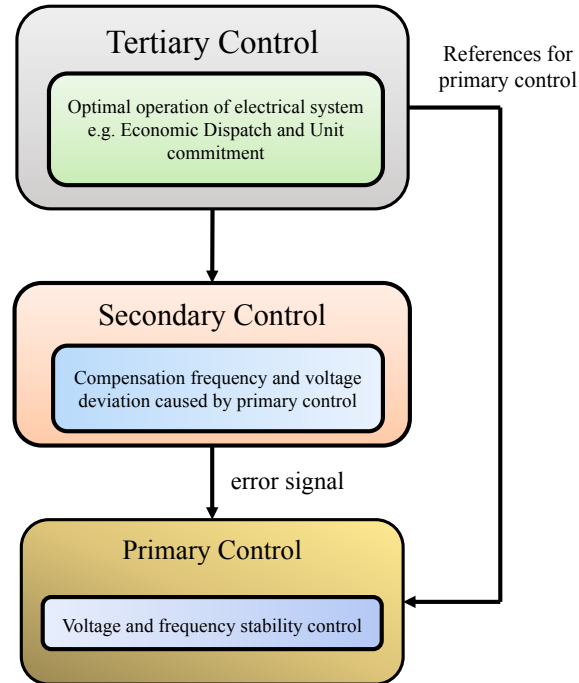
Figure 2.6: Simplified Hierarchical Control for electrical systems

bances lead to either change in the system frequency or bus voltage. Frequency is a system wide parameter whereas voltage is a local quantity[19]. In the following subsections, we will examine the role of reactive power generation control to deal with deviations in voltage and frequency.

2.3.1 Voltage Stabilization

Voltage stability is the ability of an electrical power system to preserve the steady state voltages at all buses. More specifically, it is the ability of the system to maintain or regain the state of equilibrium between power demand and power supply from its initial operating states after it has been subjected to any disturbance. In the worst case, progressive voltage drops or rises may lead to the loss of load in some areas, or possible tripping of transmission lines/transformers by their

protective systems leading to cascading voltage outages.

The phenomenon of voltage collapse is much more complicated than the voltage instability. It is the process in which a series of events accompanying voltage instability may lead to a blackout condition or unusually low voltages in a large part of the electrical power system. The major symptoms of voltage collapse may involve inadequate reactive support, low voltage profiles, heavy reactive power flows and heavily loaded systems. The voltage collapse is usually caused suddenly by low-probability multiple contingencies.

Whenever an electrical power system is exposed to a sudden rise of reactive power load demand just after a system contingency, the extra load demand is satisfied by the reactive power generation reserves of electrical generators. Generally, sufficient amount of reserve are kept for such additional load demand and the system settles down to a reliable voltage level. It is possible, however, due to this series of system conditions, that the absence of additional reactive power generation reserves may lead to a voltage collapse condition, thereby causing a limited or total blackout of the system. Therefore, it is very important to keep the sufficient amount of reactive power reserve for such conditions. Also, it is essential to design an advanced reactive power control to rectify these disturbance very fast.

2.3.2 Frequency Stabilization

Similar to voltage stability, frequency stability is about the ability of an electrical power system to maintain the steady state frequency after the system has been subjected to a severe upset resulting in a large imbalance between real power generation and power load demand. It is defined as the ability of the system

to restore equilibrium between system total generation and total load demand. The severe form of the instability may result in the sustained frequency swings causing the tripping of multiple generation units and loads.

These severe system upsets usually result in large deviations of frequency, and voltage, thereby invoking the control and protection devices. Generally, frequency instability is associated with lack of sufficient amount of real power generation reserve, slow equipment responses, and poor coordination of protection and control equipments. It is important to note that voltage magnitudes may deviate significantly during frequency excursions, especially when under-frequency load is dropped to improve the frequency. Thus, frequency deviations may cause voltage changes in the system and hence, there is an urgent need to design fast and reliable voltage and frequency control.

2.4 Existing Methods for Optimal Reactive Power Control

Voltage and frequency excursions can be significantly reduced with the help of an effective control of reactive power generation. Significant amount of research is available in the literature to control the reactive power generation[20]. Broadly speaking, there are two kinds of methods used to optimally control the reactive power generation. Centralized methods require transmission of real time system measurements from local power systems to the central controller as shown in Fig. 2.7. Information from all the buses and lines are required to send to the central controller that decides the control input for the system based on the received measurements.
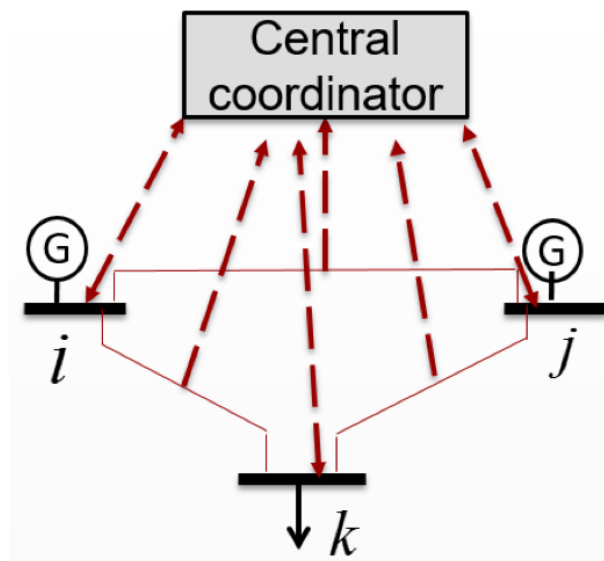
Figure 2.7: Centralized control scheme for power system

Unlike the centralized control technique, distributed techniques distribute the computation among the individual controller at the each bus as shown in Fig. 2.8. In the distributed control, each Bus Agent (BA) measures its local measurements and share it with its neighboring buses while Reactive Power Control Agent (RPCA) computes the control input for its local bus. In this way, there is no need for a centralized controller and transmission of informations from local power systems to the central controller.

2.4.1 Centralized Methods for Optimal Reactive Power Control

Centralized control schemes are the traditional control schemes that require a power controller with proper communication system to transmit information between the local electrical system and the central controller[21]. Optimal reactive power control has been explored significantly using centralized control schemes.
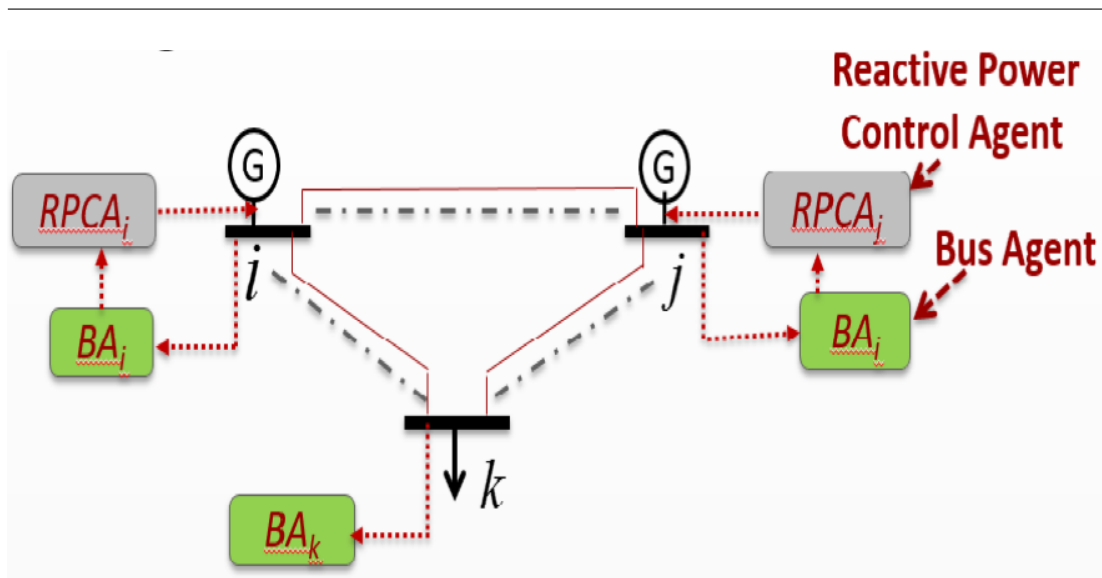
Figure 2.8: Distributed control scheme for power system

Abundant control techniques have been developed for the reactive power control such as gradient method [22], linear programming [23, 24], sequential quadratic programing algorithm [25], interior point method [26], [27], etc. Recently, many computationally intelligent based techniques have been proposed such as, Differential Evolution Algorithm [28], Gravitational Search Algorithm [29], Artificial Bee Colony [30], Enhanced Genetic Algorithm [31], and Particle Swarm Optimization (PSO) [32].

In [33], the authors proposed a centralized optimal reactive power control methodology to minimize the power loss and voltage deviation in the system. Similarly, in [34], integration of reactive power devices is proposed to provide voltage support in the distribution system. It has been implemented using centralized voltage control algorithm by dividing the distribution system into various areas.

2.4.1.1 Advantages of Centralized Techniques When comparing distributed and centralized schemes, it is found that centralized protocols show better performance in data loss recovery than the distributed protocols [35]. Also, the optimal

solution of the centralized optimal control is found to be better than that of distributed optimal control [36, 37]. The reason may be that in a distributed control, local information is shared among neighboring entities only, whereas in the centralized control, all information of the system is known that ensures the better optimal control of the reactive power. Also, most of the existing reactive power control solutions are centralized [3] and it is economical to improve the existing communication techniques than to completely reshape the overall communication paradigm. It may be expensive to deploy a controller on each DG bus.

2.4.1.2 Challenges with Centralized Techniques With so many advantages of centralized control scheme, it has also some problems. It requires an advanced and expensive communication network to transmit global information from local power systems to the centralized controller [38]. Due to slow transmission over long distances of communication network, centralized control is usually implemented off line [9]. Other shortcomings associated with it are its large sensitivity to initial conditions and mathematical restriction on objective functions, such as convexity. It has also been proved that the it may misinterpret the information if signal is noisy.

In addition to it, a centralized control technique requires transmission of massive amount of data between the local control area and the central controller, which may cause data congestion. It may be significant, especially when the control area is large and the available bandwidth of the communication channel is limited. The bandwidth requirement is evaluated by [39], which states that a bandwidth of 5 -10 Mbps and 25-75 Mbps is required for applications within one control area and for inter-area control center communication, respectively. It may further be aggravated when data from several control zones is being concentrated at the

Phasor Data Concentrator, before transmitting to the central controller.

2.4.1.3 Possible Solutions for Centralized Techniques The major challenge with the centralized control scheme is the huge amount of data transfer that may cause slow down the transmission or lose the important information. It is usually due to limited bandwidth of the communication channel. Thus, a data size reduction technique should be proposed to deal with these issues [8]. Reduction or compression of data may also minimize the communication delay, the power loss on the communication channel, and communication channel cost. There are numerous compression techniques available in the literature to deal with data size compression.

Another possible solution to its challenges is to devise a new control architecture that does not need transmission of massive amount of data from the local power system to the central controller. One of the possible solution is the distributed control scheme that commonly distributes the computation burden among numerous smaller local controllers that are placed at the monitoring positions of the power system [40].

2.4.2 Distributed Techniques for Optimal Reactive Power Control

Distributed control schemes are proved to be effective for power system applications and have been explored to a great extent for optimal reactive power control applications. Power system networks are regarded as multiagent systems (MAS) that are complex systems composed of several autonomous agents with only local knowledge, [41] but are able to interact in order to achieve a global objective

[42]. Fast communication facilities such as fiber optic, microwave and 3G are now becoming integrated parts of power systems that makes it easier to integrate MAS into power system applications [43].

In recent years, consensus-based control theory has been extensively explored in various fields. MAS framework has been adopted by many researchers to describe the communication topology among multi-agents in a physical system. These communication topologies may be different for different physical systems. Some researchers assume that agents can exchange information locally [41, 44] while others have their own definition of communication topology.

In [45], authors proposed a fully decentralized control algorithm to minimize the power loss of a microgrid. They pointed out that the performance of the proposed algorithm without communication might deteriorate noticeably compared to the case with communication. Similar studies on decentralized control to minimize power loss for smart distribution network is proposed in [46, 47]. In [48], the authors proposed a cooperative distributed optimization and control technique using local communication to minimize the voltage deviations within a grid connected microgrid. They proved that minimizing the voltage deviation naturally reduces the power loss. However, the power loss is not directly minimized, and the scalability is also not investigated.

Similarly in [3], the authors proposed MAS based optimal reactive power control algorithm to minimize the voltage deviation and power loss. It is a generic sub-gradient control strategy, which requires the information of voltage angle difference between two neighboring buses to calculate the power loss of the system. However, firstly, finding the voltage angle difference requires special techniques [3], which may lead to lengthy calculations. Secondly, considering the features

of power systems with high penetration level of DGs, the cost of reactive power generation should be considered. Thirdly, it should be emphasized that all the DGs contribute reactive power uniformly based on their capacities such that none is overloaded [49].

2.4.2.1 Advantages of Distributed Techniques Challenges associated with centralized control strategies can be resolved with distributed approach that can improve the respond speed of Optimal Reactive Power Control (ORPC) effectively by relieving the communication and computational burden of the communication channel and the central controller, respectively [50, 48], and they are proved to be suitable for online applications that require frequent control setting update [3]. In distributed scheme, there is no need of central controller rather each local entity is attached with a local controller [47].

This strategy is implemented on an MAS-based framework, where each bus in the power network is assigned with at least an agent as shown in Fig. 2.8. Each agent first calculates or measures its local state and control variables and then shares its local data with its neighbors through a local communication channel. In this way, comparatively, the size of the data size, to be transmitted, is much less than the data size, to be transmitted in a centralized control. Thus, there may no be problem of limited bandwidth.

2.4.2.2 Challenges for Distributed Techniques Although distributed approaches address the problem of data congestion, data loss and slow data transmission, yet there are some challenges associated with the distributed control. There two types of communication schemes in distributed approach: synchronizes and asynchronous scheme. Mostly, each agent in distributed approach commu-

nicates with its neighboring agents in the form of synchronized communication where each agent needs to wait for the information from its neighboring agents. This wait for the data may slow down the control process of the distributed approach.

Most of the existing physical power systems are built based on the centralized algorithms. Each system is constructed with a central controller and communication links between local power system and the central controller [51]. Communication between agents may not be available in the physical power system. That's why it may be expensive to overall build a system with two controllers on each bus and communication links between the agents.

2.4.2.3   Possible Solutions with Distributed Techniques   The possible solutions to the challenges of a distributed control can be switching to distributed control completely. It requires massive investment in the power system to fully change the control scheme by installing controller on each bus and communication links between each agent. Although initially it can be expensive yet it can make the system more reliable, fast and cost effective after the implementation. Once, real time power system is converted into the form of distributed control, the problem of single point failure of the central controller can be resolved.

Synchronized communication scheme can be improved by either switching to asynchronous scheme or synchronized scheme can be improved by numerous technique that can be developed with further research. Furthermore, it is also recommended to invest more funding the power system research so that an innovative and fast communication scheme can be designed for it. It will improve the reliability and speed of the system.

2.5 Compression Techniques

For centralized schemes, ORPC problem for a large power system requires a huge amount of data to be transmitted to the central controller. If the bandwidth of the communication network is not sufficiently large enough to support transmission of such massive amount of data, it may deteriorate the performance of the controller. To address the problem of limited bandwidth, we need to compress the sending end data.

More specifically, when transmitting power systems data over the restricted bandwidth communication channel, the amount and frequency of the data transmission have specific limits, such as Shannon's Channel Capacity, restricts the amount of digital information that can be transmitted over a given channel [52]. That is why, it is required to make the data size smaller for fast data transmission. There are a number of different compression algorithms, which can be broadly divided into two categories: lossless algorithms, and lossy algorithms.

2.5.1 Lossless Compression Techniques

As the name implies, lossless algorithms decrease the size of a given signal, while at the same time not losing any information from the original signal. For this reason, lossless compression algorithms are preferable to lossy algorithms, especially when the data needs to intact arrive at the recipient. But lossless data compression algorithms may not guarantee compression for all input type data sets.

In other words, for any lossless data compression algorithm, there may be an input data set that does not get smaller when processed by the lossless algorithm. Also,

lossless algorithms may not work perfectly for the dynamic nature of data, which is the case for the power system output data. Thus, lossless compression may not be an ideal compression technique for this specific application. Another factor is that the lossless compression scheme cannot achieve a remarkable value of compression ratio whereas our objective is to compress the data size significantly.

2.5.2 Lossy Compression Techniques

On the other hand, using lossy compression algorithms, data size can be compressed to a significant level. Very high compression ratio is possible with the lossy algorithms only. But the quality loss of the retrieved data may be noticeable. There is a trade-off between compression ratio and quality of the recovered data. Data can be sent quickly, transmitted and stored using lossy algorithms.

Another advantage of lossy compression is the generic nature of its algorithms. Lossy compression algorithms may be applied to a wide variety of applications, especially to accommodate the dynamic nature of real-time data. As power system data is always changing, thus, lossy compression algorithms are the suitable choice for this application. Therefore, based on these factors, it is recommended to use lossy algorithms for the dynamic nature of power system data.

2.5.3 Singular Value Decomposition

Singular Value Decomposition (SVD) has been successfully employed for numerous data compression related applications [53]. SVD is a lossy compression technique in which part of the information is lost when the data is compressed. In such a compression scheme, not only the redundant data but also less relevant

information is discarded. This will significantly improve the data compression. To achieve a high compression ratio and fast data transfer, SVD can be utilized to transmit data for numerous load frequency control and voltage control applications.

Let $X \in R^{(p \times q)}$ be a matrix of data needs to be compressed where each row corresponds to a PMU and each column corresponds to a time instant as shown in Fig. 2.9. SVD can be used to decompose a matrix X into a product of three matrices

$$X = U\Sigma V^T, \tag{2.10}$$

where $U \in R^{(p \times p)}$ and $V \in R^{(q \times q)}$ are the orthogonal matrices containing eigenvectors of XX^T and X^TX, respectively. $\Sigma \in R^{(p \times q)}$ is a diagonal matrix whose values are the singular values, which are square roots of the eigenvalues of XX^T or X^TX arranged in decreasing order.

(2.10) can be expressed as a sum of rank one matrices as given in 2.11

$$X = \sum_{i=1}^{p} u_i \sigma_i v_i^T = u_1 \sigma_1 v_1^T + u_2 \sigma_2 v_2^T + \cdots + u_p \sigma_p v_p^T, \tag{2.11}$$

where u_i and v_i are the left and right singular vectors, respectively, while σ_i are the corresponding singular value.

SVD can be used for data compression, enabling noise reduction and data dependences, as small singular values mainly represent the noise and interdependences in X. It can be seen in many applications that the ordered singular values in the diagonal Σ decrease rapidly. In such applications, only a few terms in (2.11) would be necessary for a good approximation of matrix X. Thus, a few singular

Time instants

$$\begin{bmatrix} X_{11} & \cdots & X_{1q} \\ \vdots & \ddots & \vdots \\ X_{p1} & \cdots & X_{pq} \end{bmatrix}$$
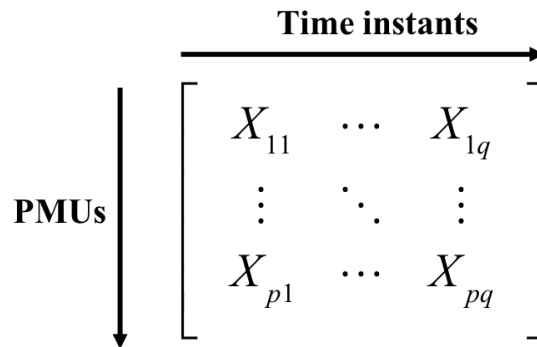
PMUs

Figure 2.9: Data matrix X

X $=$ U Σ V
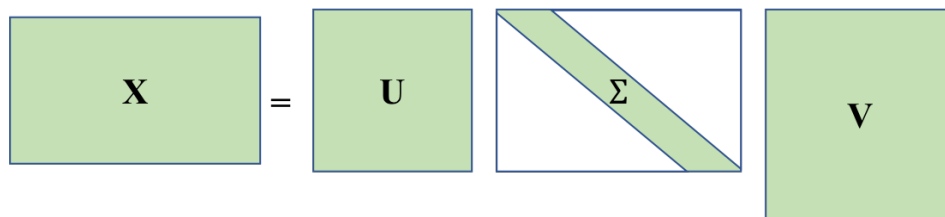
Figure 2.10: SVD of Data matrix X

values need to be retained in Σ for data compression using SVD.

A large number of smart sensors like Phasor Measurement Unit (PMUs) can be deployed in power systems, which will collect and transmit enormous amounts of data to the central controller for power system control applications.

2.5.3.1 Data Collection Let's consider, for example, that measurements from p different PMUs in an area of power system, taken over q time instants, need to be transmitted through communication network to serve. This set of input measurements can be put in the form of a matrix X, with each number of row containing the measurement taken from a given PMU and each column containing the measurement at a given instant as shown in Fig.2.9. Representation of data in this form can be easily manipulated for data compression.

2.5.3.2 Data Compression Matrix X can be factorized into three matrices by applying the SVD. It can be shown in 2.12 and can be schematically represented in Fig.2.10. Matrix V^T in (2.10) is hereafter written as just V in order to simplify the notation.

$$X^{(p \times q)} = U^{(p \times p)} \Sigma^{(p \times q)} V^{(q \times q)}, \tag{2.12}$$

where Σ is a diagonal matrix that contains the SVs of X, ordered from the highest to the lowest. Data can be compressed significantly by utilizing the fact that matrices of power system data contain spatial-temporal correlation that leads to only a few Singular Values (SVs) actually being non-negligible. Thus, a good approximation of matrix X can be obtained by keeping only the SVs found to be significant in matrix Σ . Assume that only r SVs are to be retained in Σ and let the matrix XR denotes the approximated reduced matrix from matrix X. The matrix XR can be computed by replacing Σ by Σ' in (2.10), yielding 2.13

$$XR = U\Sigma'V^T, \tag{2.13}$$

where each matrix takes the form of

$$XR = \begin{bmatrix} XR_{11}^{(r \times r)} & XR_{12}^{(r \times (q-r))} \\ XR_{21}^{((p-r) \times r)} & XR_{22}^{((p-r) \times (q-r))} \end{bmatrix},$$

$$U = \begin{bmatrix} U_{11}^{(r \times r)} & U_{12}^{(r \times (p-r))} \\ U_{21}^{((p-r) \times r)} & U_{22}^{((p-r) \times (p-r))} \end{bmatrix},$$

$$V = \begin{bmatrix} V_{11}^{(r \times r)} & V_{12}^{(r \times (q-r))} \\ V_{21}^{((q-r) \times r)} & V_{22}^{((q-r) \times (q-r))} \end{bmatrix},$$

$$\Sigma' = \begin{bmatrix} \Sigma_{11}^{'(r \times r)} & 0 \\ 0 & 0 \end{bmatrix}.$$

Performing matrix multiplication on the right hand side of 2.13, XR can be represented in 2.14

$$\begin{bmatrix} XR_{11} & XR_{12} \\ XR_{21} & XR_{22} \end{bmatrix} = \begin{bmatrix} U_{11}\Sigma'_{11}V_{11} & U_{11}\Sigma'_{11}V_{12} \\ U_{21}\Sigma'_{11}V_{11} & U_{21}\Sigma'_{11}V_{12} \end{bmatrix}. \tag{2.14}$$

It can be seen from (2.14) that the only matrices needed to compute the reduced matrix XR are: $\Sigma_{11}^{'(r \times r)}$; $U_{11}^{(r \times r)}$; $U_{12}^{((p-r) \times r))}$; $V_{11}^{(r \times r)}$; and $V_{12}^{(r \times (q-r))}$. Considering the dimensions of each submatrix and knowing that Σ' is diagonal, it can be observed that total number of elements to be transmitted for those submatrices equals $(p + q + 1) \times r$.

2.5.3.3 Compression Ratio Compression Ratio (CR) is defined as the ratio of size of original data by size of compressed data. A $CR=10$ means that the data has been compressed with the ratio 10:1. CR is computed by 2.15, that expresses the ratio between total number of elements in the original matrix X (measurements) and the total number of elements in the submatrices that are needed to compute the matrix XR

$$CR = \frac{p \times q}{(p + q + 1) \times r}. \tag{2.15}$$

It can be seen from (2.15) that, given a measurement set, the effectiveness of the data compression will depend on the number of SVs, to be retained after performing the SVD. Communication network bottleneck limits the value of CR that can be considered acceptable for a given compression task. So, alternatively, it is possible to rearrange (2.15) so that one can directly compute the number of SVs that need to be retained in order to achieve a given CR as given in 2.16

$$r = \frac{p \times q}{(p + q + 1) \times CR}.$$
(2.16)

(2.16) can be used to directly compute number of SVs that will meet a given CR requirement. However, it should be noted that r can take only positive integers because it represents the number of SVs to be retained in Σ. For practical purposes, a rounding of r to the nearest positive integer value will be a good approximation to meet the specified CR requirement.

2.5.3.4 Computation of Loss of information Lossy compression methods can be very effective for data compression, but this happens with a cost, which is the loss of information that cannot be retrieved when the original signal is reconstructed. Thus, it is advisable to compress the data in such a way that a good trade-off between the CR and loss of information is achieved. Data compression, in other words, should not result in the loss of information that renders the reconstructed matrix of limited use. Loss of information, in this thesis, is measured in terms of the mean absolute error (MAE) and mean percentage error (MPE) observed when comparing the reconstructed data matrix with original input data as given in 2.17 and 2.18

$$MAE = \frac{1}{p \times q} \sum_{i}^{p} \sum_{j}^{q} \mid X(i,j) - XR(i,j) \mid, \qquad (2.17)$$

$$MPE = \frac{1}{p \times q} \sum_{i}^{p} \sum_{j}^{q} \mid \frac{X(i,j) - XR(i,j)}{X(i,j)} \mid \times 100. \qquad (2.18)$$

2.5.4 Compressive Sensing

Another lossy compression technique is the compressive sensing (CS) which takes advantage of sparse signal structures, is considered as a promising joint data compression and reconstruction method to transmit information efficiently [54]. As the data obtained from observing a physical system like power system, inherently contains spatial and temporal correlation [55], it can be compressed before transmitting through the unreliable communication channel and recovered at the receiving end. In power system applications, real-time data of bus voltages and line currents in each area can be first sampled and compressed before being transmitted through the communication network. At the receiving end, it is first decoded and recovered accurately by the central controller. The size of transmitted data can be significantly reduced with the use of CS.

CS has been utilized in many applications of signal processing e.g. a CS-based data loss recovery algorithm to improve the communication efficiency by reducing the communication burden and thus, saving the power demand is presented in [56], which is further improved in [57] with low space complexity, low floating-point calculations, and low time complexity robust CS framework. Recently, a data reduction scheme by removing redundant phasor information before transmission is proposed in [58] in order to reduce the amount of data.

2.5.4.1 Compression Using CS Power system data such as bus voltage magnitudes, angles, and line currents can be monitored with the help of Phasor Measurement Units (PMUs) at each interval of time and need to be transmitted to the central controller. To start compression, if there are n PMUs in the power system control area, at each time step k, the state measurements vector $x(k)$ taken from n sensors of the power system control area can be compressed into m linear measurements (such that $m < n$, and $y \in \mathbb{R}^m$) [59] as 2.19

$$y(k) = \Phi \mathbf{x}(k) + \mathbf{N}(k) = \Phi \Psi \theta(k) + \mathbf{N}(k) = \Upsilon \theta(k) + \mathbf{N}(k), \qquad (2.19)$$

where m is a function of the number of non-zero elements of the vector $x(k)$, $x(k) = \Psi \theta(k)$ is the representation of $\mathbf{x}(k)$ into its basis matrix $\Psi \in \mathbb{R}^{m \times n}$ and the vector of transform coefficients $\theta(k) \in \mathbb{R}^n$. $\mathbf{N}(k)$ is the Gaussian additive white noise vector with zero mean and variance in the signal. $\Phi \in \mathbb{R}^{m \times n}$ is the measurement matrix and $\Upsilon = \Phi \Psi \in \mathbb{R}^{m \times n}$ is the sensing matrix. In power system applications measurement vector, $\mathbf{x}(k)$ can be the voltage and reactive power magnitudes measured at the load buses. 2.19 will be used to compress measured data vector before sending it through the communication channel.

For compression, by using DCT basis, the basis of the state measurements vector $\mathbf{x}(k)$ is first changed into transformation coefficients vector $\theta(k)$. Then, the transformation coefficients vector $\theta(k)$ is compressed into size $m \times 1$ using measurement matrix $\Phi \in \mathbb{R}^{m \times n}$ of size $m \times n$ where $m << n$. After compression, the compressed data is transmitted through communication channel. Note that, any universal data independent basis can be considered as a basis matrix $\Psi \in \mathbb{R}^{n \times n}$. Some of the available transformations may include the discrete cosine transform (DCT) basis, the discrete Fourier transform (DFT) basis, and the discrete wavelet

transform (DWT), etc.

2.5.4.2 Recovery using CS At the end of communication channel, recovering of the original measured data vector can be done by solving 2.20 for $\hat{\theta}(k)$. However, decoding of 2.20 is an NP-hard problem involving l_0-norm minimization. Thus, l_1-norm minimization which is the convex approximation of l_0-norm is adopted as 2.20

$$\hat{\theta}(k) = arg\ min_{\theta(k)}||\theta(k)||_1 \quad \text{subject to} \quad y(k) = \Upsilon\theta(k) + \mathbf{N}(k), \qquad (2.20)$$

where $\hat{\theta}(k)$ is the vector of transformation coefficients of the measurement vector. After recovering transformation coefficients vector $\hat{\theta}(k)$, the state measurement vector is calculated as 2.21

$$\hat{x}(k) = \Psi\hat{\theta}(k), \qquad (2.21)$$

where $\hat{x}(k)$ is the vector of recovered measurements. fig.2.11 shows the pictorial representation of CS where state measurement vector $\mathbf{x}(k)$ is being compressed using encoding algorithm of 2.19 and recovered using 2.20 and 2.21.

2.5.4.3 Compression Ratio The performance of CS can be evaluated by the following two criterions:

- Compression ratio (ρ) :

$$\rho = \frac{\text{The size of data being transmitted without CS}}{\text{The size of data being transmitted with CS}}, \qquad (2.22)$$
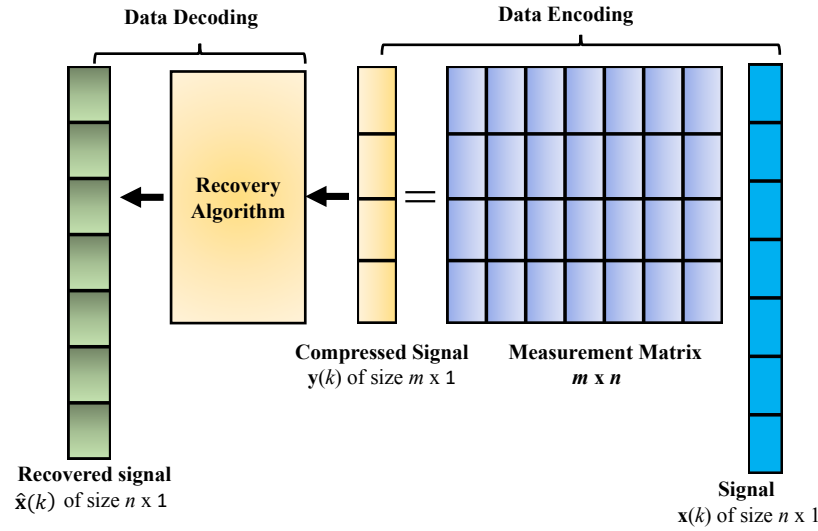
Figure 2.11: Compression and Recovery of x using CS

- Signal to Noise Ratio (SNR) :

$$SNR = \frac{-20 \log ||x - \hat{x}||}{||x||}.$$ (2.23)

2.6 Fault Detection Techniques

Power system protection is a very important branch of power engineering that deals with the protection of power systems, more specifically to identify the abnormal conditions and faults in the system. There are many techniques used to detect the abnormal conditions in the system. There are some related more toward control engineering approach, while others are more towards mathematical, statistical and Artificial Intelligence approach. Some recent interesting work can be seen in [60, 61, 62, 63, 64, 65]. One of the recent fault detection technique is known as Mathematical Morphology Singular Entropy (MSE) that combines

the concepts of Mathematical Morphology (MM) , Singular Value Decomposition (SVD) and Information Entropy to detect abnormal conditions in power systems.

2.6.1 Mathematical Morphology Singular Entropy

As mentioned in the previous section, Mathematical Morphology Singular Entropy (MSE) utilizes three different techniques: Mathematical Morphology (MM), Singular Value Decomposition (SVD) and Information Entropy, and then combines them to detect the abnormal conditions. Here is a brief overview of these three approaches.

2.6.1.1 Mathematical Morphology Mathematical Morphology is a concept based on the set theory [66] and has been established by introducing the fundamental operations on two sets. One of the set is given measured signal and other set is a function known as the structuring element (SE) which is used to process the given signal. SE is used as a probe which translates over the given signal.

Morphological operators are the set transformations which are highly efficient for feature extraction and de-noising the noisy signals while preserving the nature of signals [67]. Two basic morphological operators are dilation and erosion which together make a pair of dual transforms. Let $\boldsymbol{x}(k)$ denote the state measurement vector obtained from power system and $\boldsymbol{g}(s)$ denote the structuring element, then mathematically, the dilation ($\oplus$) and erosion ($\ominus$) of $\boldsymbol{x}(k)$ by $\boldsymbol{g}(s)$ are given by 2.24 and 2.25

$$(x \oplus g) = \max_{s} \quad x(k+s) + g(s), \qquad (2.24)$$

$$(x \ominus g) = \min_{s} \quad x(k+s) - g(s), \tag{2.25}$$

where s is the vector of structuring element [68].

Dilation operator computes the maximum value within the neighborhood of $\boldsymbol{x}(k)$ and erosion operator calculates the minimum value within the neighborhood of $\boldsymbol{x}(k)$. Intuitively, dilation can be considered as swelling of $\boldsymbol{x}(k)$ while erosion can be imagined as shrinking of $\boldsymbol{x}(k)$. SE can have different shapes and sizes depending on the problem to be solved. A simple case of SE is of the form $\boldsymbol{g}(s) = 0$ and it is called (known as) "flat SE". A SE is a shape that is used to probe an image. Flat structuring elements are binary in nature and are sometimes considered as masks.

Most of the time, flat structuring elements are centered and are square matrices, with an odd size: 3×3, 5×5, etc. These matrices consist of $0's$ and $1's$ and are typically much smaller than the image being processed. It is common to use flat structuring elements in morphological applications. In order to filter the noise from signal, Mathematical Morphological Filter (MMF) is designed by averaging the dilated and eroded waveforms as 2.26 :

$$x_{filter}(k) = \frac{(x \oplus g)(k) \; + \; (x \ominus g)(k)}{2}, \tag{2.26}$$

where $\boldsymbol{x}_{filter}(k)$ is the filtered output of $\boldsymbol{x}(k)$. By applying different shapes and lengths of SE, filter can de-noise the input signal in different levels.

2.6.1.2   Singular Value Decomposition SVD has already been explained in this chapter and hence, only a very brief working of SVD is given here. It is used to decompose a matrix $A \in \mathbb{R}^{m \times n}$ into two orthonormal matrices $L \in \mathbb{R}^{m \times m}$

and $M \in \mathbb{R}^{n \times n}$ and a rectangular diagonal matrix $\Sigma \in \mathbb{R}^{m \times n}$ as given in 2.27 [69]

$$A = L\Sigma M^{T},\tag{2.27}$$

where Σ consists of positive square roots of eigenvalues known as singular values of A. Singular values (σ) are arranged in its descending order in Σ. By decomposing the matrix of measured state data using SVD, the state data can be represented in a decreasing order of their magnitudes using singular values.

2.6.1.3 Information Entropy In information theory, information entropy is the expected value of the information contained in each message. In other words, it is the measure of uncertainty in each data package as defined by [70] 2.28

$$E = \sum_{i=1}^{n} p_i \, ln(p_i),\tag{2.28}$$

where $0 \leq p_i \leq 1$ is the probability of occurrence of an event where $\sum_{i=1}^{n} p_i = 1$ and n is the total number of events or total number of data packages. When all probabilities are equal to each other, the information entropy E reaches its maximum value $ln(n)$ means that it is the most uncertain situation.

2.7 Summary

This chapter first introduces the basic fundamentals concepts about apparent power generation, real power generation and reactive power generation. Then it presents the importance of reactive power generation and power factor improvements. After explaining various means of power factor improvements, it presents

hierarchical control for power systems which is used for voltage and frequency stabilization of power systems.

Furthermore, this chapter presents various existing control paradigms for power system: centralized and distributed. It describes advantages, disadvantages, solutions to existing challenges within control paradigms. It then moves on to different compression techniques, their benefits and mathematical formulations. Finally, it presents the importance of power system protection and mathematical morphology singular entropy as a fault identification technique.

Chapter 3

Singular Value Decomposition based Load Frequency Control: The Secondary Control

With the recent expansion and growing complexity of power system to realize the growing load demand, the massive amount of information that needs to be transmitted for real-time monitoring, and control purposes, has risen rapidly. The accurate and timely transmission of this enormous amount of data poses great challenge to the existing communication network [71]. This chapter proposes a novel Singular Value Decomposition (SVD) based real-time Load Frequency Control (LFC) of a multi-area power system. According to the proposed strategy, the measured data in each control area is decomposed using SVD before being transmitted through the communication network, and only the most valuable information is transmitted to the control center [72].

The proposed strategy is capable of significantly reducing the volume of the data

to be transmitted through the communication network and accurately recovering the original data. These features are illustrated by the test results that demonstrate the effectiveness of the proposed SVD based load frequency control strategy.

In this chapter, a real-time SVD based frequency control strategy is proposed for a multi-area interconnected power system. The real- time data at each control area is first sampled and decomposed before being transmitted through the communication network. To address the problem of time delay and packet drop, model predictive control (MPC) technique, which minimizes a finite-horizon cost function in a receding horizon manner, is introduced. The proposed algorithm is reliable, robust, and its effectiveness is demonstrated through simulations. The contributions of this chapter are:

- Real-time load frequency control is implemented for a multi-area power system.

- SVD is introduced to reduce the size of transmitted data significantly at a very fast rate.

- Comparison of results of SVD with CS as a compression technique is presented to realize the importance of SVD

- MPC is introduced to effectively handle the data delay and packet loss problem.

This chapter is organized as follows: Section 3.1 discusses the related work and motivation behind the frequency control and use of SVD to compress the size of data transmission. Section 3.2 introduces the SVD based LFC, our proposed

method to regulate frequency of a multi-area power system while decreasing the size of real-time data at the same time. Settings for testing the proposed algorithm are given in Section 3.3 with results and their discussions are followed in Section 3.4. Finally, the findings are summarized in Section 3.5.

3.1 Motivation and Related Work

With the rapid growth in electric energy demand and the increasing attention to lessen the environmental impact of the power systems, the penetration level of renewable distributed energy sources, the scale of power systems and the information handling quantity have kept increasing [73]. The transmission of massive amount of real-time system data poses great challenges for reliable, safe, robust and economical operation of the next-generation power system[74].

LFC is a very important control technique for supplying sufficient and high quality electric power in a very efficient and cost-effective way[74, 75, 76]. Its main objective is to control the frequency deviations within the permissible range by controlling the real power output generation of the generating units and balancing the tie-line power interchange in response to generation and load variations. It is an area wide control scheme which rectifies frequency deviation produced by load variation in its area. Initially, the primary control tries to minimize those deviations but since it is a proportional controller, the response is not free from deviation. Load Frequency Control rectifies the miniature deviations existing after the operation of primary control.

Load frequency control is an area-wide control scheme that requires the local data to be sent to the central controller of the control area. Real-time system state

measurements are transmitted from massive number of distributed generation units to the control center in a conventional centralized LFC strategy [77].The operating timescale of this type of control is ranging from few seconds to minutes. The transmission of information is happened to have communication delays due to several factors including transmission protocol used, data package size, network communication load etc. [78]. The amount of data being gathered and transmitted is so big that all of it may not be able to be transmitted at the rates at which it is gathered. The communication system, thus, needs to be designed to transmit only the necessary data to the control center [79]. However, it is extremely challenging to identify the necessary data in a real-time manner to preserve the integrity of important information. Therefore, there is an urgent need to develop advanced information processing techniques to support real-time control and management.

Recently, CS which takes advantage of the sparse signal structures has been utilized by many researchers to reduce the communication delay and cost of data transmission [33]. A dynamic CS framework, where continuous-time sparse signal is sampled and reconstructed afterwards based on the prior signal knowledge, is proposed in [80] for a real-time control application. In [58], an amount of data reduction scheme is proposed by removing redundant phasor information to identify only the important information. Similarly, in [56], a CS-based data loss recovery algorithm is proposed to improve the communication efficiency by reducing the communication burden.

In [81], authors propose real-time CS based strategy for the load frequency control of a multi-area power system. The measured data in each control area is compressed before being transmitted through the communication network, and

then recovered at the end of communication channel. The proposed strategy can significantly reduce the size of transmitted data. However, LFC is a secondary control that is a fast control strategy usually of an order of few seconds.

But using of CS as compression technique may slow down the data transmission process. In CS, we need to design a basis matrix that transforms the measurement vector into a new basis. CS also requires a measurement matrix which is used to compress the measurement data into smaller dimension. Formulation of basis matrix and measurement matrix in CS makes the process slow. In addition to it, various reconstruction algorithms can be used to recover the original data. Some of the algorithms are convex optimization based and others are greedy algorithms [82].

These algorithms further, consume time in recovering the original data. Furthermore, the effectiveness of CS based compression algorithms relies on the bases selection for the temporal and spatial compression. If the optimal bases are not utilized for compression, it may result in a slower transmission of data. In an application of LFC, data needs to be transmitted at a very fast rate and CS may not comply with the rate of transmission required by LFC. Therefore, there is an urgent need to develop a fast advanced information processing technique to support real-time LFC scheme.

Singular Value Decomposition has been successfully employed for data compression related applications [53, 83]. SVD is a lossy compression technique in which part of the information is lost when the data is compressed. In such a compression, not only the redundant data but also less relevant information is discarded. This will significantly improve the data compression. Along with this compression requirement, it is, further, required for the compression technique to be fast
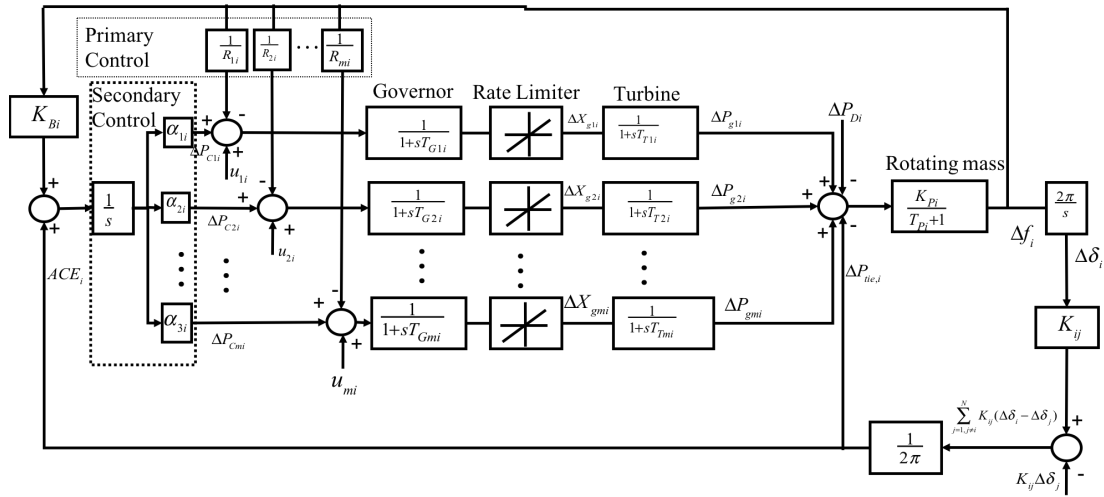
Figure 3.1: i^{th} control area with multiple generators in a multi-area power system

in order to match the rate of response scale for fast Load Frequency Control scheme. Singular Value Decomposition satisfies both of these requirements, that is why, Singular Value Decomposition has been used.

3.2 The Proposed Method: SVD Based LFC

SVD based LFC approach consists of two parts: 1) SVD part and 2) the LFC part. Formulation of SVD along with its application as compression technique has been discusses in 2.5.3. In this section, we will discuss the formulation of LFC for a multi-area power system.

3.2.1 Load Frequency Control

Frequency of a system can be controlled by varying the real power generation in the system. Frequency control of a multi-area power system is shown in Fig.3.1, where i^{th} control area with m number of generators is connected with its jth

neighbor. Although the power system is highly non-linear physical system, the linearized model is valid in frequency control application because only small variations and disturbances are expected during normal operation of power system [84].

Equations governing small signal dynamic operation of the ith control area of a multi-area power system are shown from 3.1 through 3.4.

$$
\Delta\dot{f}_i(t) = -\frac{\Delta f_i}{T_{Pi}} + \frac{K_{Pi}}{T_{Pi}}\sum_{k=1}^{m_i}\Delta P_{gki}(t) - \frac{K_{Pi}}{T_{Pi}}\Delta P_{Di}(t)
$$
$$
-\frac{K_{Pi}}{2\pi T_{Pi}}\sum_{j=1,j\neq i}^{N} K_{ij}(\Delta\delta_i(t) - \Delta\delta_j(t)),
$$
(3.1)

$$
\Delta\dot{P}_{Di}(t) = -\frac{\Delta P_{gki}(t)}{T_{Tki}} + \frac{\Delta X_{gki}(t)}{T_{Tki}},
$$
(3.2)

$$
\Delta\dot{X}_{gki}(t) = \frac{-\Delta f_i(t)}{R_{ki}T_{Gki}} - \frac{\Delta X_{gki}(t)}{T_{Gki}} - \frac{P_{Cki}(t)}{T_{Gki}} + \frac{u_{ki}(t)}{T_{Gki}},
$$
(3.3)

$$
\Delta\dot{P}_{Cki}(t) = \alpha_{ki}[K_{Bi}\Delta f_i(t) + \frac{1}{2\pi}\sum_{j=1,j\neq i}^{N} K_{ij}(\Delta\delta_i(t) - \Delta\delta_j(t))],
$$
(3.4)

where Δf_i, ΔX_{gki}, ΔP_{gki}, $\Delta\delta_i$, ΔP_{Cki}, and ΔP_{Di} are the changes in frequency, governor value position, power output, rotor angle deviation, integral control of the kth generator, and supply demand mismatch disturbance, respectively. K_{Pi}, R_i, and K_{Bi} are power system gain, droop control coefficient, and frequency bias factor, respectively. T_{GKi}, T_{Tki} and T_{Pi} are the time constants of governor, turbine and power system, respectively. α_{ki} and K_{ij} are the integral control gain that also contains participation factor of the generator; and the interconnection gain between two interconnected areas. Vectors of state variables and control variables in the ith control area with m_i generators are shown in 3.5 and 3.6, respectively.

$$x_i(t) = [\Delta f_i, \Delta P_{g1i}, \cdots, \Delta P_{gmi}, \Delta X_{g1i}, \cdots, \Delta X_{gmi},$$

$$\Delta P_{C1i}, \cdots, \Delta P_{Cmi}, \Delta \delta_i]^T_{n_i \times 1}, \tag{3.5}$$

$$u_i = [0, \underbrace{0, \cdots, 0}_{m_i}, u_{1i}, \cdots, u_{mi}, \underbrace{0, \cdots, 0}_{m_i}, 0]^T_{n_i \times 1}, \tag{3.6}$$

where n_i is the size of the state variables in control area i with $n_i = 3m_i + 2$. In this problem of Load Frequency Control, the number of state variables needs to be transmitted from a local area to the central controller are of size (3m+2). For a power system with N control areas, vector of state variables, control variables and disturbance term (change in load demand) are given in 3.7, 3.8 and 3.9, respectively.

$$X(t) = [x_1(t), \cdots, x_N(t)]^T, \tag{3.7}$$

$$U(t) = [u_1(t), \cdots, u_N(t)]^T, \tag{3.8}$$

$$\Delta P_D(t) = [\Delta P_{D1}, \cdots, \Delta P_{DN}]^T. \tag{3.9}$$

Based on 3.7 to 3.9, the dynamic equations of LFC can be written in standard state space form as 3.10.

$$\dot{X}(t) = AX(t) + BU(t) + F\Delta P_D(t), \tag{3.10}$$

where,

$$A_{ii} = \begin{bmatrix} \frac{-1}{T_{Pi}} & \frac{K_{Pi}}{T_{Pi}},\cdots,\frac{K_{Pi}}{T_{Pi}} & 0,\cdots,0 & 0,\cdots,0 & \frac{-K_{Pi}}{T_{Pi}}\sum_{j=1,j\neq i}^{N}T_{ij} \\[2em] 0 & 0,\cdots,\frac{-1}{T_{Tki}},\cdots,0 \quad 0,\cdots,\frac{-1}{T_{Tki}},\cdots,0 & 0,\cdots,0 & 0 \\[2em] \frac{-1}{R_{ki}T_{Gki}} & 0,\cdots,0 & 0,\cdots,\frac{-1}{T_{Gki}},\cdots,0 \quad 0,\cdots,\frac{-1}{T_{Gki}},\cdots,0 & 0 \\[2em] \alpha_{ki}K_{Bi} & 0,\cdots,0 & 0,\cdots,0 & 0,\cdots,0 & \alpha_{ki}\sum_{j=1,j\neq i}^{N}T_{ij} \\[2em] 2\pi & 0,\cdots,0 & 0,\cdots,0 & 0,\cdots,0 & 0 \end{bmatrix}$$

Figure 3.2: Diagonal entries of matrix A

$$A = \begin{bmatrix} A_{11} & A_{12} & \cdots & A_{1N} \\ A_{21} & A_{22} & \cdots & A_{2N} \\ A_{31} & \vdots & \vdots & \vdots \\ A_{N1} & A_{N2} & \cdots & A_{NN} \end{bmatrix},$$

The diagonal entriess of A are shown in 3.2.

$$B = diag[B_1, B_2, \cdots, B_N],$$

$$B_i = [0, \underbrace{0, \cdots, 0}_{m_i}, \frac{1}{T_{G1i}}, \cdots, \frac{1}{T_{G1m}}, \underbrace{0, \cdots, 0}_{m_i}, 0]^T,$$

$$F = diag[F_1, F_2, \cdots, F_N],$$

$$F_i = [-\frac{K_{Pi}}{T_{Pi}}, \underbrace{0, \cdots, 0}_{m_i}, \underbrace{0, \cdots, 0}_{m_i}, \underbrace{0, \cdots, 0}_{m_i}, 0]^T.$$

We adopt a discrete-time approach and take sample-hold effects into account. The discrete-time expression of 3.10 can be written as 3.11

$$X(k+1) = A_d X(k) + B_d U(k) + F_d(k), \tag{3.11}$$

where, $A_d = e^{AT_s}, B_d = \int_0^{T_s} e^{A\tau} d\tau B,$
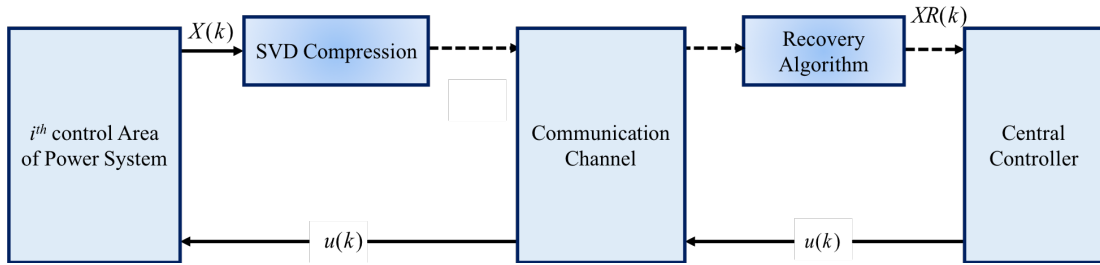
Figure 3.3: SVD based communication between power system and central controller

$$F_d(k) = \int_0^{T_s} e^{A\tau} F \Delta P_D((k+1)T_s - \tau) d\tau.$$

If the sampling time,T_s, for conversion from continuous to discrete-time is significantly small and mismatch disturbance is constant during one sampling period, 3.11 can be further simplified as 3.12

$$X(k+1) = (I + T_s A)X(k) + T_s BU(k) + T_s F \Delta P_D(k). \qquad (3.12)$$

3.2.2   Proposed Algorithm

There exists a large number of controllable generation units in each control area. As per 3.11, huge number of data needs to be transmitted towards the control center through an unreliable communication network for a multi-area power system as shown in Fig.3.3. Conventional methods will require a communication network with large bandwidth and high reliability to enable the real-time operation of power system, which is highly expensive for implementation [85, 86]. However, owing to the interconnectivity of devices in power grid, this data naturally exhibits spatio-temporal correlation. Thus, it can be efficiently compressed using

SVD and then reconstructed by exploiting the joint spatial-temporal correlation among the measured data.

As working of SVD is explained is explained in 2.5.3, $X(k)$, given in 3.5 is the original data received from the PMUs installed in the system. This data is compressed using SVD before sending it through the communication channel. At the receiving end, it will be recovered using the approach described in 2.5.3.1. Finally, recovered data is sent to the central controller that decides the control input for LFC of the system.

In Load Frequency Control, the number of state variables needs to be transmitted from an area are given in 3.5 and that are of size $(3m + 2)$. For simplicity, lets assume $3m + 2 = p$. These measurements are monitored for a data window of q. Thus, the data that is transmitted from local area without compression is of the size of $p \times q$. The size of measurements that are transmitted with compression using SVD are explained in Chapter 2 in the form of 2.15 and its size is $(p+q+1) \times r$ where, $r(r \ll p, q)$ is the singular values retained after compression.

Data window of each PMU contains q sets of data for q time steps, but not all data need to be transmitted at each step. Initially, the data window is initiated with $q-1$ sets of data for the initial $q-1$ time steps to form matrix X. With the next data set coming in, the earliest data set will be pushed out of the matrix X. In other words, earliest received q data sets will be stored in matrix X. When $(q + 1)^{th}$ set of data coming in, the earliest set will be pushed out. As given in Fig.3.3, following steps are involved while implementing the proposed algorithm.

1. As shown in 2.10, data matrix X is formed.

2. SVD is performed to obtain U, Σ' and V.

Table 3.1: Convergence time comparison between SVD and CS

SVD		CS	
CR	Time(s)	CR	Time(s)
1:1	0.84	1:1	0.95
2:1	0.81	2:1	0.80
3:1	0.75	3:1	0.70
4:1	0.70	4:1	–
5:1	0.61	5:1	–
6:1	0.56	6:1	–
7:1	0.50	7:1	–

3. According to 2.16, r is chosen to achieve a given CR.

4. Submatrices $\Sigma_{11}'^{(r\times r)}$; $U_{11}^{(r\times r)}$; $U_{12}^{((p-r)\times r))}$; $V_{11}^{(r\times r)}$; and $V_{12}^{(r\times(q-r))}$ are formed.

5. Reconstruct matrix X by computing XR according to (2.14).

6. The loss of information is evaluated by computing MAE and MPE using 2.17 and 2.18, respectively.

Before sending the compressed data through the communication network, it is possible to check if the loss of information is acceptable. If it is not acceptable, data compression should be performed again by increasing the value of r. This will reduce the loss of information but with the cost of making data compression less effective. Once a trade-off between CR and loss of information is achieved, the data can be transmitted.

3.3 Experiment Settings

To evaluate the proposed method , a power system of three-control areas is chosen, where the average values of parameters for three areas A_i, B_i are directly taken

Table 3.2: Comparison of error between CS and SVD

SVD			CS		
CR	MAE	MPE(100%)	CR	MAE	MPE(100%)
1:1	0.00	0.00	1:1	0.00	0.00
2:1	0.001	0.251	2:1	0.001	0.8
3:1	0.003	0.406	3:1	0.002	0.95
4:1	0.004	0.479	4:1	−	−
5:1	0.004	0.532	5:1	−	−
6:1	0.007	0.710	6:1	−	−
7:1	0.009	1.004	7:1	−	−

from [87]. Model parameters for F_i are also given in the same paper. Values for time constants and gains as given in [87] are used to calculated the plant parameters.

To test the proposed SVD based Load Frequency control strategy on given three-area interconnected power system with six generators in each control area, MATLAB on MacBook pro of 3.1 GHz Intel Core $i5$ and memory of 8 GB is utilized.

3.4 Results and Discussion

Convergence of control variable of three areas is shown in Fig 3.4 which shows that the control variable changes to minimize the frequency deviation in each area, finally converging to zero. It means that control variable reaches to zero and no further action is required to stabilize the frequency. Frequency deviation using our proposed algorithm reaches to zero as shown in 3.5. Two lines of frequency deviation are shown using CS based LFC and SVD based LFC. It can be observed that SVD based LFC has faster convergence than CS based LFC. Time taken by SVD is 0.5s whereas taken by CS based LFC is 0.6s approximately.

To compare the speed of convergence, both algorithms are tested with the same
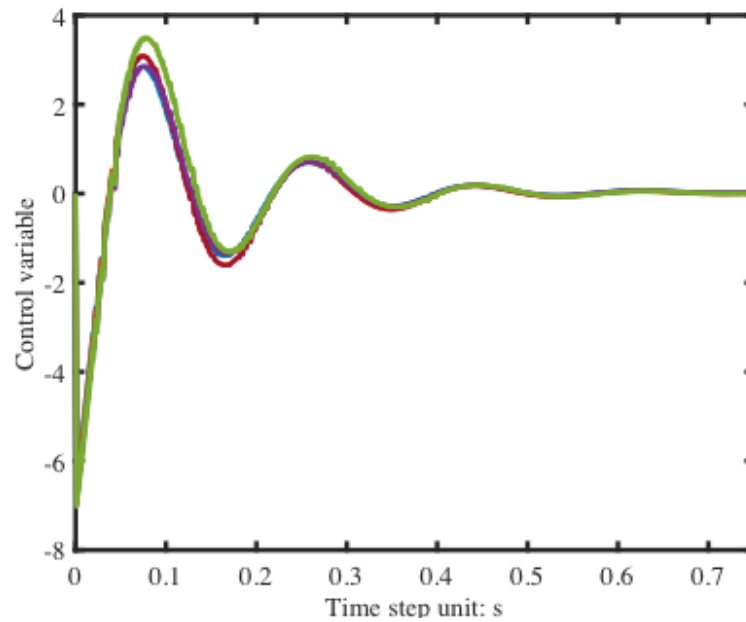
Figure 3.4: Control variable of three areas

three-area power system and results are tabulated in Table 3.1. It is observed that SVD based algorithm converges faster than the CS based LFC algorithm. Also the achievable compression ratio is higher for SVD based LFC which can compress seven times of the original data. However, it increases the error between original data and the reconstructed data as shown in 3.2. Mean Average Error for CR of 3:1 is more for SVD based algorithm than that of CS based LFC. Thus, there should be some trade off between the compression ratio and error in the reconstructed data. Compression ratio should be decreased if error is more than the permitted error and should be checked before adopting the final CR.

It should be noted that power system state measurements may sometimes be noisy. If noisy signal is sent to the central controller, it may have error in the control input. So, to send a noiseless signal to the secondary controller, an effective filter should be designed in LFC application. Also, any fault or disturbance in local systems should be identified locally before sending it to the central con-
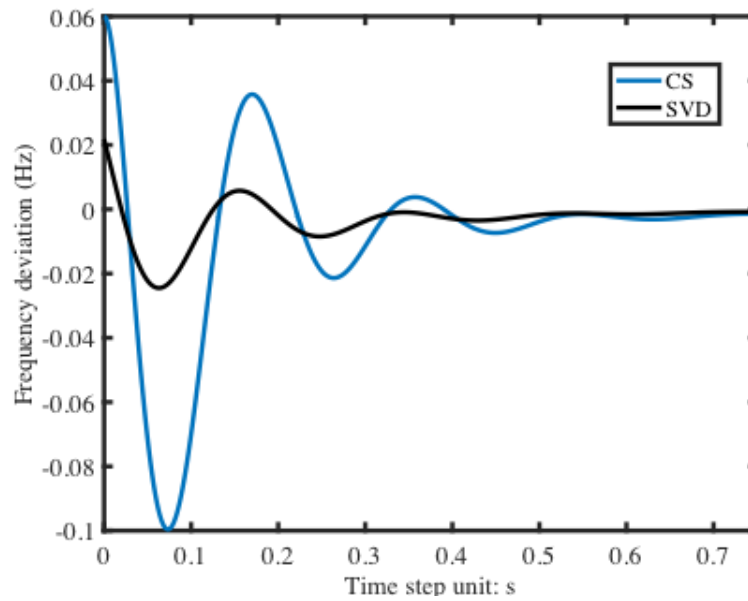
Figure 3.5: Frequency deviation of the power system

troller. Reason for identifying it locally is that it may slow down the protection system if information is first sent to the central controller and then control signal is fed back to local systems all the way from the central controller.

However, filtering technique and fault identification scheme are not designed for LFC application because the number of signals being sent to the central controller in LFC are of diverse characteristics, each having different bandwidth and nature, a single unique filter of specific bandwidth and parameters, will not be able to reduce noise from all incoming signals. Hence, the design of filter and fault identification scheme is unique for each signal type. Implementation of such a scheme with filters local to each signal will increase system cost to a huge extent which is why it may not be techno-economically feasible to implement these schemes in LFC.

3.5   Summary and Contributions

In the real-time centralized load frequency control application, a large amount of data need to be shared with the control center via a timely and accurate data transmission scheme. However, due to the continuous rapid expansion of smart grid, the amount of data is so massive that it poses challenge to an effective transmission of real-time data.

This chapter proposes a methodology for data compression of real-time centralized load frequency control of a three-area interconnected power system using the SVD technique. The proposed methodology can help the existing communication network to cope with the challenge of transmitting an enormous volume of real-time data. The proposed algorithm is tested on a three-area power system to verify the effectiveness of the proposed algorithm. The obtained results show that a significant reduction in the volume of data can be achieved.

Chapter 4

Compressive Sensing and Mathematical Morphology Singular Entropy Based Real-Time Voltage Control: The Secondary Control

This chapter presents an improved secondary voltage control (SVCON) methodology incorporating compressive sensing (CS) for a multi-area power system. SVCON minimizes the voltage deviation of the load buses while CS deals with the problem of the limited bandwidth capacity of the communication channel by reducing the size of massive data output from phasor measurement unit (PMU) based monitoring system. The proposed strategy further incorporates the application of a Morphological Median Filter (MMF) to reduce the noise from the

output of the PMUs.

To keep the control area secure and protected locally, Mathematical Singular Entropy (MSE) based fault identification approach is utilized for fast discovery of faults in the control area. Simulation results with 27-bus and 486-bus power systems show that CS can reduce the data size up to 1/10th while the MSE based fault identification technique can accurately distinguish between fault and steady state conditions.

The prime control objective of the proposed control strategy is to improve the voltage profile of load buses in a multi-area power system which is achieved by using secondary voltage control. In addition to it, the communication burden of the power system data transmission is decreased using CS. Another advantage of the proposed control scheme is to detect abnormal loading conditions/faults locally with the help of MSE. The main contributions of this chapter are a unified method that jointly addresses these problems.

- Real-time SVCON is proposed to minimize the worst-case voltage deviation of the control area by adopting an infinite norm minimization problem.

- CS is used to encode and decode the real-time power system data to deal with the issues of data congestion and limited bandwidth.

- To deal with the noise in the signals, MMF is proposed to reduce the noise in the PMU output.

- MSE based fault identification approach is employed for the fast identification of disturbances in the control area.

This chapter is structured as follows. Section 4.1 presents the related work and

motivation for this chapter. Section 4.2 talks about the Secondary Voltage Control (SVCON), its formulation and proposed method of SVCON. Section 4.3 presents the implementation of CS and MSE based SVCON algorithm. Section 4.4 details the simulation settings used to test the proposed algorithm followed by Section 4.5 presenting the detailed results and their discussions. Finally, Section 4.6 concludes the chapter with summary of the important findings.

4.1 Motivation and Related Work

Nowadays, distributed generation (DG) is increasing in the power system due to the environmental and economical motivation. The integration of massive DGs introduces intermittency, which makes the power system architecture susceptible to disturbances. These disturbances may cause severe voltage deviations or even voltage collapse in the power system. Therefore, adequate voltage control is very important to avoid voltage abnormalities in power systems.

The hierarchical voltage control adopted in various countries can be considered as a solution to the problem of voltage collapse and instability [88]. Hierarchical voltage control usually consists of three control levels: primary, secondary and tertiary. The primary control is a local control and its main role is to automatically maintain the generator bus voltages close to their reference values by acting on generator exciters. However, primary voltage control is not always sufficient to cope with voltage violations associated with load changes[20]. When the load increases, the primary control technique keeps the generator bus voltage close to its reference value. However, this control does not ensure the voltage regulation of all the load buses in the network.

To maintain the load bus voltage within the permissible limits, Secondary Voltage Control (SVCON) is utilized in [89], which is a feedback control strategy to minimize the voltage deviation of load buses. SVCON was first established in Europe and since then many researchers have utilized it in several countries like Brazil [90], Canada [91] and China [92]. For the implementation of SVCON, the power system network is divided into several distinct zones where the voltage of each zone is controlled through automatic adjustment of voltage regulating units. The size of the adjustments is determined by the difference between the current load bus voltage and the predefined reference value of the bus. Thus, for the reliable functioning of SVCON, all the load buses need to be monitored all the time. However, due to high cost, not all buses are equipped with PMUs for complete monitoring. The load buses which are equipped with PMUs, are called pilot buses while the rest are known as non-pilot buses [93].

Several SVCON approaches have been proposed in the recent literature. Gu et al. [94] designed a non-linear state estimator based decentralized SVCON scheme for voltage regulation which incorporates the effects of communication latency, whereas Wang et al. [95] designed a coordinated SVCON strategy through a fuzzy logic scheme. As the number of pilot buses are usually less than the total number of load buses in a control area, the SVC problem can be mathematically viewed as an under-determined problem. Several methods exist in the literature to solve the under-determined SVCON problem. Infinite norm regularization technique is used to minimize the worst-case voltage deviation [96]. Similarly, Chebyshev norm is utilized to design an optimal control strategy to minimize the worst-case voltage deviation.

The real-time monitoring of load buses is usually accomplished using PMUs.

Recent literature cites the usage of PMUs in power system applications [97, 98]. They are capable of providing fast and synchronized measurements and have the capability to overcome the interference from external conditions. The PMU measurements, however, may suffer from different issues related to cyber physical attacks, sensor failures and data congestion. The centralized SVCON requires transmission of massive amount of data between the local control area and the central controller, which may cause data congestion. Data congestion may be significant, especially when the control area is large and the available bandwidth of the communication channel is limited.

Bandwidth requirement is evaluated by [39], which states that a bandwidth of 5 - 10 Mbps and 25 - 75 Mbps is required for applications within one control area and for inter control center communications, respectively. It may further be aggravated when data from several control zones is being concentrated at the Phasor Data Concentrator, before transmitting to the central controller. Thus, a data size reduction technique should be proposed to deal with these issues. Reduction or compression of data may also minimize the communication delay, the power loss on the communication channel, and communication channel cost.

CS is regarded as a promising joint data acquisition and reconstruction method to deal with the problem of limited bandwidth and data congestion. The data retrieved from the PMUs can be compressed before sending through the communication channel and can be recovered at the end of communication channel. Plenty of research has been performed to recover the signal at the end of communication channel [80, 99]. A CS based control strategy is developed for load frequency control in a multi-area power system network [81]. This strategy helps reduce the transmission data loss and increase the reliability of the communica-

tion network.

Performance of CS may be affected by the noise in the signal, which may induce error in the signal processing and degrade the systems dynamic performance [100]. In order to deal with such problems, several noise filtering techniques have been developed in the recent literature [101, 102]. Based on the theory of Mathematical Morphology (MM) , a mathematical morphological filter (MMF) is proposed in [103], which helps smooth sharp edges, narrow valleys and gaps in a contour. The MMF filter has been found to be effective in the removal of signal noise in power systems applications.

Apart from noise in the signals, abrupt load changes/faults in the power system may lead to significant deterioration of the terminal voltage. There has always been a need to design a fault identification technique that can observe changes in the signal waveforms locally and can activate the control action.

Recent literature in fault identification suggests MM based [59] and Morphology Singular Entropy (MSE) based [104] fault identification techniques. For rapid identification of disturbance, the signal should be analyzed before being sent to communication channels. Thus, a MSE-based fault identification technique is proposed which can detect the abnormality in the signal waveform accurately.

The prime control objective of the proposed control strategy is to improve the voltage profile of load buses in a multi-area power system which is achieved by using secondary voltage control. In addition to it, the communication burden of power system data transmission is decreased using CS. Another advantage of the proposed control scheme is to detect abnormal loading conditions/faults locally with the help of MSE.

4.2   Secondary Voltage Control

In the power system hierarchical control, secondary voltage control deals with the regulation of load bus voltages only. The primary control/ local control deals with the voltage regulation of source buses. As load buses have no sources connected on them, so primary control cannot regulate their states and thus, secondary control comes into operation and regulates the load buses. Thats why, this chapter considers regulating the voltage of load buses in the proposed algorithm of secondary voltage control.

SVCON minimizes the load bus voltage deviations within power systems. Voltage deviation is calculated by the difference between the measured bus voltage and its predefined reference value as 4.1:

$$\Delta|V_L| = |V_L| - |V_L{}^*|, \tag{4.1}$$

where V_L is the load bus measured voltage and $V_L{}^*$ is its predefined reference voltage. V_L is usually measured with the help of PMUs, attached on the selected buses as shown in Fig.4.1, which explains the working diagram of SVCON in a power system network. In a control area of power system, there are load buses, capacitor buses and generator buses. Any change in load on load bus or on capacitor bus will affect the voltage of the respective buses. Thus, monitoring of state variables $x = [V_L, Q_L]$ should always be performed and sent to SVCON unit to regulate them. SVCON unit, in turn changes the control input vector $u = [\Delta V_G, \Delta Q_G]$ to regulate the state measurements vector.
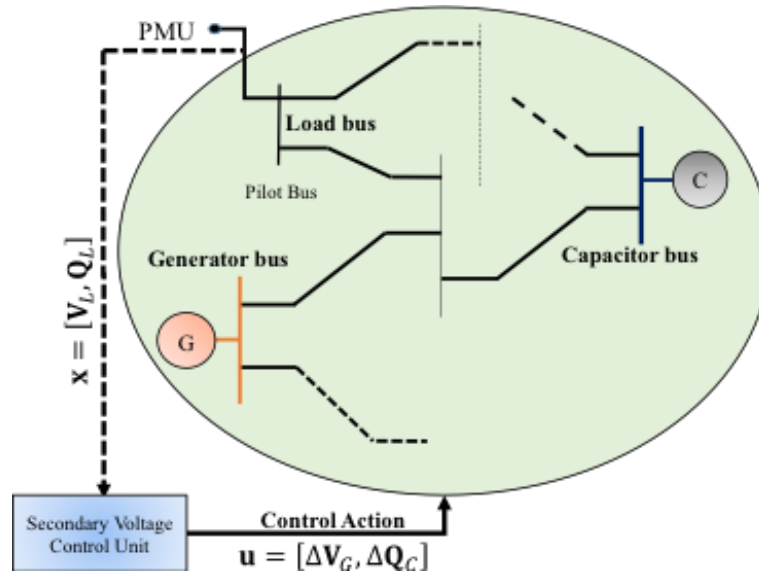
Figure 4.1: Overview of the Secondary Voltage Control

4.2.1 Problem Formulation

In the centralized control of SVCON, the transmission of massive data incurs delays in data arrival at the receiving station. To deal with this problem in SVCON, CS can be used to decrease the data size and hence decrease the communication delays in the data transfers. In CS based SVCON, problem occurs when a fault or abnormal loading condition happens in power system. We propose to minimize the worst-case scenario of the voltage deviation. As CS works on the assumption that temporal and spatial correlation exits in the power system data but in case of faults, this correlation may not exist. To deal with this problem, faults should be identified locally and alarm/protection devices should be activated to avoid any abnormal condition.

MSE has been used to address this problem in CS based SVCON. Thus, the proposed control algorithm examines the voltage deviation of each bus in the control area and identifies the bus with the worst voltage deviation. The SV-

CON algorithm generates the control output based on the maximum load bus voltage deviation and hence, it is performed by formulating it as an infinite norm minimization problem as 4.2.

$$\underset{u}{\text{minimize}} ||\Delta|V_L|||_\infty, \tag{4.2}$$

where $\mathbf{u}$ is the control output of the SVCON algorithm which includes the voltage regulating variables e.g. reactive power generation change from capacitor banks and voltage change of the voltage controlled buses etc. Solving the infinite norm minimization problem, generates the optimal $\mathbf{u}$ for which the maximum deviation is minimum.

The equality constraint of the SVCON problem is given by power balance equations of the control area. Power balance equations are non-linear functions of the bus voltages (V), active power (P) injection and reactive power (Q) injection of the buses as given in 4.3. Non-linear equality constraints governing power flow in the control area of the power network have been described in detail in [96].

$$f(\mathbf{V}, \mathbf{u}, \mathbf{P}, \mathbf{Q}) = 0. \tag{4.3}$$

The inequality constraints of the optimization problem are governed by the upper and lower bounds of the control variable $\mathbf{u}$. If the upper and lower bounds be denoted by $\overline{\mathbf{u}}$ and $\underline{\mathbf{u}}$ respectively, then the constraints are given by 4.4 .

$$\underline{\mathbf{u}} \leq \mathbf{u} \leq \overline{\mathbf{u}}. \tag{4.4}$$

4.2.2   Proposed SVCON Approach

DC power flow approximation has been recognized as valid approximation within real power P and phase angle [105]. At the same time, DC approximation for reactive power and voltage magnitude V has also been explored by many recent researchers [96, 106] and is considered to be a reasonable approximation for fast analysis of power system. The nonlinear equality constraint can be linearized using linearized model of decoupled power flow equations where real power changes are assumed to be less sensitive to changes in the voltage magnitude. Thus, the approximate model of the small disturbance voltage-VAR control can be represented by a linear relation between the reactive power and the voltages of the generator, capacitor and load buses as given in 4.5 [96, 97].

$$
\begin{bmatrix} \Delta Q_G \\ \Delta Q_C \\ \Delta Q_L \end{bmatrix} = \begin{bmatrix} B_{GG} & B_{GC} & B_{GL} \\ B_{CG} & B_{CC} & B_{CL} \\ B_{LG} & B_{LC} & B_{LL} \end{bmatrix} \begin{bmatrix} \Delta|V_G| \\ \Delta|V_C| \\ \Delta|V_L| \end{bmatrix},
\tag{4.5}
$$

where, B represents the system susceptance matrix, subscript L represents the load bus, subscript G represents the generator bus which can be used as voltage-controlled bus when $\Delta|V_G|$ is considered as control variable. Subscript C represents the capacitor bank, which can also be used as voltage-controlled bus when ΔQ_C represents the control variable.

From 4.5, the components $\Delta|V_C|$ and $\Delta|V_L|$ can expressed in 4.6 and 4.7 respectively.

$$
\Delta|V_C| = B_{CC}^{-1}\Delta Q_C - B_{CC}^{-1}B_{CG}\Delta|V_G| - B_{CC}^{-1}B_{CL}\Delta|V_L|,
\tag{4.6}
$$

$$\Delta|V_L| = B_{LL}^{-1}\Delta Q_L - B_{LL}^{-1}B_{LG}\Delta|V_G| - B_{LL}^{-1}B_{LC}. \tag{4.7}$$

Substitute the term of $\Delta|V_C|$ from 4.6 into 4.7 yields as 4.8,

$$\Delta|V_L| = B_{LL}^{-1}\Delta Q_L - B_{LL}^{-1}B_{LG}\Delta|V_G| - B_{LL}^{-1}B_{LC}\times$$
$$[B_{CC}^{-1}\Delta Q_C - B_{CC}^{-1}B_{CG}\Delta|V_G| - B_{CC}^{-1}B_{CL}\Delta|V_L|]. \tag{4.8}$$

From 4.8, it is evident that, the load bus voltage change $\Delta|V_L|$ can be expressed as a function of the reactive power load change $(\Delta|Q_L|)$ and the control output (u), as given in 4.9.

$$\Delta|V_L| = J_1\Delta Q_L - J_2 u, \tag{4.9}$$

where

$$J_1 = (B_{LL} - B_{LC}B_{CC}^{-1}B_{CL})^{-1}, \tag{4.10}$$

$$J_2 = J_1[(B_{LG} - B_{LC}B_{CG} \quad B_{LC}B_{CC}^{-1}], \tag{4.11}$$

$$u = [\Delta|V_G| \quad \Delta Q_C]. \tag{4.12}$$

By utilizing DC Decoupled power flow of 4.5, the equality constraint of 4.3 is already incorporated in 4.9. Thus, infinite norm minimization problem of 4.2 can be rewritten as 4.13.

$$\underset{u}{\text{minimize}}||J_1\Delta Q_L - J_2 u||_\infty \quad \text{subject to} \quad \underline{\mathbf{u}} \le \mathbf{u} \le \overline{\mathbf{u}}. \tag{4.13}$$

The optimal solution of the 4.13 generates the optimal value of control input $\mathbf{u}$, which consists of the vector of generator bus voltage change and the vector of capacitor bus reactive power generation change. Each reactive power source is limited with a maximum value $\overline{\mathbf{u}}$ and minimum value $\underline{\mathbf{u}}$. If the control input

u exceeds its limits, the proposed algorithm will restrict it within its lower and upper bounds. Monitoring the vector of reactive power load change ΔQ_L, can be achieved by deploying PMUs on load buses. However, currently, all load buses are not equipped with PMUs and hence, it is required to design a method to estimate reactive power load changes on the non-pilot load buses.

4.2.2.1 Only Partial Load Buses are Equipped with PMUs For the case when partial load buses are equipped with PMUs, voltage measurements $\Delta|V_p|$ are available only at the given pilot buses. It means $\Delta|V_p|$ has only some elements of vector $J_1 \Delta Q_L$. Using only the rows of corresponding pilot buses in J_1 and denoting it as J_p, the optimal reactive power load change on all buses ΔQ_L^*, can be estimated by solving the under-determined system of 4.14 [96].

$$\Delta Q_L^* = J_p^T (J_p J_p^T)^{-1} \Delta|V_p|. \tag{4.14}$$

After obtaining ΔQ_L^*, infinite norm minimization problem in 4.13 can be solved for the optimal **u**. Based on the new control input u^{k+1} for every new iteration, $\Delta|V_L^{k+1}|$ is calculated using 4.9, as shown in Fig.4.2. The Pilot bus voltage deviation, $\Delta|V_p^{k+1}|$ can be taken out from the set consisting of the deviation of all the load buses to calculate the pilot bus voltage $|V_p^{k+1}|$ for the next iteration as given in 4.15.

$$|V_p^{k+1}| = |V_p^k| + \beta \Delta|V_p^{k+1}|, \tag{4.15}$$

where, an acceleration parameter β with a value of 0.5, is incorporated in 4.15 to further speed up the update process. The proposed algorithm provides an optimal control output when the predefined value of tolerance ϵ is reached as

4.16.

$$|V_p^{k+1}| - |V_p^k| < \epsilon, \qquad (4.16)$$

where ϵ is the predefined value of tolerance, which is chosen as 0.001 in this chapter. Once the predefined value of tolerance is achieved, the proposed algorithm will stop and produce the optimal u^*.

The performance of the SVCON algorithm can be expressed as the root mean square value of voltage deviations at all load buses given by 4.17

$$x_{rms} = \sqrt{\frac{1}{l} \sum_{i=1}^{l} (|V_L| - |V_L^*|)^2}, \qquad (4.17)$$

where l is the total number of load buses.

4.3 Implementation of CS and MSE based SVCON Algorithm

This section provides information regarding the implementation of proposed algorithm. It outlines the steps taken by the algorithm to achieve the optimal control input incorporating MSE and CS simultaneously.

4.3.1 MSE Implementation

SVCON of the power system is performed by dividing it into several control areas as shown in Fig 4.3. It shows that real time data $x_i(k)$ from each area is first filtered using MMF and checked for any abnormal condition using MSE. In the simulation, pre-recorded data is not used rather the real-time data of
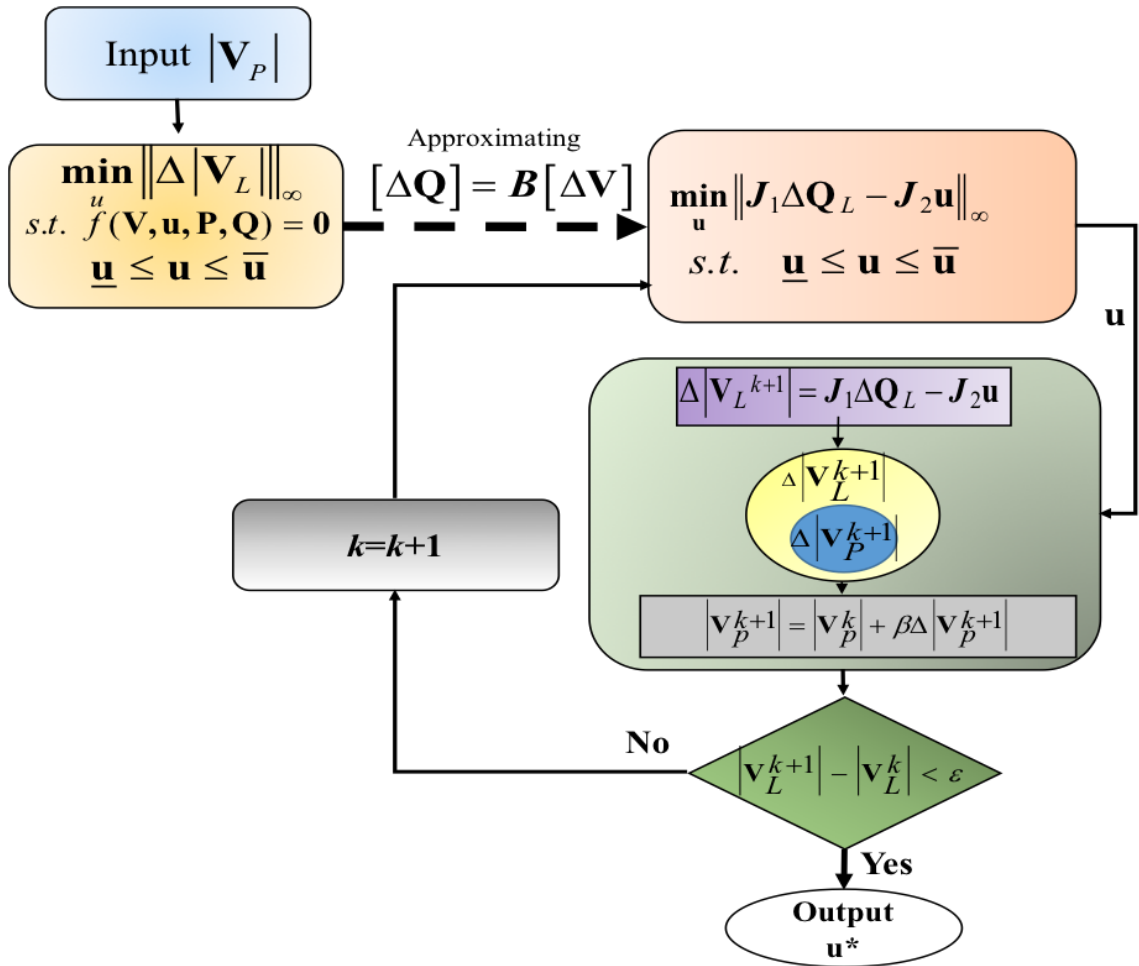
Figure 4.2: Flowchart for SVCON algorithm

$x_i(k) = [V(k) \quad Q(k)]$ is measured at each instance k. Here, real time power system states data from i^{th} control area $x_i(k)$ consist of load bus voltage and load bus reactive power load demand are measured online at each instance. It is assumed that data measuring techniques are ideal and measured data has no uncertainties. These measured states may introduce some random noise due to sensor inefficiency or harmonics present in the power system. To deal with such scenarios, $x_i(k)$ is passed through MMF to eradicate the noise from the signal.

Before sending the system data to the central controller for system state observation and generation of a control output, it is recommended to check the system states locally for any fault or abnormal condition. For fast local control action for faults, MSE is calculated locally and a control signal is sent back to the control area to raise an alarm or initialize the relay when value of entropy exceeds a certain pre-set limit. Following steps are taken to calculate the MSE:

Step 1: Suppose a signal with a data window length of w contains $w \geq 1$ consecutive readings of a signal x at the time step k is given as $x(k) = [x(k - w + 1) \cdots x(k)]$. Now, MMF defined in 2.26 is applied to construct a matrix H from $x(k)$. By choosing a flat SE of different sizes with its origin in the middle, matrix H is given as 4.18

$$\mathbf{H} = \begin{bmatrix} h_1(w - k + 1) & \cdots & h_1(k) \\ \vdots & \ddots & \vdots \\ h_m(w - k + 1) & \cdots & h_m(k) \end{bmatrix}, \qquad (4.18)$$

where $h_i(k)$ is the output of MMF filter at $x(k)$ for different length of SE when length of SE is increased from 1 to m at a step of 1. First row of H is the same as the input data $x(k)$. As the length of SE increases, more details
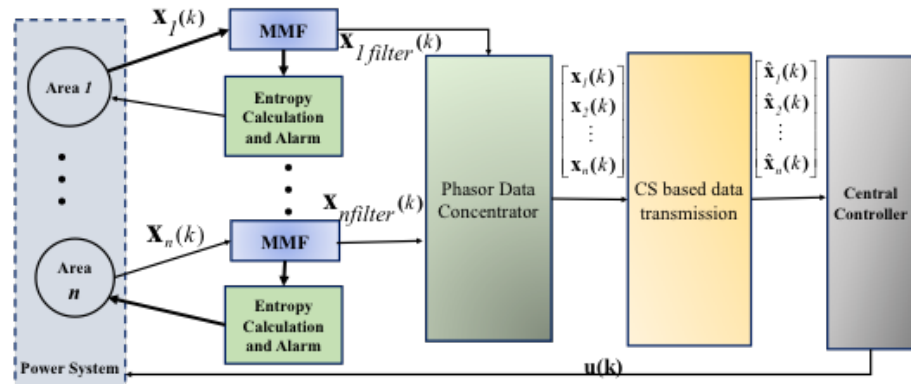
Figure 4.3: Extensive working of the proposes CS and MSE base SVCON algorithm

are eliminated from $x(k)$ [104] which implies that different rows preserve information at different levels.

Step 2: After formation of H, it is decomposed using SVD and only those singular values can be selected which represent the main components of the signal.

Step 3: Assume, m_1 is the number of selected singular values retained in step 2, then the probability p_j associated with σ_j is calculated as 4.19

$$p_j = \frac{\sigma_j}{\sum_{j=1}^{m_1} \sigma_j}. \tag{4.19}$$

Step 4: Finally, entropy (E) of $x(k)$ can be calculated as per 2.28 .

It can be further explained from 2.28 and 4.19 that E will be zero for a pure sinusoidal input $x(k)$ because in this situation, only first singular value is nonzero with a probability of 1. Any change in the signal will lead to a higher entropy.

4.3.2 CS Implementation

After filtering the data and testing it for any abnormal condition, data from each control area is concatenated at PDC and sent to the central control through communication channel. To reduce the data size, CS is utilized to compress the data and recover it at the end of communication channel. In the application of SVCON, the recovered data is calculated as 2.21 given as 4.20

$$\hat{x}(k) = [\hat{V}(k) \quad \hat{Q}(k)]. \tag{4.20}$$

The data obtained from monitoring the power system inherently contains spatial and temporal correlation. Because of this inherent property, the monitored data can be compressed before transmitting through the communication channel. Likewise, it can be recovered successfully at the end of communication channel using various recovery techniques. In this chapter, the Orthogonal Matching Pursuit (OMP) algorithm is utilized to solve the optimization problem. OMP is a recursive algorithm and provides faster rate of convergence especially in the case of non-orthogonal directories [107].

Finally, the central controller decides the SVCON control action based on the recovered data and sends it back to each control area as explained in Fig.4.3. It is important to note that filter should be placed prior to the fault identification. MMF filter removes the noise from system states by its dilation and erosion operations, after which the signal is sent to the fault identification scheme (MSE). If the signal was directly sent to the MSE scheme without being filtered, the noise present in the signal may raise a false alarm thereby leading to unnecessary tripping of the system. Thus, in order to prevent unnecessary tripping, the fault
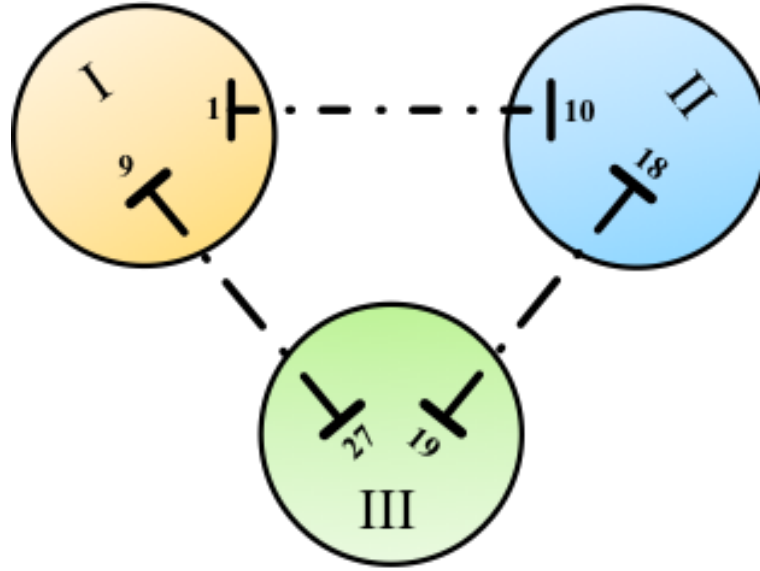
Figure 4.4: 27-bus power system, comprising of three control areas of 9 buses in each control area

identification technique is preceded by an MMF filter.

4.4 Simulation Settings

The proposed algorithm is tested on two multi-areas power system: 27-bus power system and 846-power system. Both power systems are further divided into three sub-areas. 27-bus power system comprises of 9 buses in each area while 846 bus system has 162 buses in each areas. 27-bus power system has been shown in Fig 4.4. It is built by connecting 3 control areas with modified IEEE 9- bus system [108] in each area. The impedances for all the tie-lines are set to 0.02+j0.07 p.u. In each area, bus no. 7, 8 and 9 are selected as load buses.

In this case, all the load buses are assumed to have PMU on them for monitoring of voltage deviation. However, system will also be tested for partial buses with PMUs and will be shown in the results section. Bus no. 2 and 3 are equipped

Table 4.1: Event sequences of load changes on 9-Bus Control Area

Time stamp	Event No.	Bus No	Load Type	Load Change
21s	Event1	7,8,9	Reactive Load	1.03× Initial
42s	Event2	7,8,9	Reactive Load	0.97× Event1

with capacitor banks while 4, 5 and 6 are voltage controlled buses, which can change their bus voltage to improve the voltage profile of the load buses.

Similar to 27-Bus system, 486-bus power system is built by connecting 3 areas with 162-buses in each area as shown in Fig. 4.5. Parameters of the 162-bus system can be found in [108], where each control area contains 32 generators and 50 capacitor banks to regulate the voltage of load buses. The impedances for all the tie-lines are set to 0.028+j0.096 p.u.

To test the given multi-areas power system, they are first modeled in PSCAD and various load changing condition and faults conditions are applied in PSCAD. Real-time data is saved from PSCAD and used in MATLAB to test our proposed algorithm. MATLAB is implemented in (13-inch, 2017, Four Thunderbolt 3 Ports) with processor 3.1 GHz Intel Core i5 and internal memory of 8 GB 2133 MHz LPDDR3.

4.4.1 Load Changing Conditions

To test the proposed algorithm in real-time conditions, a series of load changing events are introduced on various buses as given in Table.4.1. At 21st second, reactive power load was raised to 1.03 times the initial load. Similarly, at 42nd second, load was reduced to 0.97 times the event1 load.
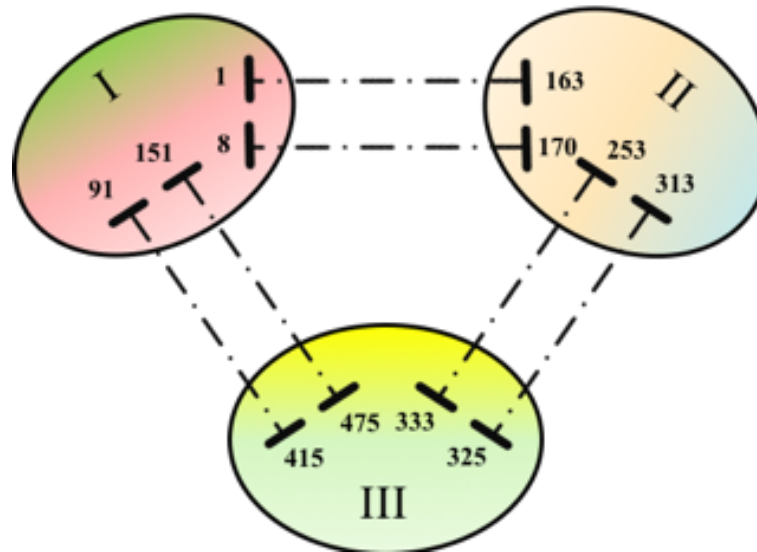
Figure 4.5: 486-bus power system, comprising of three control areas of 162 buses in each control area

4.5   Simulation Results and Discussions

This section shows the simulation results for two power systems: 27-bus power system and 846-power system. It discusses the various observations found in the results

4.5.1   27-Bus Power System

For the results in Figs.4.6 - 4.10, compression ratio of 2 is used. Various values of compression ratios are tested to investigate its effect on the system performance and results are shown in the tabular form in part C of this Section. The voltage profile improvement of the load buses in control area I is shown in Fig.4.6. It shows that SVCON algorithm is very fast in improving the load bus voltage close to the reference value.
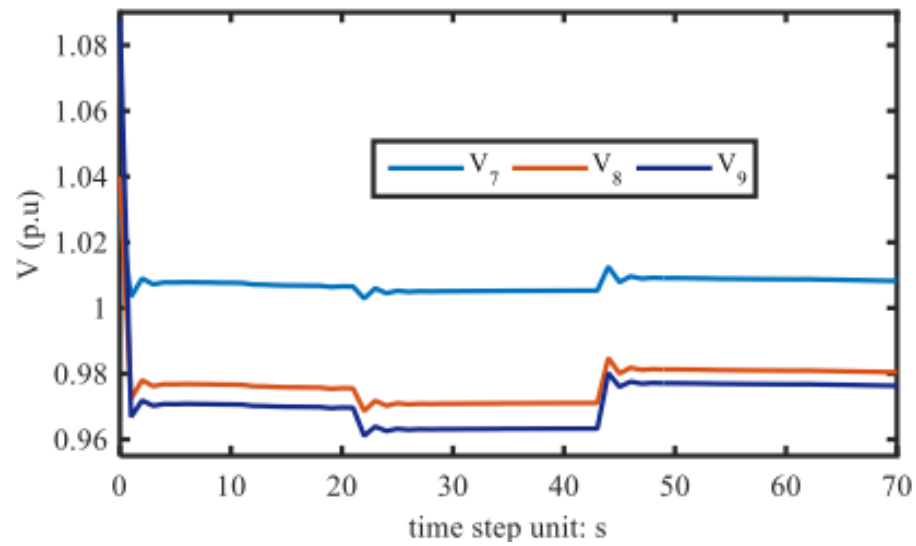
Figure 4.6: Load voltage results of the 27-bus power system
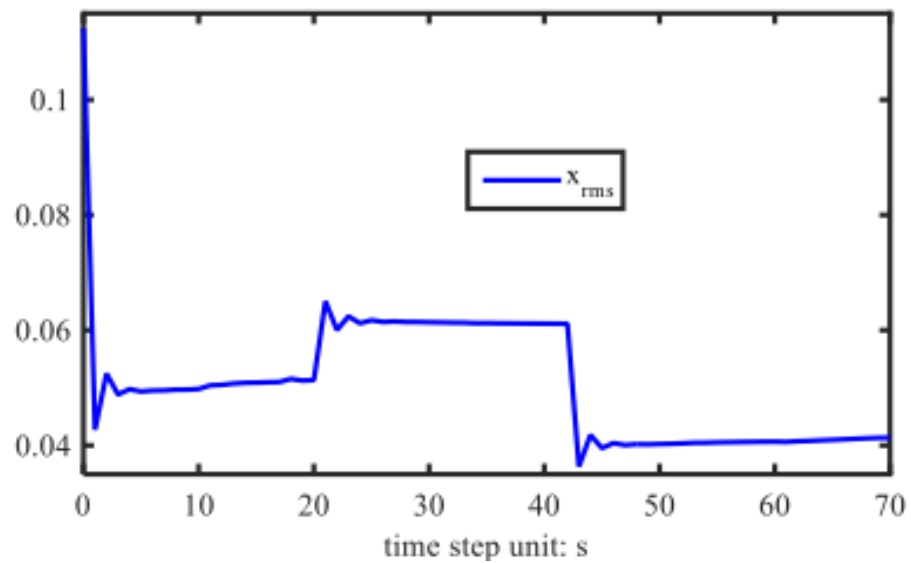
Figure 4.7: X_{rms} value of voltage deviation of the 27-bus power system
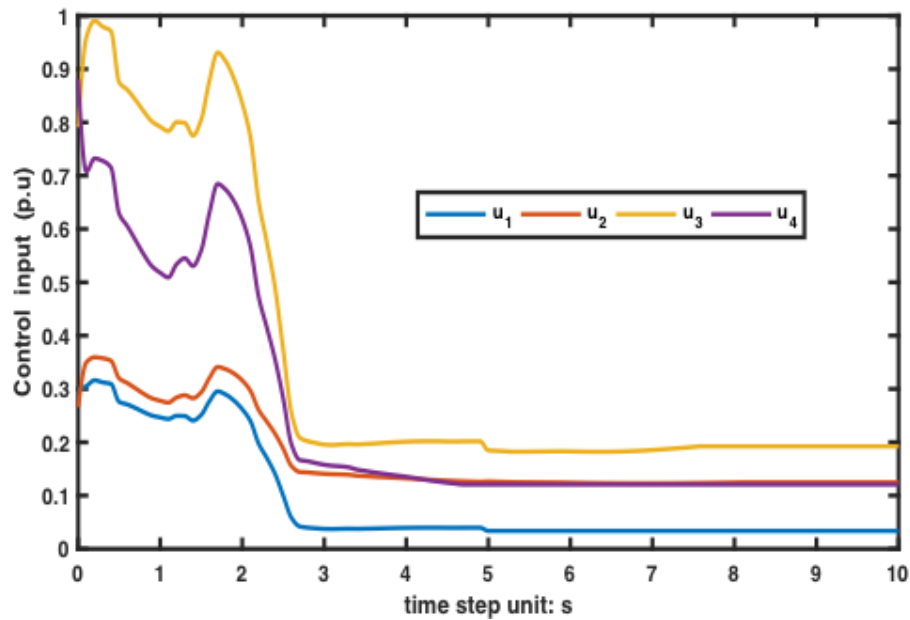
Figure 4.8: Optimal control input for SVCON in control area I

To analyze the behavior of the algorithm in case of changing reactive power loads, load voltages falls down at 21st when the reactive power load is increased by 1.03 times and voltage improves at 42nd when reactive power load decreases by 0.97 times. The response of the proposed control algorithm during instances of load changes substantiates its performance and adaptability.

RMS value of the voltage deviation is calculated using 4.17 and shown in Fig.4.7. It is clear that proposed algorithm minimizes the voltage deviation of the load buses, where overloaded buses have higher voltage deviations. The optimal control input which minimizes the voltage deviation in control area I of the system is shown in Fig.4.8. It clearly exhibits that it converges to its optimal value to regulate the voltage deviation in the system.
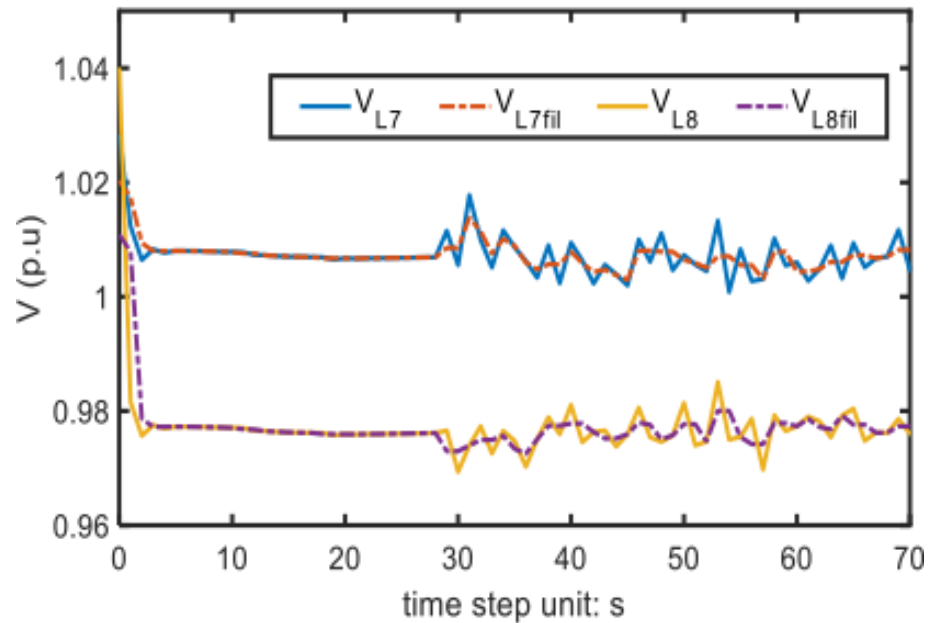
Figure 4.9: Voltage profile with & without MMF

4.5.2 Filtering of power system signals

To test the effectiveness of MMF, white Gaussian noise with zero mean and 40 SNR is introduced in the load bus voltage of bus 8 at 30s as shown in Fig. 4.9. It shows that noise in the voltage signal of bus 8 also introduces small noise in its neighboring buses. Thus, it is important to use the filtered signal for control of the system. From Fig. 4.9, it can be observed that the proposed MMF reduces the noise peaks in the output voltage signal.

To investigate the working of fault identification by calculating its MSE, the MSE of the noisy voltage signals of bus 7-9 is calculated and shown in Fig.4.10. It exhibits that the maximum value of MSE due to noise is for the voltage signal of bus 8 and its value oscillates between 0 and 0.015 nat. This value is far less than 0.05 which is the pre-set value, to send an actuation signal to the protection relay. Thus, in this case the proposed control strategy will assume it as a noise
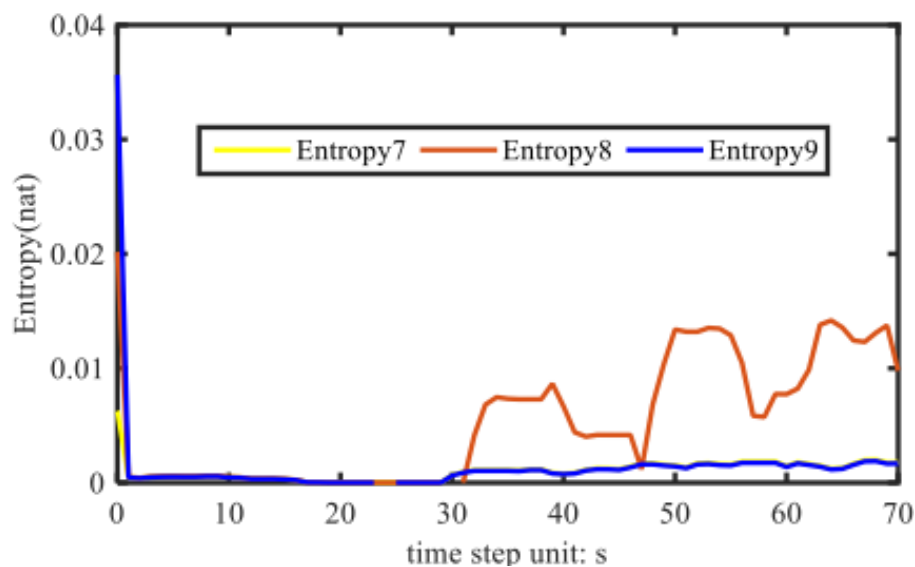
Figure 4.10: Entropy variation of voltage profiles bus 7, bus 8 and bus 9

and will not send a triggering signal to the relay.

To test the working of proposed MSE method for fault identification, reactive power load is increased by 1.75 times on bus 8 at 20th second as shown in Fig.4.11 where X represents the $X - axis$ value of time step in seconds while Y represents the $Y - axis$ value of voltage in p.u. and entropy in nat. Due to this severe overloading condition, V_8 falls to 0.8454 p.u. and the measured entropy rises to 0.08685 nat. This value is higher than the pre-set threshold value of 0.05 and thus an actuation signal will be sent to the protection relay to activate the circuit breakers or raise an alarm.

The proposed SVCON algorithm will work satisfactory as long as at least one load bus is a pilot bus. To find the optimal control input using 4.13, we need to calculate ΔQ_L using 4.14 and ΔQ_L will be undefined if J_p is zero or in other words, no load bus is selected as pilot bus. Thus, at least one of the load bus need to be attached with PMU. For 27-bus power system, authors have performed simulations for different number of pilot buses. Total number of load buses in
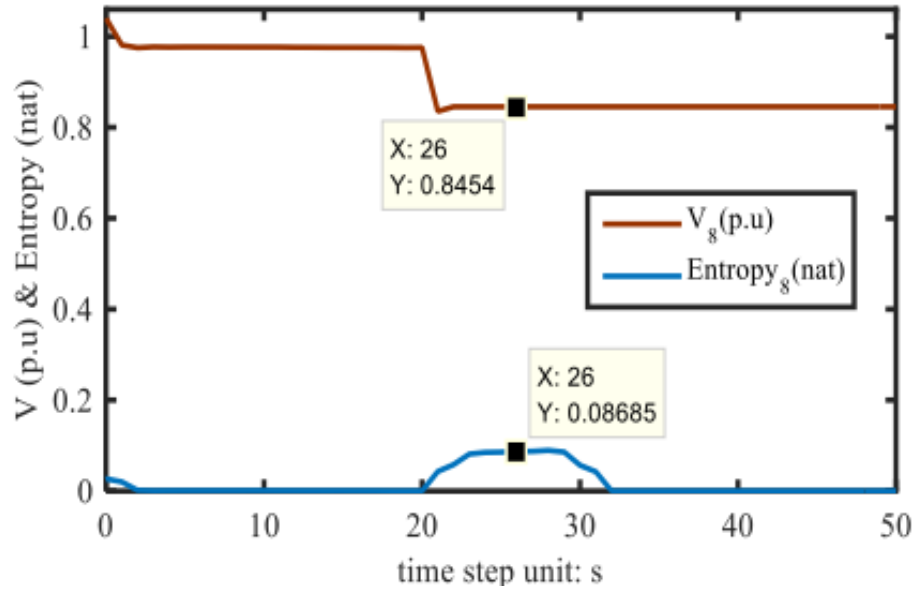
Figure 4.11: Entropy change when V8 falls to 0.85 p.u.

27-bus power system are 9. Authors varied pilot buses from one to nine and calculated the root mean square value of voltage deviation for each case. Fig.4.12 shows how increasing number of pilot buses improves the voltage deviation. Thats why it is always recommended to connect a PMU on each load bus of power system.

4.5.3 486-Bus Power System

To test the proposed algorithm's performance on a large-scale control area, a test case on 486-bus power system is performed and to test the proposed algorithm on the real-time power system, reactive power loads of the control area III are changed to 1.20 times and 0.80 times of the initial loads on all load buses at t=10s and t=20s, respectively.

Voltage profile of the load buses in control area III is shown in Fig.4.13. It exhibits that the voltage profile improves from 1.15 p.u. to a permissible operating voltage
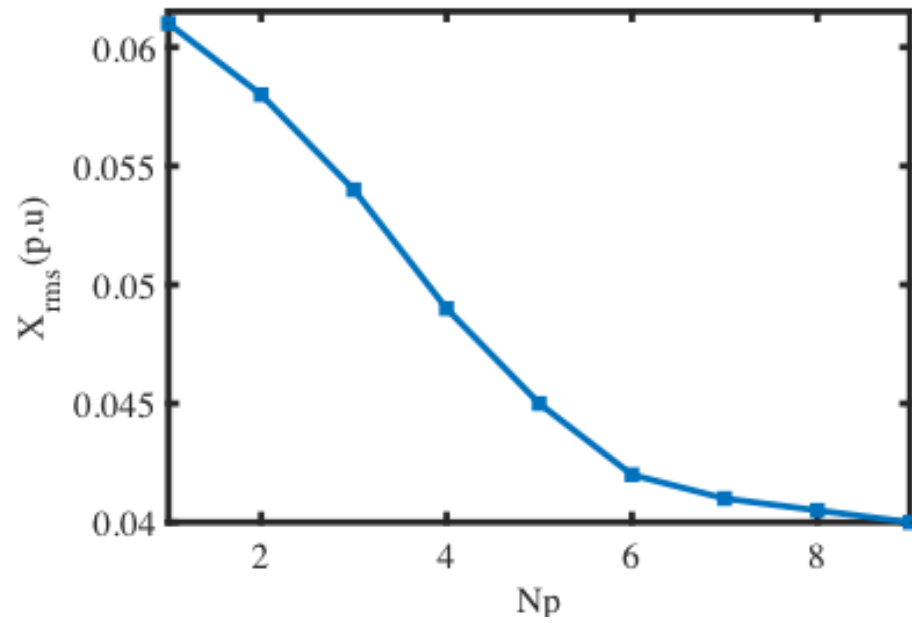
Figure 4.12: Number of pilot buses vs root mean square value of voltage deviation
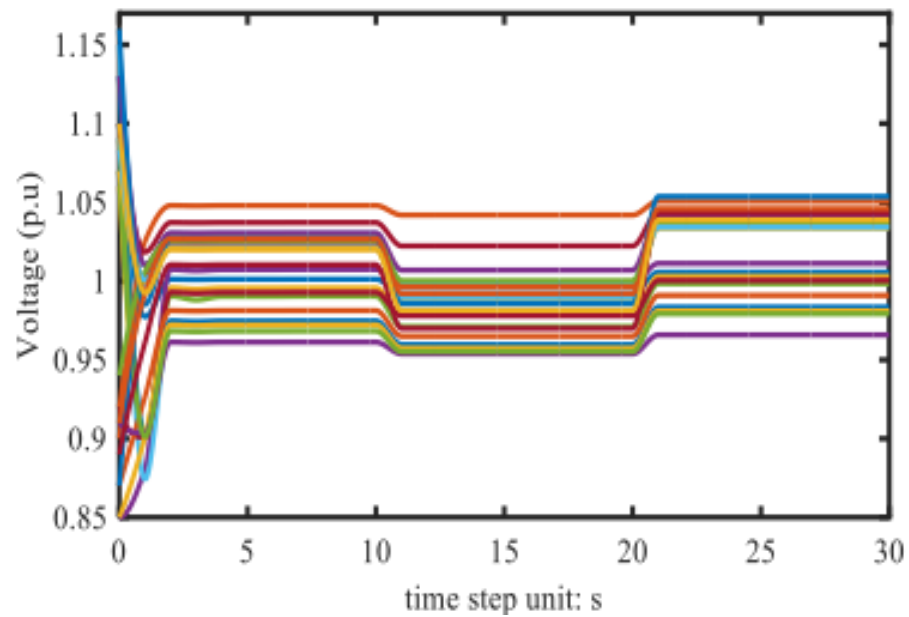
Figure 4.13: Load bus voltage results of the 486-bus system in control area III

range of 0.95 p.u. to 1.05 p.u. As the reactive power load increases at t=10s, voltage profile deteriorates. However, the proposed algorithm still keeps it within the permissible operating range. Similar is the case when reactive power load is dropped at t=20s. RMS value of the voltage deviation of the control area III is shown in Fig.4.14, which shows that load change increases the voltage deviation in the system.

To analyze the effect of CS on the communication delay of data transfer, proposed SVCON algorithm is implemented without using CS. Real time data of the three control areas is transferred through the communication channel simultaneously. The obtained results are then compared with the results obtained by using CS for data reduction as shown in Fig. 4.15. The solid lines show plots without CS and dotted lines show plots with CS. When CS is utilized to compress the power system data, it decreases the communication delays during the data transfer. It is clear that the use of CS relieves the communication congestion and thus, decreases the communication delay during data transfer.

Secondary voltage control is observed to be very fast and can converge to its optimal value within couple of seconds. However, this fast SVCON cannot disturb the primary control in source buses because operating time of secondary is far less than the primary control. Primary control usually operates in micro/ milliseconds whereas the proposed fast secondary control takes few seconds to change the control variable settings.

In real-time scenarios, secondary control is a centralized control that observes states of individual area, concatenates states of multiple areas, compresses them, transmits them through unreliable communication channel, recovers the original states at the end of communication channel and sends to the central controller
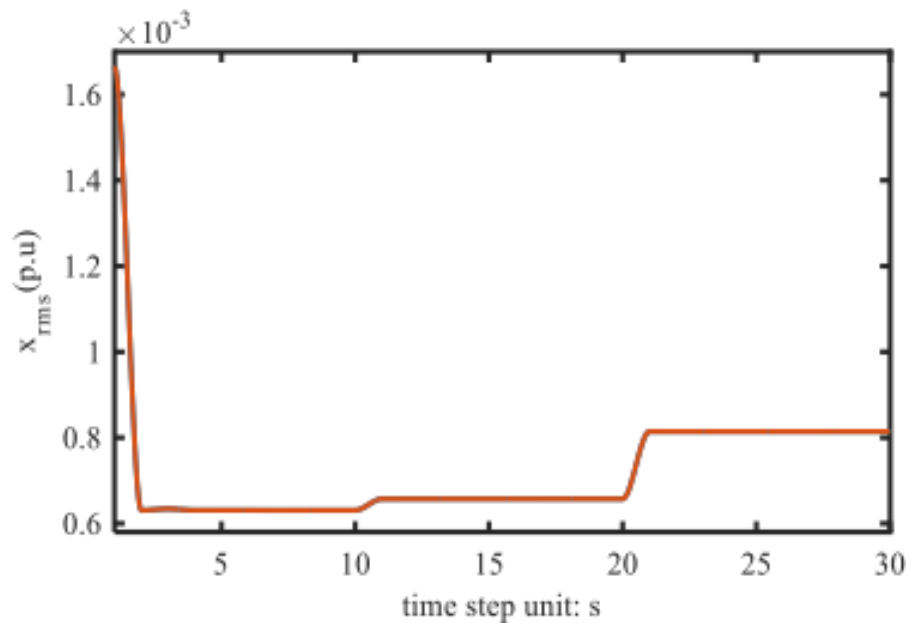
Figure 4.14: RMS of the load bus voltage deviation of the 486-bus system in control area III

that calculates the control variables and sends back to the system through communication channel. These all activities consume time which is much higher than the primary control that is a local control with no communications between local power system and the central controller.

4.5.4 Achieveable Compression Ratio

CS based SVCON algorithm is tested for various compression ratios and its corresponding SNR of the recovered signal. It is observed that as the compression ratio of the CS increases, the quality of recovered signal deteriorates, as shown in Table.4.2. It shows that the maximum compression ratio achieved for 27-bus power system is 6, after which the recovered signal does not produce any useful state information. The maximum compression obtained for 486-bus power system is 10. It implies that as the size of power system increases, the achievable com-
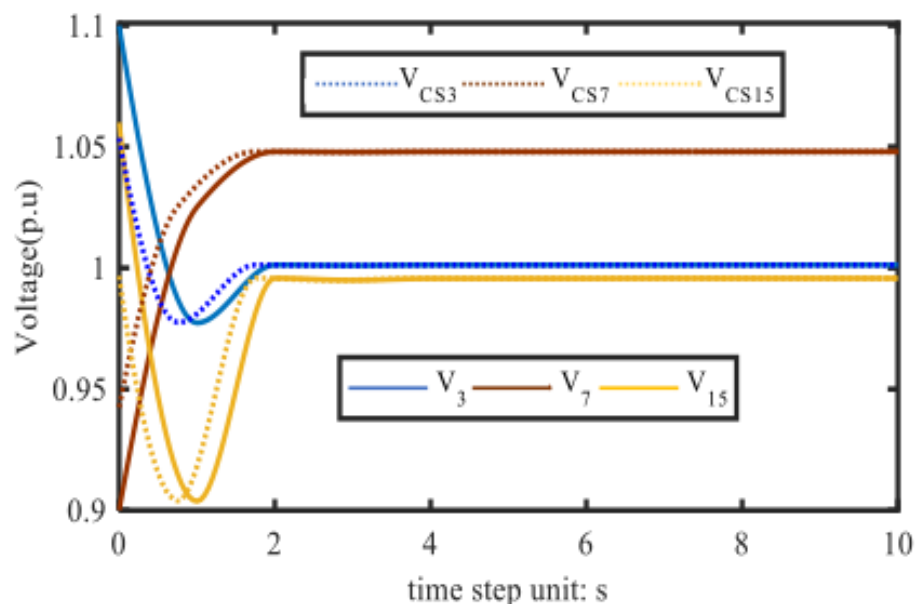
Figure 4.15: Voltage profile comparisons under the communication delay

Table 4.2: Values of achievable compression ratios

27- bus power system		486-bus power system	
Compression Ratios (ρ)	SNR	Compression Ratio (ρ)	SNR
1.5	86.76	2	90.67
3	75.14	4	81.39
4	66.3	6	68.01
5	53.49	8	52.82
6	36.87	10	35.65
7	-	12	-

pression ratio grows. It means use of CS is more effective for large power systems where data size is massive. Thus, the results corroborate that the proposed CS based SVCON algorithm can reduce data congestion significantly.

It is important to understand that in Chapter 4, compressive sensing is utilized for secondary voltage control while in Chapter 3, singular value decomposition is used for load frequency control. There is a reason for using two different schemes for the same purpose of compression. Voltage deviation is a local parameter to each bus of the power system whereas frequency deviation is a system vari-

able. Minimizing voltage deviation will require basis elements which take into account spatial and temporal correlations whereas minimizing frequency deviation demands faster compression techniques. Thus, Load Frequency Control can be better implemented using SVD and secondary voltage control fits into the paradigm of compressive sensing technique.

4.6 Summary and Conclusion

This chapter incorporates a CS based technique to reduce the data size for meeting the bandwidth requirement for real-time secondary voltage control of large power system networks. The obtained results demonstrate that CS decreases the communication delay during the data transmission for large power systems by reducing the data size to a factor of 10.

Further, the MMF is introduced to eradicate the noise present in the states of the power system. Furthermore, MSE based fault identification technique is proposed to clear faults locally in the control area in a fast and efficient way. Results show that in case of faults or abnormal conditions, the entropy of the RMS value of the voltage exceeds the preset limit and a switching signal is sent to the relay to raise an alarm or activate the breakers.

Chapter 5

Distributed Optimal Reactive Power Control: The Tertiary Control

To accommodate the increasing penetration level of distributed generators (DGs) in the electrical energy distribution system, appropriate reactive power control of DGs, which can lead to the voltage profile improvement and power loss minimization, should be addressed [109]. This chapter proposes a consensus-based distributed algorithm for the reactive power control of DGs in the power system to optimize the multi-objective function, which includes power loss, voltage deviation and cost of the reactive power generation of DGs [110]. The formulated problem is proved to be convex. The proposed algorithm is tested on 6-bus and 34-bus systems to validate its effectiveness and scalability. The proposed algorithm is also compared to the centralized technique Particle Swarm Optimization (PSO), which demonstrates the effectiveness of the proposed distributed algo-

rithm.

In this chapter, a new distributed algorithm based on MAS framework has been proposed to minimize the power loss, voltage deviation and cost of DGs reactive power generation. In this work, fully coupled distribution system is considered which means that power loss on the line is affected by both voltage magnitude and the voltage angle of the both sides of buses across the line. To address different DGs capacities and realize equal contribution of reactive power generation, reactive power fair utilization ratio has been introduced and the gradients constructed in this chapter, are reduced to be more compact.

The opportunity cost of reactive power generation is very important to include in the multi-objective function otherwise reactive power generation may decrease the real power output and it may not accommodate the sudden load changes of the power system. According to the proposed algorithm, each DG is assigned with one agent which communicates with its neighboring agents only and updates its local reactive power generation according to simple rules based on consensus algorithm. The major contributions of this chapter are summarized as follows:

- A new algorithm based on MAS framework has been proposed to address multi-objective function: the power loss, voltage deviation and the opportunity cost of DGs reactive power generation, simultaneously.

- The formulated problem has been given the form of a convex function by shaping it as a quadratically constrained quadratic program (QCQP).

- The proposed algorithm is distributed in nature as information sharing among neighboring buses only is required to optimize the objective function.

- Consensus algorithm is introduced, which can achieve reactive power fair utilization ratio for all DGs with different capacities.

- Power system is assumed as a fully coupled power system which takes into account effects of voltages and its angles (both local and neighboring) on the power loss.

This chapter is organized as follows: Section 5.1 describes the motivation behind distributed control and related work for tertiary control of reactive power generation. Section 5.2 gives the problem formulation for objective function and the constraints. Convexity Analysis is provided in Section 5.3. Implementation of the proposed ORPC is provided in Section 5.4. Simulation results and their discussions are given in Section 5.5 and finally, the findings are summarized and concluded in Section 5.6.

5.1 Motivation and Related Work

Distributed renewable energy sources are being deployed rapidly in the electrical energy distribution system to reduce carbon emission, lower environmental impact and improve energy diversity [111, 112]. However, integration of DGs poses challenging control issues to the system due to the intermittent nature of the renewable energy sources [113, 114]. One important issue is the bus voltage deviation from the acceptable limits. As a result, prolonged voltage deviation can cause dire consequences to the equipment connected with the deviated voltage source [115]. Active power loss is another important issue which should be minimized. Reactive power generation has been widely used to control the voltage

of the buses as well as minimize the power loss in the conventional power system [48].

When the active power generation by the inverters of DGs is less than their actual power ratings, the remaining capacity of DGs generation may be used to produce reactive power [116, 117]. The appropriate control of DGs reactive power may result in the improvement of system voltage profile and the loss minimization [118]. However, the optimal injection of reactive power to minimize the power loss and voltage deviation has always been a challenging task, especially for distribution network with high penetration level of DGs.

Power loss and voltage regulation can be improved in islanded microgrids by uniformly sharing reactive power loads among parallel-connected inverters proportionally. Many power sharing control strategies have been proposed in literature e.g. uniform power sharing among parallel inverters is achieved by selecting controller gains proportionally [119] and a Linear Matrix Inequality (LMI) based decentralized feedback control is designed to achieve power sharing among different generation units [120]. A consensus-based distributed voltage control strategy is proposed in [121, 122] for uniform reactive power sharing in autonomous microgrids with dominantly inductive power lines. Finally, Han, et al. [123] reviewed and categorized various power sharing control approaches.

In this chapter, optimal reactive power generation is generated to minimize multi-objective objective function: power loss, voltage deviation and reactive power generation opportunity cost simultaneously. It has been achieved using gradient based distributed algorithm. In addition to it, all generators are ensured to have equal contribution towards reactive power generation to achieve the optimal objective function.

5.2 Problem Formulation

Optimal reactive power control of DGs plays an important role in power system control and operation, which can lead to improved voltage profile, minimal active power loss and cost of controllable reactive power generation. Therefore, the objective function to be optimized is formulated as the combination of three sub-functions as given in 5.1.

$$
\begin{aligned}
\underset{Q_i,V_i,\delta_i,\alpha_i}{\text{minimize}} \quad & W_1 P_{loss} + W_2 D_V + W_3 C_Q, \\
\text{subject to} \quad P_i &= V_i \sum_{j=1}^{n} V_j Y_{ij} \cos(\theta_{ij} + \delta_j - \delta_i), \\
Q_i &= -V_i \sum_{j=1}^{n} V_j Y_{ij} \sin(\theta_{ij} + \delta_j - \delta_i), \\
\underline{P}_{Gi} &\leq P_{Gi} \leq \overline{P}_{Gi}, \\
\underline{Q}_{Gi} &\leq Q_{Gi} \leq \overline{Q}_{Gi}, \\
\underline{V}_i &\leq V_i \leq \overline{V}_i,
\end{aligned}
\tag{5.1}
$$

where W_1, W_2 and W_3 are the weight coefficients, which describe the preference of DGs suppliers. P_{loss}, D_V and C_Q are the power loss, voltage deviation and cost of reactive power generation, respectively. Y_{ij} and θ_{ij} is the magnitude and angle of the Y bus entry, V_i, V_j and δ_i, δ_j are bus voltage magnitudes and angles of i and j, respectively. $\overline{P}_{Gi}$, $\underline{P}_{Gi}$, $\overline{Q}_{Gi}$, $\underline{Q}_{Gi}$, $\overline{V}_i$ and $\underline{V}_i$ are the maximum and minimum active power ratings of generator i; maximum and minimum reactive power ratings of generator i; and upper and lower ratings of bus voltage of i_{th} bus, respectively.

Although non linear power balance constraints, limit constraints for real power

generation and limit constraints for voltage of the generators are shown in 5.1, however, these constraints are not considered in optimization problem. Only limit constraints for reactive power generation are considered in the optimization problem. It is assumed that the active power generation by the inverters of DGs is less than their actual power ratings, the remaining capacity of DGs generation may be used to produce reactive power [116, 117]. In our case, we assume that reactive power generation of DGs is the surplus amount of generation i.e. more than the required load demand and thus, it will not have an effect on the real power generation. That's why these constraints are not considered in this problem.

Furthermore, authors also realize that power loss minimization will have an impact on the real power generation. The decrease in power loss will cause drop in the required real power generation and vice versa but as we have assumed that the real power generation is sufficient enough to meet the load demand, we have not considered the effect of power loss on the real power generation.

Commonly, it is assumed that reactive power generation is provided free from the generation companies and consumers are not charged for it. Thus, it is often debatable to include cost of reactive power generation in the minimization objective function. The reason for including reactive power cost in our objective function is that it generates the optimal value of reactive power. If we do not take reactive power cost into account, the generation cost may rise unnecessarily.

The objective function given in 5.1 can be minimized by using the reactive power control of DGs. However, to address different DGs capacities and realize equal contribution of reactive power generation, utilization ratio α_{qi} is defined as 5.2

$$\alpha_{qi} = \frac{Q_i}{\overline{Q}_i} \quad with \quad \overline{Q}_i = \sqrt{S_i^2 - P_i^2}, \tag{5.2}$$

where α_{qi} is the reactive power utilization ratio, Q_i and $\overline{Q}_i$ are the present and maximum available reactive power generation, S_i and P_i are the maximum apparent power generation capacity and the real power generation of the DG i, respectively. Unlike traditional dispatchable generators, renewable energy sources, such as solar or wind which are intermittent in nature, are dynamic and thus non-dispatchable [124]. Therefore, reactive power bounds of DGs are determined by using power triangle equation of 5.2 where apparent and real power are measured or predicted for renewable sources and reactive power bounds are then calculated.

5.2.1   Power Loss Formulation

Individual formation of three sub-functions will be presented, starting with power loss in section 5.2.1. The first term of 5.1 is related to the active power loss, which can be derived as [111, 125, 33] 5.3 :

$$P_{Gi} - P_{Li} - V_i \sum_{j=1}^{n} V_j Y_{ij} \cos(\theta_{ij} + \delta_j - \delta_i) = 0. \tag{5.3}$$

5.3 can be simplified in polar form as 5.4

$$P_i = V_i^2 G_{ii} + \sum_{j=1,j\neq i}^{n} V_i V_j Y_{ij} \cos(\theta_{ij} + \delta_j - \delta_i), \tag{5.4}$$

where $P_i = P_{Gi} - P_{Li}$, is the scheduled real power from bus i, G_{ii} is the conductance of the Y_{ii}. In power system, total active power generation is either consumed by the loads or wasted in the form of losses, hence, the total power loss

P_{loss} can be obtained by taking the summation of 5.3 on both sides for all buses as 5.5 [126]

$$P_{loss} = \sum_{i=1}^{n} P_{Gi} - \sum_{i=1}^{n} P_{Li} = \sum_{i=1}^{n}\sum_{j=1}^{n} V_i V_j Y_{ij} \cos(\theta_{ij} + \delta_j - \delta_i). \qquad (5.5)$$

Using $\delta_{ji} = \delta_j - \delta_i$, 5.5 can written as 5.6

$$P_{loss} = \sum_{i=1}^{n}\sum_{j=1}^{n} V_i V_j Y_{ij} \cos(\theta_{ij} + \delta_{ji}). \qquad (5.6)$$

To optimize 5.1, a consensus based gradient approach is proposed which requires the gradient of the objective function. The gradient of the objective function w.r.t state variable α_{qi} can be determined as 5.7

$$\frac{\partial f}{\partial \alpha_{qi}} = W_1 \frac{\partial P_{loss}}{\partial \alpha_{qi}} + W_2 \frac{\partial D_V}{\partial \alpha_{qi}} + W_3 \frac{\partial C_Q}{\partial \alpha_{qi}}. \qquad (5.7)$$

Using the chain rule for the partial derivative, gradient for power loss can be expanded as 5.8

$$\frac{\partial P_{loss}}{\partial \alpha_{qi}} = W_1 \left(\frac{\partial P_{loss}}{\partial V_i} \frac{\partial V_i}{\partial \alpha_{qi}} + \sum_{j \in N_i} \frac{\partial P_{loss}}{\partial V_j} \frac{\partial V_j}{\partial \alpha_{qi}} + \frac{\partial P_{loss}}{\partial \delta_i} \frac{\partial \delta_i}{\partial \alpha_{qi}} + \sum_{j \in N_i} \frac{\partial P_{loss}}{\partial \delta_j} \frac{\partial \delta_j}{\partial \alpha_{qi}} \right) \frac{\partial Q_i}{\partial \alpha_{qi}}.$$
$$(5.8)$$

It should be emphasized here that usually in AC power flow, the effect of V_i on P_i and δ_i on Q_i is ignored. Known as decoupled power flow, it is a very strong assumption and it cannot be ignored especially in distribution networks where the resistance of the transmission line is not negligible [127].

As shown in 5.8, the gradient of power loss w.r.t α_{qi} can be calculated as the sum of four terms, where the first term is determined as 5.9

$$\frac{\partial P_{loss}}{\partial V_i} = \frac{\partial}{\partial V_i} \sum_{j=1}^{n} \sum_{k=1}^{n} V_j V_k Y_{jk} \cos(\theta_{jk} + \delta_{kj}). \tag{5.9}$$

There are three possible combinations for 5.9 [3]

$$\frac{\partial P_{loss}}{\partial V_i} = \begin{cases} 2V_i^2 G_{ii} & for \quad j = i, k = i, \\[2ex] \sum_{k=1,k\neq i}^{n} V_k Y_{ik} \cos(\theta_{ik} + \delta_{ki}) & for \quad j = i, k \neq i, \\[2ex] \sum_{j=1,j\neq i}^{n} V_j Y_{ji} \cos(\theta_{ji} + \delta_{ij}) & for \quad k = i, j \neq i, \\[2ex] 0 & otherwise. \end{cases} \tag{5.10}$$

5.10 can be further simplified as 5.11

$$\begin{aligned} \frac{\partial P_{loss}}{\partial V_i} &= 2V_i^2 G_{ii} + \sum_{k=1,k\neq i}^{n} V_k Y_{ik} \cos(\theta_{ik} + \delta_{ki}) + \sum_{j=1,j\neq i}^{n} V_j Y_{ji} \cos(\theta_{ji} + \delta_{ij}), \\ &= 2V_i^2 G_{ii} + \sum_{j=1,j\neq i}^{n} V_j G_{ij} \cos(\theta_{ij} + \delta_{ji}) = 2\sum_{j=1}^{n} V_j Y_{ij} \cos(\theta_{ij} + \delta_{ji}). \end{aligned} \tag{5.11}$$

According to 5.3, multiplying and dividing by V_i on both nominator and denominator of right side of 5.11 makes 5.12

$$\frac{\partial P_{loss}}{\partial V_i} = \frac{2P_i}{V_i}. \tag{5.12}$$

$\frac{\partial V_i}{\partial Q_i}$ can be derived as follows [48]

$$\begin{aligned} Q_i = Q_{Gi} - Q_{Di} &= -\sum_{j=1}^{n} V_i V_j Y_{ij} \sin(\theta_{ij} + \delta_{ji}), \\ &= -V_i^2 B_{ii} - \sum_{j=1,j\neq i}^{n} V_i V_j Y_{ij} \sin(\theta_{ij} + \delta_{ji}). \end{aligned} \tag{5.13}$$

where Q_{Gi}, Q_{Di} are the reactive power generation and load at bus i, and Q_i is

the scheduled reactive power from bus i, 5.13 can be expanded as 5.14

$$\frac{\partial Q_i}{\partial V_i} = -2V_i B_{ii} - \sum_{j=1, j\neq i}^{n} V_j Y_{ij} \sin(\theta_{ij} + \delta_{ji}). \tag{5.14}$$

The right hand side of 5.14 can be easily rewritten as 5.15

$$\frac{\partial Q_i}{\partial V_i} = \frac{-2V_i^2 B_{ii} - V_i \sum_{j=1, j\neq i}^{n} V_j Y_{ij} \sin(\theta_{ij} + \delta_{ji})}{V_i}. \tag{5.15}$$

The nominator on the right hand side of 5.15 can be replaced by Q_i, according to 5.13 as 5.16

$$\frac{\partial Q_i}{\partial V_i} = \frac{Q_i}{V_i} - V_i B_{ii}. \tag{5.16}$$

For second term of gradient of power loss, as P_{loss} is calculated for the whole system, $\frac{\partial P_{loss}}{\partial V_j}$ will have the same relation as $\frac{\partial P_{loss}}{\partial V_i}$ but j will have different neighbors than i

$$\frac{\partial P_{loss}}{\partial V_j} = 2 \sum_{k=1}^{n} V_k Y_{jk} \cos(\theta_{jk} + \delta_{kj}). \tag{5.17}$$

According to 5.3, multiplying and dividing by V_j on both nominator and denominator of right side 5.17, makes 5.18

$$\frac{\partial P_{loss}}{\partial V_j} = \frac{2P_j}{V_j}. \tag{5.18}$$

Similarly, $\frac{\partial Q_i}{\partial V_j}$ can be determined as 5.19

$$\frac{\partial Q_i}{\partial V_j} = -V_i Y_{ij} \sin(\theta_{ij} + \delta_{ji}). \tag{5.19}$$

The second term of gradient of power loss with respect to voltage becomes as

5.20

$$\sum_{j \in N_i} \frac{\partial P_{loss}}{\partial V_j} \frac{\partial V_j}{\partial Q_i} = \sum_{j \in N_i} \frac{2P_i}{-V_i V_j Y_{ij} \sin(\theta_{ij} + \delta_{ji})}. \tag{5.20}$$

Next, the third term can be determined as 5.21

$$\frac{\partial P_{loss}}{\partial \delta_i} = \begin{cases} 0 & for \quad j = i, k = i, \\ \sum_{k=1}^n V_i V_k Y_{ik} \sin(\theta_{ik} + \delta_{ki}) & for \quad j = i, k \neq i, \\ -\sum_{j=1}^n V_j V_i Y_{ji} \sin(\theta_{ji} + \delta_{ij}) & for \quad k = i, j \neq i. \end{cases} \tag{5.21}$$

5.21 can be further simplified as 5.22

$$\frac{\partial P_{loss}}{\partial \delta_i} = \sum_{k=1, k \neq i}^n V_i V_k Y_{ik} \sin(\theta_{ik} + \delta_{ki}) - \sum_{j=1, j \neq i}^n V_j V_i Y_{ji} \sin(\theta_{ji} + \delta_{ij}),$$
$$= 2 \sum_{j=1, j \neq i}^n V_i V_j Y_{ij} \sin(\theta_{ij} + \delta_{ji}). \tag{5.22}$$

According to 5.13, 5.22 is rewritten as 5.23

$$\frac{\partial P_{loss}}{\partial \delta_i} = -2(Q_i + V_i^2 B_{ii}). \tag{5.23}$$

Now, $\frac{\partial \delta_i}{\partial Q_i}$ can be calculated from Q_i as 5.24

$$\frac{\partial Q_i}{\partial \delta_i} = \begin{cases} 0 & for \quad j = i, \\ \sum_{j=1, j \neq i}^n V_i V_j Y_{ij} \cos(\theta_{ij} + \delta_{ji}) & for \quad otherwise. \end{cases} \tag{5.24}$$

According to 5.3, 5.24 becomes 5.25

$$\frac{\partial Q_i}{\partial \delta_i} = P_i - V_i^2 G_{ii}. \tag{5.25}$$

Last term of gradient of power loss can be determined as follows

$$\frac{\partial P_{loss}}{\partial \delta_j} = 2 \sum_{k=1,k\neq j}^{n} V_j V_k Y_{jk} \sin(\theta_{jk} + \delta_{kj}). \tag{5.26}$$

According to 5.13, 5.26 becomes as 5.27

$$\frac{\partial P_{loss}}{\partial \delta_j} = -2(Q_j + V_j^2 B_{jj}). \tag{5.27}$$

$$\frac{\partial Q_i}{\partial \delta_j} = -V_i V_j Y_{ij} \cos(\theta_{ij} + \delta_{ji}). \tag{5.28}$$

Thus, last term of gradient of power loss will be 5.29

$$\sum_{j\in N_i} \frac{\partial P_{loss}}{\partial \delta_j} \frac{\partial \delta_j}{\partial Q_i} = 2 \sum_{j\in N_i} \frac{Q_j + V_j^2 B_{jj}}{V_i V_j Y_{ij} \cos(\theta_{ij} + \delta_{ji})}. \tag{5.29}$$

$\frac{\partial Q_i}{\partial \alpha_{Qi}}$ can be calculated as 5.30

$$\frac{\partial Q_i}{\partial \alpha_{Qi}} = \overline{Q}_i. \tag{5.30}$$

5.2.2 Voltage Deviation Formulation

The second term of the objective function, which is the voltage deviation between voltage magnitude and its reference is given as 5.31

$$D_V = \sum_{i=1}^{n} (V_i - V_i^*)^2, \tag{5.31}$$

where V_i^* is the reference voltage for bus i. The derivative of D_V w.r.t state variable α_{qi} can be determined as 5.32

$$\frac{\partial D_V}{\partial \alpha_{qi}} = W_2 \left(\frac{\partial D_V}{\partial V_i} \frac{\partial V_i}{\partial Q_i} \frac{\partial Q_i}{\partial \alpha_{qi}} \right), \qquad (5.32)$$

where $\frac{\partial D_V}{\partial V_i}$ is determined as 5.33

$$\frac{\partial D_V}{\partial V_i} = 2(V_i - V_i^*). \qquad (5.33)$$

$\frac{\partial V_i}{\partial Q_i}$ and $\frac{\partial Q_i}{\partial \alpha_{qi}}$ can be obtained from 5.16 and 5.30, respectively. Thus, the gradient of voltage deviation is given as 5.34

$$\begin{aligned}
\frac{\partial D_V}{\partial \alpha_{qi}} &= 2W_2(V_i - V_i^*)\left(\frac{V_i}{Q_i - V_i^2 B_{ii}} \right)\overline{Q}_i, \\
&= \frac{2V_i W_2 \overline{Q}_i (V_i - V_i^*)}{Q_i - V_i^2 B_{ii}}.
\end{aligned} \qquad (5.34)$$

5.2.3   Reactive Power Cost Formulation

The third term of the objective function, the cost of reactive power generation, is simply approximated as [128, 129] 5.35

$$C_Q = k_i Q_i^2, \qquad (5.35)$$

where k_i is the cost coefficient for reactive power generation. Various lost opportunity cost models for generators exit in the literature [130, 131, 132]. The critical element of the cost calculation is the value of, ΔP which, in turn, depends on the desired reactive schedule and the reactive capability curve of the generator. In our case, we utilized a single term quadratic function for reactive power cost,

kQ^2 as a demonstration to generate an optimal value of reactive power. The derivative of the cost w.r.t. α_{qi} is calculated as 5.36

$$\frac{\partial Q_C}{\partial \alpha_{qi}} = W_3\left(\frac{\partial Q_C}{\partial Q_i}\frac{\partial Q_i}{\partial \alpha_{qi}}\right) = 2W_3 k_i Q_i \overline{Q}_i. \tag{5.36}$$

Finally, all the terms in 5.7 are known, and 5.7 can be obtained as 5.37

$$\begin{aligned}\frac{\partial f}{\partial \alpha_{qi}} = 2W_1\overline{Q}_i\Big\{ &\frac{P_i}{Q_i - V_i^2 B_{ii}} + \sum_{j\in N_i}\frac{P_i}{-V_iV_jY_{ij}\sin(\theta_{ij}+\delta_{ji})} - \frac{Q_i + V_i^2 B_{ii}}{P_i - V_i^2 G_{ii}} \\ &+ \sum_{j\in N_i}\frac{Q_j + V_j^2 B_{jj}}{V_iV_jY_{ij}\cos(\theta_{ij}+\delta_{ji})} + \frac{2V_iW_2\overline{Q}_i(V_i - V_i^*)}{Q_i - V_i^2 B_{ii}} + 2W_3 k_i Q_i \overline{Q}_i.\end{aligned} \tag{5.37}$$

It is worthy to note that only admittance of the transmission line connecting two buses and local information, such as bus voltage, voltage reference, reactive power capacity, are required to calculate the gradient. No global parameter of the power system is required.

5.3 Convexity Analysis

To express problem 5.1 as a quadratic cone quadratic programming (QCQP), equality constraints jointly, can be reformulated as Branch Injection Model (BIM) of power flow, defined by Kirchhoffs laws as given as 5.38 [133]

$$\vec{S}_i = \sum_{j=1}^{n}\vec{Y}_{ij}^{H}\vec{V}_i(\vec{V}_i^{H} - \vec{V}_j^{H}), \tag{5.38}$$

where S represents the apparent power, $\rightarrow$ represents the complex quantity and H represents its Hermitian. 5.38 can be rewritten in terms of current injection

from bus i as 5.39 :

$$\vec{S}_i = \vec{V}_i \vec{I}_i^H = (e_i^H \vec{V})(\vec{I}^H e_i), \tag{5.39}$$

Where e_i is the n-dimensional vector with 1 in the i_{th} entry and 0 elsewhere. Here, $\vec{I} = \vec{Y}\vec{V}$, thus 5.37 can be rewritten as 5.40:

$$\vec{S}_i = tr(e_i^H \vec{V} \vec{V}^H \vec{Y}^H e_i) = tr(\vec{Y}^H e_i e_i^H)\vec{V}\vec{V}^H = \vec{V}^H \vec{Y}^H \vec{V}, \tag{5.40}$$

where $\vec{Y}_i^H =: e_i e_i^H \vec{Y}$ is an $n \times n$ matrix with its i_{th} row equal to i_{th} row of $\vec{Y}$ matrix and all other rows equal to zero. Hermitian and skew Hermitian components of $\vec{Y}_i^H$ and $\vec{Y}^H$ are defined as 5.41:

$$\begin{aligned} \Phi_i &= \frac{\vec{Y}_i^H + \vec{Y}_i}{2}; \quad \text{and} \quad \Psi_i = \frac{\vec{Y}_i^H - \vec{Y}_i}{2}, \\ \Phi &= \frac{\vec{Y}^H + \vec{Y}}{2}; \quad \text{and} \quad \Psi = \frac{\vec{Y}^H - \vec{Y}}{2}. \end{aligned} \tag{5.41}$$

Using 5.41, equality constraints of 5.1 can be reformulated as 5.42 :

$$P_i = \vec{V}^H \Phi_i \vec{V} \quad \text{and} \quad Q_i = \vec{V}^H \Psi_i \vec{V}. \tag{5.42}$$

Let $J_i := e_i e_i^H$ denote the Hermitian matrix with a single 1 at $(i,i)_{th}$ entry and 0 elsewhere, problem formulation 5.1 can be written as QCQP in 5.43 :

$$\begin{aligned} \vec{V}^H(W_1\Phi + W_2 I + W_3 \Psi)\vec{V} &- 2W_2 V^{*H}\vec{V} - 1^H P_D + W_2 V^{*H} V^*, \\ \text{subject to} \quad P_i &= \vec{V}^H \Phi_i \vec{V}; \quad Q_i = \vec{V}^H \Psi_i \vec{V}, \\ \vec{V}^H \Phi_i \vec{V} &\le \overline{P}_i; \quad \vec{V}^H(-\Phi_i)\vec{V} \le -\overline{P}_i, \\ \vec{V}^H \Psi_i \vec{V} &\le \overline{Q}_i; \quad \vec{V}^H(-\Psi_i)\vec{V} \le -\overline{Q}_i, \\ \vec{V}^H J_i \vec{V} &\le \overline{V}_i; \quad \vec{V}^H(-J_i)\vec{V} \le -\overline{V}_i. \end{aligned} \tag{5.43}$$
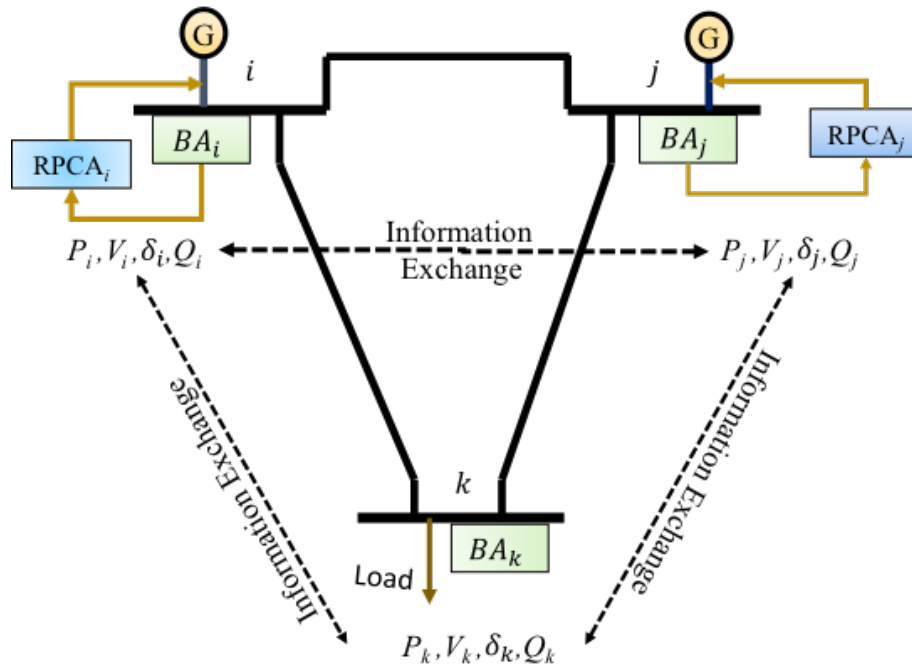
Figure 5.1: Scheme of the communications among agents

Even though different sets of equations define the optimization model 5.1 and 5.43 in terms of their own variables, yet both are models of the Kirchhoff's laws and both mathematical models are equivalent in the precise sense, which means any result in one model is derivable in the other [133]. In this chapter, we expressed the OPF problem as QCQP using BIM. In the similar work, some other authors have attempted to express their optimization model as Semidefinite Programming (SDP) [134] or Second Order Cone Problem (SOCP) [135], depending on their own applications.

5.4   Implementation of Reactive Power Control

Implementation of the ORPC algorithm can be further divided into three part: first part is the proposed algorithm; second is the the power system test cases on

which proposed algorithm is tested and third is the selection of weight coefficients for three sub-functions.

Specifically, we propose a consensus based distributed algorithm that is possibly suboptimal, but nonetheless has the interesting property of achieving close to uniform utilization ratios.

5.4.1 Proposed ORPC

Proposed algorithm is implemented by considering power system as MAS where each bus is equipped with a bus agent (BA) responsible for obtaining the local measurement of four state variables of P_i, Q_i, V_i & δ_i and exchanging the information with its neighboring agents. The communication network for the MAS framework is designed in such a way that two neighboring agents (NA) communicate with each other only if their corresponding buses are electrically coupled. In addition, each DG bus is attached with a Reactive Power Control Agent (RPCA) which receives information from BA and decide its control output. Communication of state variables among various buses is graphically explained in Fig. 5.1.

The reactive power utilization ratio of every bus in the power system is discovered iteratively as 5.44

$$\alpha_i[k+1] = \sum d_{ij}\alpha_i[k] - \epsilon \frac{\partial f}{\partial \alpha_{qi}}, \qquad (5.44)$$

where ϵ is the step size that can be adjusted to control the converging speed, d_{ij}

is designed as 5.45 [136]

$$d_{ij} = \begin{cases} \frac{2}{(n_i+n_j+1)} & for \quad j \in N_i, \\ 1 - \sum_{j \in N_i} \frac{2}{(n_i+n_j+1)} & for \quad\quad i = j, \\ 0 & otherwise, \end{cases} \quad (5.45)$$

where n_i and n_j are the numbers of agents connected to agents i and j, respectively. N_i denotes neighboring agent set of agent i. α_{qi} is the optimization variable being calculated to a uniform value using consensus based algorithm. From α_{qi}, reactive power generation will be calculated for each generator. This reactive power generation is the control variable/intermediate variable for each generator that will change voltage magnitudes and phase angles of the generators.

The utilization ratio, α_{qi} will be updated iteratively for a given number of iterations, which is predetermined by the size and connectivity of the power system, until an optimal solution of the objective function is achieved [137]. 5.44 Our consensus based proposed algorithm is trying to reach a consensus on utilization ratios, α among all generators and results show that all generators are operating at the same uniform utilization ratio. However, this does not imply that the converged solution is globally optimal in nature. Nonetheless, the proposed algorithm provides a good approximation to the global optimum solution.If all generators achieve the same α, it may not be the optimal solution because 5.44 does not involve any hard constraint that may force α to reach the equal value. Nonetheless, it is the attribute of proposed distributed algorithm that it reaches the consensus.
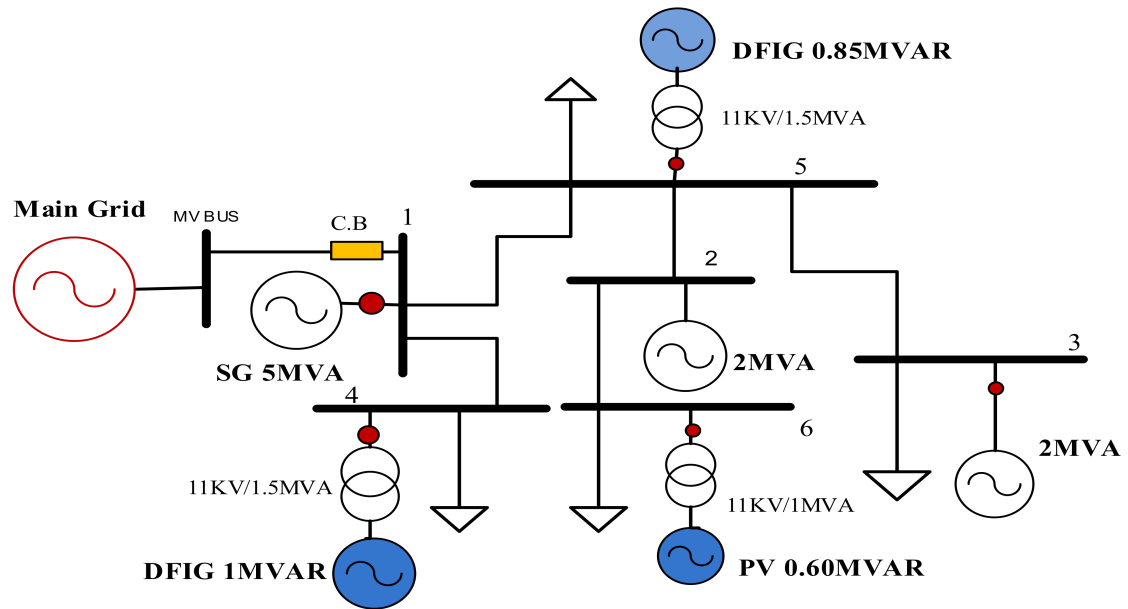
Figure 5.2: Six-bus radial distribution network

5.4.2   Test Cases

In this section, two case studies are presented to exhibit the effectiveness of proposed distributed control algorithm: 6-Bus and 34-Bus system. The 6-Bus radial distribution network is shown in Fig.5.2, in which bus 1 is a slack bus, attached to the main grid. Three DGs with reactive power ranges -0.30 to 0.56 MVAR, -0.45 to 0.75 MVAR and -0.35 to 0.60 MVAR are attached at bus 4, 5 and 6 respectively. The line data for the given system is shown in Table.5.1. Reactive power generation from these DGs is utilized to minimize the power loss and voltage deviation of the system, taking the reactive power generation cost into account simultaneously. Reference voltages for 6 buses is assigned as 1.04, 1.03, 1, 1, 1, and 1 in an ascending order.

Table 5.1: Distribution line data for the 6-bus system

From	To	R(p.u.)	X(p.u.)	From	To	R(p.u.)	X(p.u.)
1	4	0.05	0.095	2	6	0.07	0.115
1	5	0.08	0.125	3	5	0.12	0.165
2	5	0.1	0.145				

Table 5.2: Event sequences of load changes on 6-bus system

Iteration No.	Event No.	Bus No.	Load Type	Load Change
25	Event 1	[4, 5, 6]	React. Load	1.2× Initial
50	Event 2	[3, 4, 5, 6]	Real Load	1.05× Event 1
75	Event 3	[4, 5, 6]	React. Load	0.80× Event 2
100	Event 4	[3, 4, 5, 6]	Real Load	0.95× Event 3

5.4.3 Selection of weight coefficients

Usually, weights for multi-objective function are determined by specific applications and the method of finding weights may vary for each specific problem. In our application, three sub-functions are determined in different units: power loss and voltage deviation are determined in p.u. while reactive power cost is calculated in dollars. In order to give equal contributions to each of the three sub-functions, reactive power cost weight coefficient is divided by 10^2 to convert it into p.u.

As voltage deviation is formulated by taking the square of voltage difference, its value will be of the order 10^{-2}. Therefore, weight coefficient to the voltage deviation is given as of the order of 10^2 to give equal contributions from each sub-function. Three sub-objective functions: power loss, voltage deviation and reactive power cost are weighted as 3.5, 150 and 0.28 respectively. However, the weight coefficients can be changed to any value depending on DGs suppliers preferences.
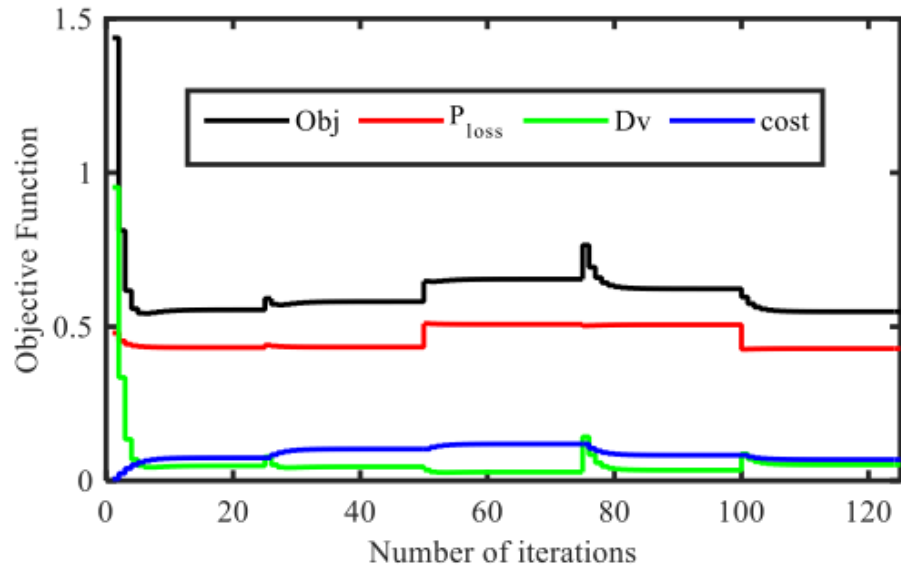
Figure 5.3: Objective function convergence for 6-bus system using real bus angles in the power loss function
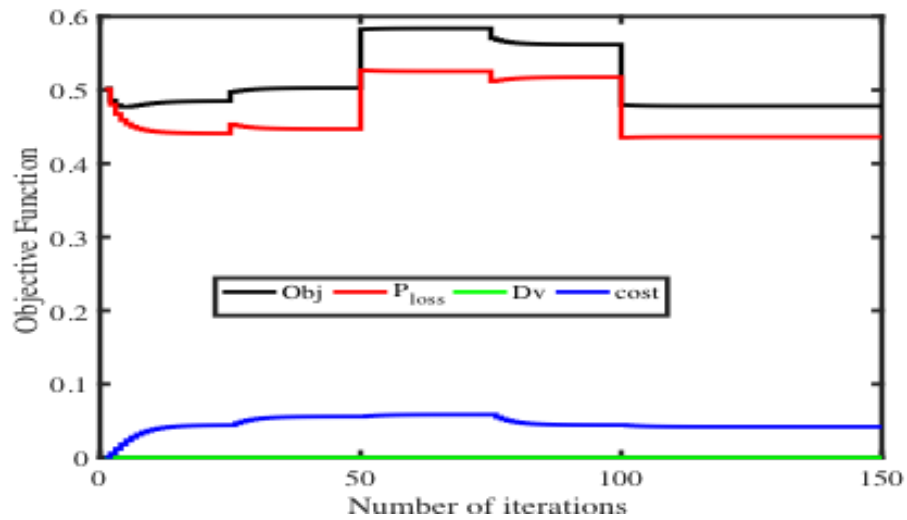

Figure 5.4: Objective function convergence for 6-bus system without Dv

5.5 Simulation Results and Discussions

In the first scenario, the gradient of power loss is calculated including $\cos(\delta_{ij})$ and results are shown in shown Figs.(5.3 - 5.7). In the second scenario, the gradient of power loss is simplified by ignoring the bus angle difference between two neighboring buses ($\delta_{ij} = 0$) as shown in Figs.(5.8 - 5.11). Both Figs.(5.3 - 5.7) & Figs.(5.8 - 5.11) exhibit the update of objective functions, reactive power generation, fair utilization ratio and voltage of the non-PV bus buses, respectively. To test the effectiveness of the proposed algorithm, an event sequence of load demand variation is introduced in the existing power distribution system as given in Table.5.2.

5.3 clearly shows that the value of voltage deviation is quite small, roughly of the order 10^{-2} p.u, thus, implicitly ignoring D_V from the objective function should not bring any significant change in the final optimal objective function. To see the impact of ignoring D_V on the objective function, the algorithm is simulated with $W_2 = 0$. The obtained results shown in 5.4 validate our logic and does not bring any significant change in the final optimal objective function.

The objective function, along with its individual sub-functions, converges to their optimal value before 10th iteration. When reactive power load demand rises at 25th iteration, it is compensated by the reactive power generation sources at bus 4, 5 and 6th buses as evident from Fig.5.5 & Fig. 5.6. Similarly, change in real power load and decrease in reactive power load is counteracted by their respective generators [138].

It is important to note that proposed algorithm strives to attain the reference voltages of the load buses immediately after the abrupt load changes take place
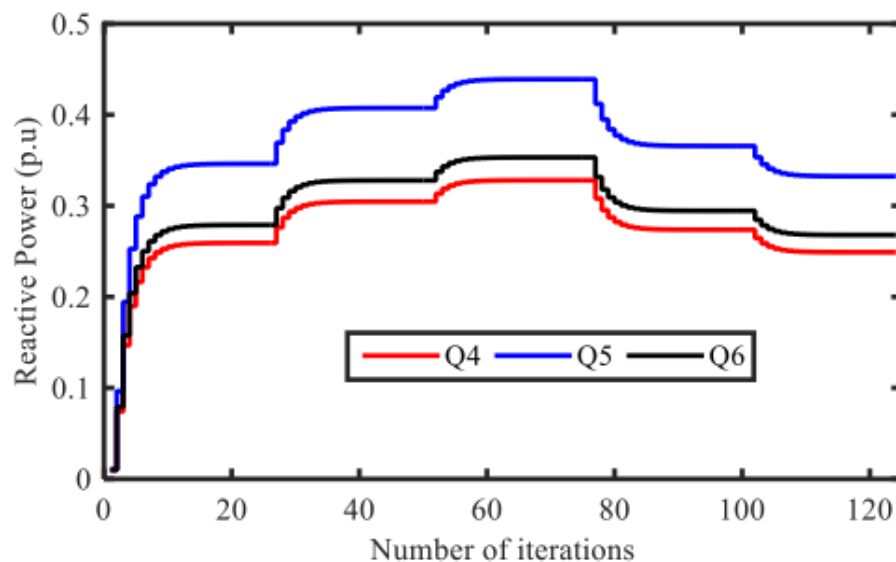
Figure 5.5: Reactive power generation update for 6-bus system using real bus angles in the power loss function

on the energy system as shown in Fig.5.7. Another important observation is to spot the behavior of the power loss in case of abrupt real power load changes. Increase/decrease of real power demand means flow of higher/lower current through lines, which increases/decreases the power loss on the lines as evident from Fig.5.3.

As included in the problem formulation, each DG should contribute reactive power uniformly based upon its available capacity. Thus, Fig. 5.6 manifests that the reactive power utilization ratio (α) converges to a common value of 0.47 for every DG till 25th iteration, before any load change occurs. It is because our consensus based proposed algorithm is trying to reach on a agreement for uniform utilization ratio among all DGs and results show that all DGs are operating at the same uniform utilization ratio. However, this does not imply that the converged solution is globally optimal in nature. Without loss of generality, we can definitely propose that the algorithm provides a good approximation to the global optimum solution.
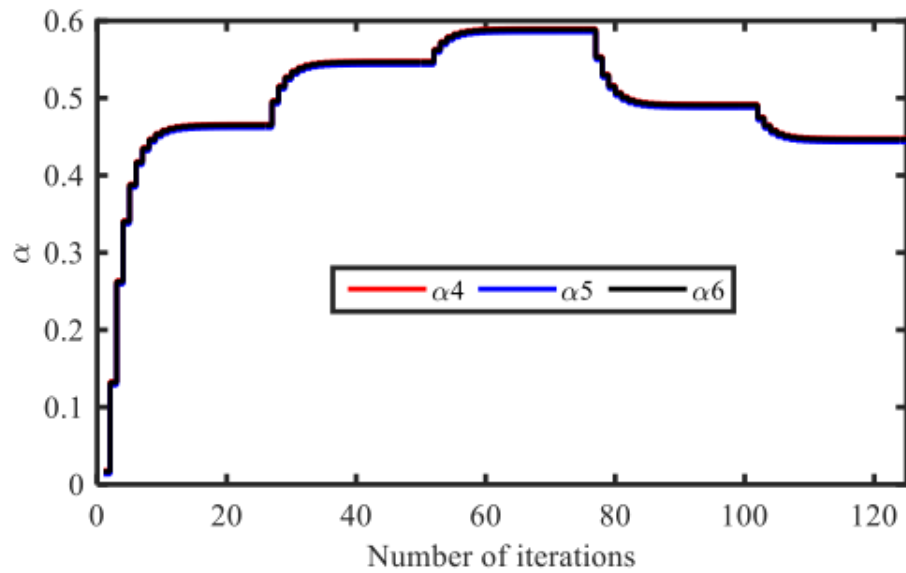
Figure 5.6: Utilization ratio update for 6-bus system using real bus angles in the power loss function
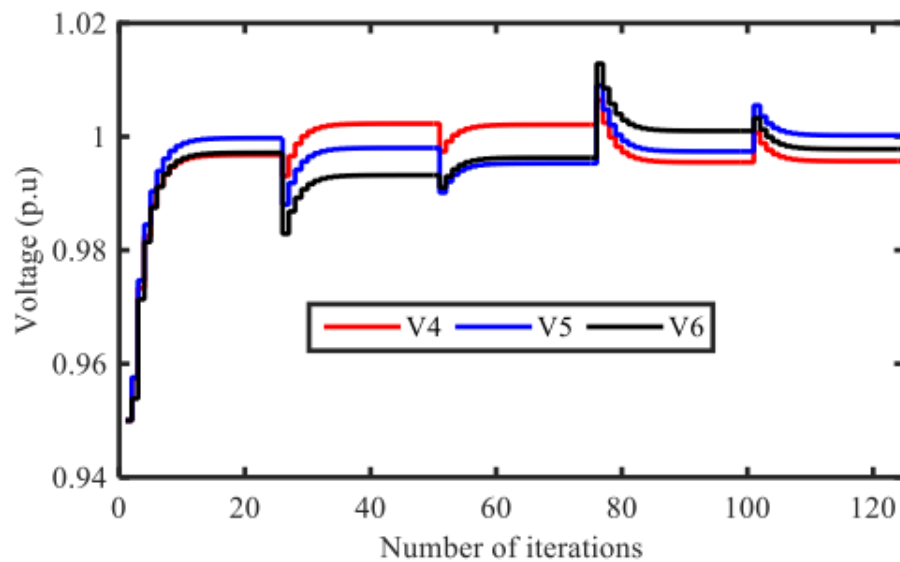
Figure 5.7: Updates of improved voltage profile for 6-bus system using real bus angles in the power loss function
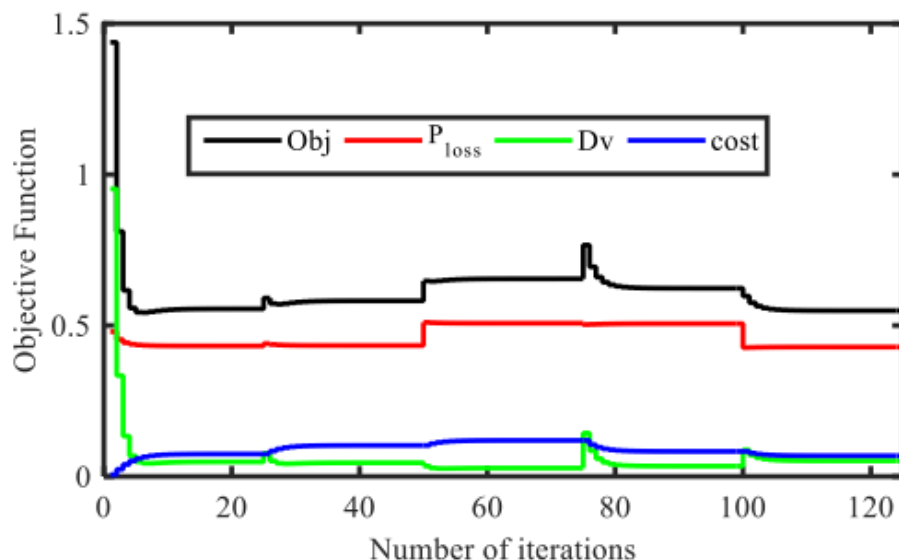
Figure 5.8: Objective function convergence for 6-bus system using voltage angle approximation

Figs.(5.8 - 5.11) show the simulation results of the second scenario: the angle differences between two neighboring buses are approximated to zero. Comparing of Figs.(5.3 - 5.7) and Figs.(5.8 - 5.11) show that no significant difference between the two graphs is observed. After analyzing both the results closely, it is found that with approximation of $\cos(\delta_{ij}) = 1$, it conforms to the original value with a small error of only 0.22%. According to [3], special techniques are required to obtain the information of angle differences, which may make the online application very complicated and computationally expensive. From authors work, it is concurred that making approximation of $\cos(\delta_{ij}) = 1$ is a valid approximation and angle difference may be approximated to zero when the system is operating in the steady state condition.

To authenticate the efficacy of proposed distributed algorithm, it is compared with centralized control technique of PSO [139]. The adopted PSO uses 20 particles and converges at 28th iteration, which means 560 calculations in total. It is noticed that results obtained from the both approaches are identical. Table.
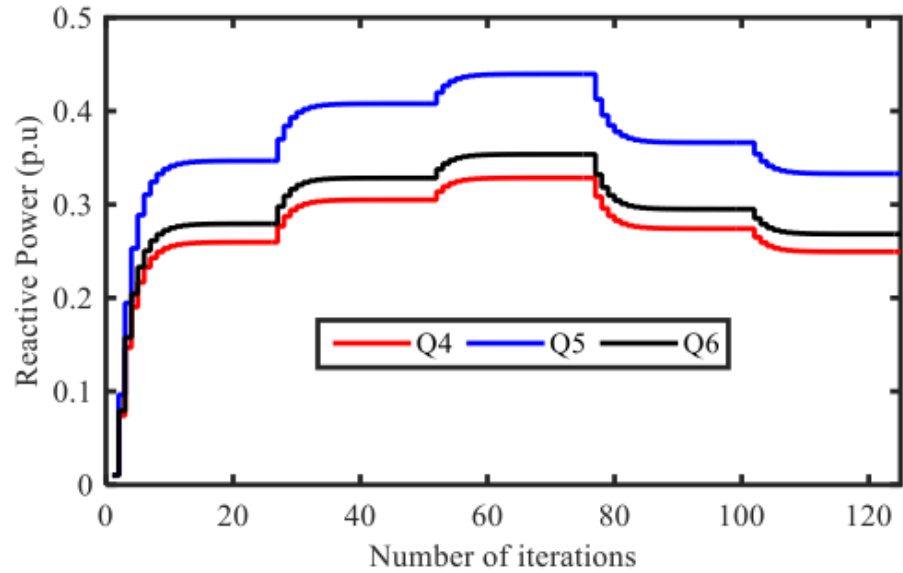
Figure 5.9: Reactive power generation update for 6-bus system using voltage angle approximation
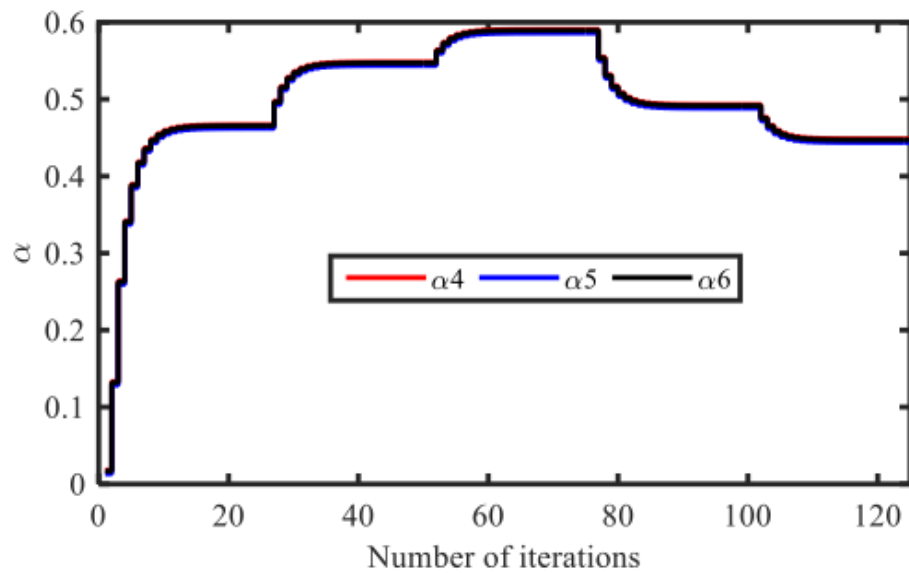
Figure 5.10: Utilization ratio update for 6-bus system using voltage angle approximation

Table 5.3: Simulation results summary for 6-Bus System

Variables	Distributed	Centralized PSO
Q4	0.2596	0.2589
Q5	0.2793	0.2791
Q6	0.3466	0.3460
V1	1.030	1.030
V2	1.040	1.040
V3	1.000	1.000
V4	1.000	1.00
V5	0.998	0.992
V6	0.997	.991
Power Loss	0.4323	0.4223
Objective Function	0.5446	0.5383

5.3 is provided to compare the values of reactive power generations, voltage magnitudes, power loss and objective function for the proposed algorithm and the centralized approach.

Voltage angle differences of lines in the 6-bus radial system is shown in Fig.5.12. The angle difference changes during the load changing condition and gets restored to its previous state immediately when the external loading is removed. Fig.5.12 shows that voltage angles changes much more in case of real power load change than that of reactive power load change. It is also clear that the magnitude of angle differences is close to zero and has very limited effect on the optimal solution of the proposed distributed algorithm. Thus, angle difference can be approximated to zero, which can reduce the computational burden of the controller and make the algorithm fast [140].

Measuring the angle difference slows down the convergence rate of the algorithms and incurs an additional computational cost on the controller. It is clear from the graph that angle difference is small and the proposed algorithm may not require its measurement for decision of the control action. This substantiates the
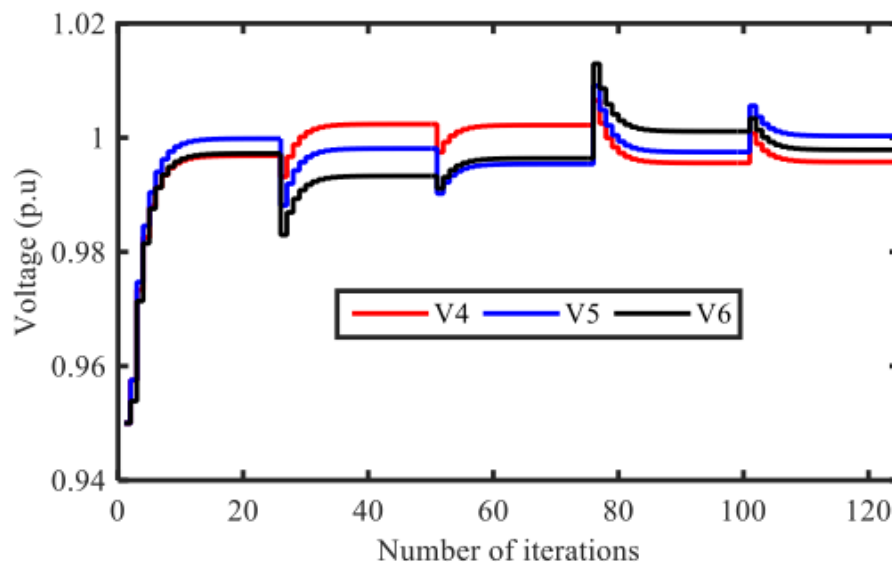
Figure 5.11: Updates of improved voltage profile for 6-bus system using voltage angle approximation

Table 5.4: Reactive power generation output for two cases for 6-bus system

Bus No.	$W_1=1$, $W_3=0$	$W_1=1$, $W_3=0$	Maximum Q
Q_4	0.67818	0.72410	0.80
Q_5	0.37380	0.37864	0.75
Q_6	0.37478	0.50000	0.50
Power loss	0.18701	0.17915	–

assumption of considering $\cos(\delta_{ij}) = 1$ and validates the claim that algorithm can provide comparable results to the one without an approximation.

To discover the impact of considering the cost of reactive power generation, the proposed algorithm has been tested with $W_2 = 0, W_3 = 0$ as shown in Table.5.4. It is observed that reactive power generation may rise when we ignore reactive power cost in the objective function. Here, W_1 and W_3 are the weights for the power loss and reactive power generation cost, respectively. It is evident that reactive power generation cost increases in case of $W_3=0$ leading to the operation of Q_6 at its maximum available ratings.
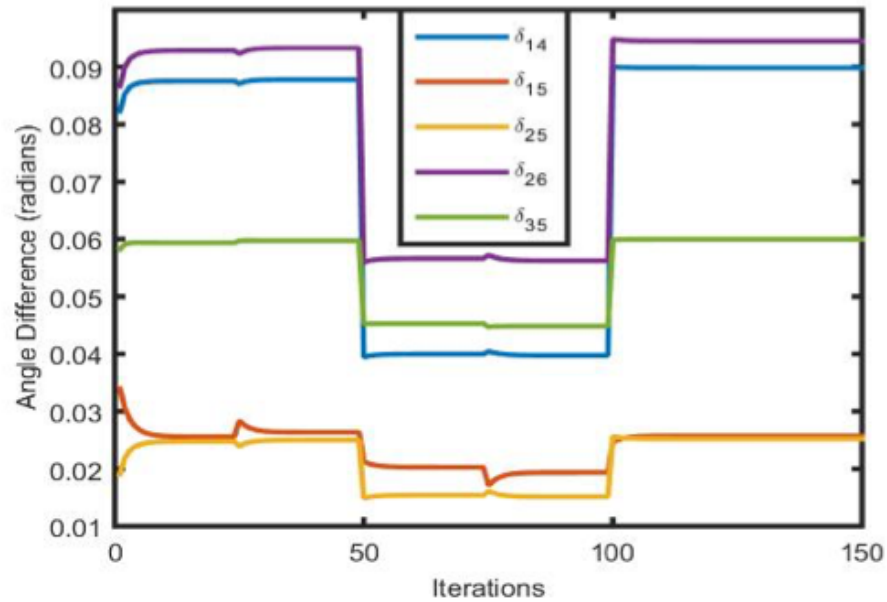
Figure 5.12: Voltage angle difference of all lines in 6 bus distribution network

Table 5.5: Distribution line data for the 34-bus system

From	To	R(p.u.)	X(p.u.)	From	To	R(p.u.)	X(p.u.)
1	2	0.117	0.1085	17	19	0.2079	0.1994
2	3	0.10725	0.09875	19	20	0.189	0.1805
3	4	0.16445	0.15595	20	21	0.189	0.1805
4	5	0.1495	0.141	21	22	0.262	0.2535
4	6	0.1495	0.141	20	23	0.262	0.2535
6	7	0.3144	0.3059	23	24	0.3144	0.3059
7	8	0.2096	0.2011	23	25	0.2096	0.2011
8	9	0.3144	0.3059	25	26	0.131	0.1225
9	10	0.2096	0.2011	26	27	0.1048	0.0963
10	11	0.131	0.1225	27	28	0.1572	0.1487
11	12	0.10148	0.09298	28	29	0.1572	0.1487
9	13	0.1572	0.1487	25	30	0.1572	0.1487
13	14	0.2096	0.2011	30	31	0.1572	0.1487
13	15	0.1048	0.0963	31	32	0.2096	0.2011
15	16	0.0524	0.0439	31	33	0.1572	0.1487
16	17	0.1794	0.1709	33	34	0.1048	0.0963
17	18	0.16445	0.15595	-	-	-	-
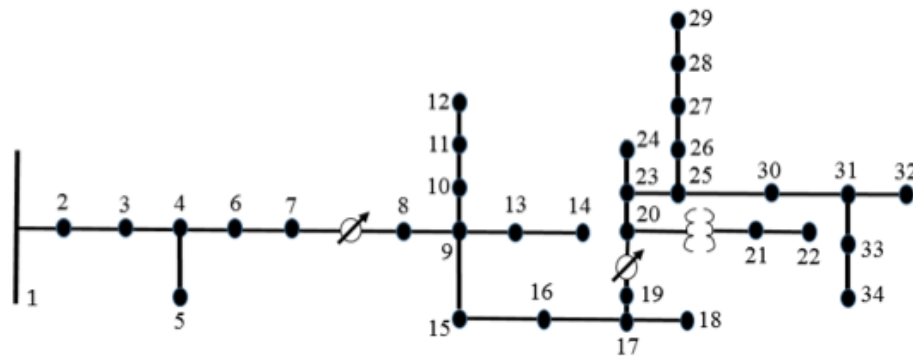
Figure 5.13: Schematic diagram of 34-bus system

5.5.1   34-Bus Radial Distribution System

A 34-bus radial distribution network [141] with the topology and line data as given in Fig.5.13 and Table.5.5 respectively, is being utilized for validation of the proposed algorithm. 9 DGs for reactive power control are connected at bus 4, 8, 12, 16, 20, 21, 23, 27 and 28, whose reactive power generation capacities are predicted as 0.6, 0.75, 0.75, 0.675, 0.9, 0.675, 0.75, 0.85, and 0.95 MVAR, respectively. DGs attached at bus 4, 8, 20, 23 and 27 are PV generators while DGs attached at bus 12, 16, 21 and 28 are DFIGs. Reference voltages are taken as given in [141]. Cost coefficient (k_i) for reactive power generation is set to 1 whereas coefficients for power loss, voltage deviation and reactive power cost are chosen as 2, 100 and 0.1 respectively.

Results for the 34-bus system show that the proposed algorithm is faster than the centralized approach as visible in Figs.5.14 & 5.15. It exhibits that the distributed algorithm achieves the optimal solution, equal to the centralized approach but within much less time. The detailed comparison between the proposed distributed algorithm and the centralized approach is provided in Table.5.6, which shows that power loss, objective function and reactive power updates. Figs.5.16 & 5.17 reveal
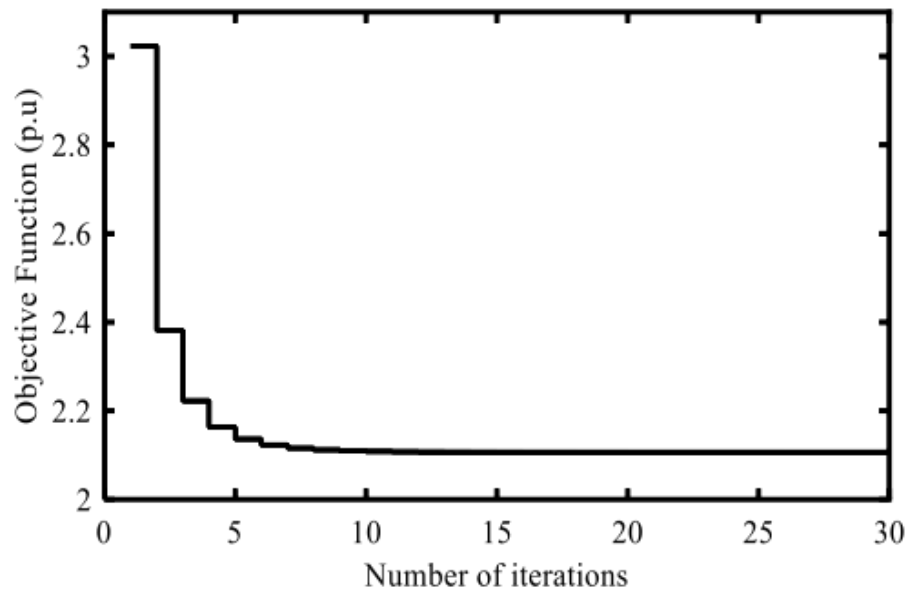
Figure 5.14: Convergence of proposed distributed algorithm of 34-bus system
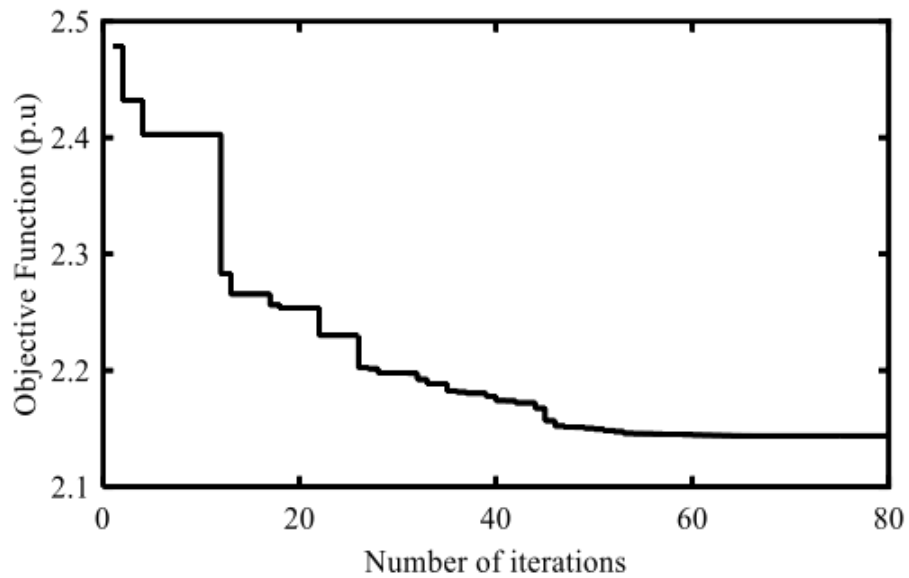
Figure 5.15: Convergence of centralized algorithm for 34-Bus System

Table 5.6: Reactive power generation output for two cases for 34-bus system

Variables	Distributed	Centralized PSO	Maximum Q
Q_4	0.510	0.514	0.600
Q_8	0.637	0.640	0.750
Q_{12}	0.637	0.637	0.750
Q_{16}	0.574	0.572	0.675
Q_{20}	0.765	0.770	0.900
Q_{21}	0.574	0.570	0.675
Q_{23}	0.638	0.638	0.750
Q_{27}	0.720	0.720	0.850
Q_{28}	0.797	0.800	0.950
Power Loss	1.7982	1.8020	–
Objective Function	2.107	2.109	–

the convergence of the reactive power generations for DGs and the fair utilization ratio converges α, respectively. Fair utilization ratio attains a ratio of 0.85 for each DG, which means every DG is 85% of the maximum generating reactive power generation capability.

5.6   Summary and Conclusion

This chapter proposes a distributed consensus-based optimal reactive power control algorithm for multiple DGs in an electrical distribution system. The effectiveness of the proposed distributed algorithm is validated by comparing to the centralized algorithm: PSO, for 6-bus and 34-bus systems. The proposed algorithm achieves the following four main merits.

- The proposed distributed algorithm effectively minimizes the objective function consisted of active power loss, voltage deviation and reactive power generation opportunity cost. Only information exchange among neighboring buses is used to attain the optimal solution.
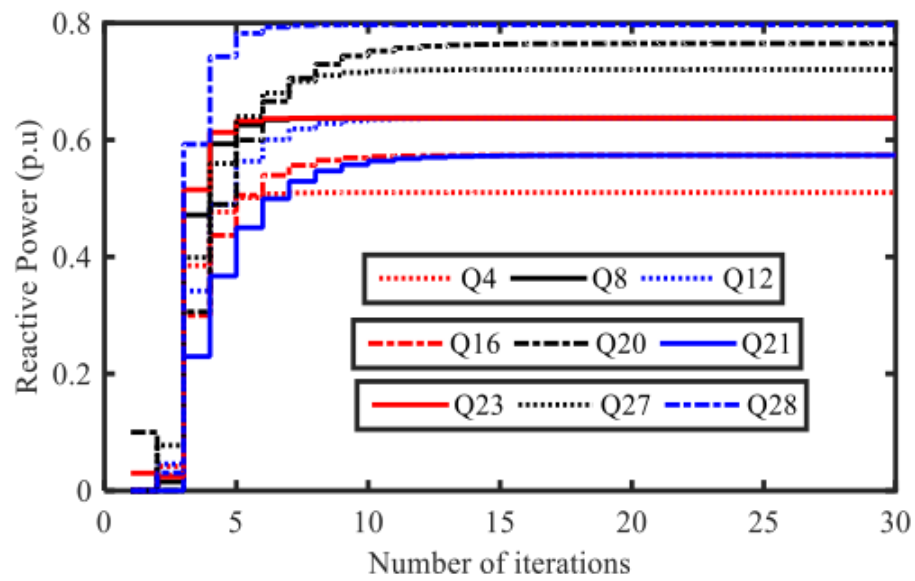
Figure 5.16: Reactive power generation updates of 34-bus system
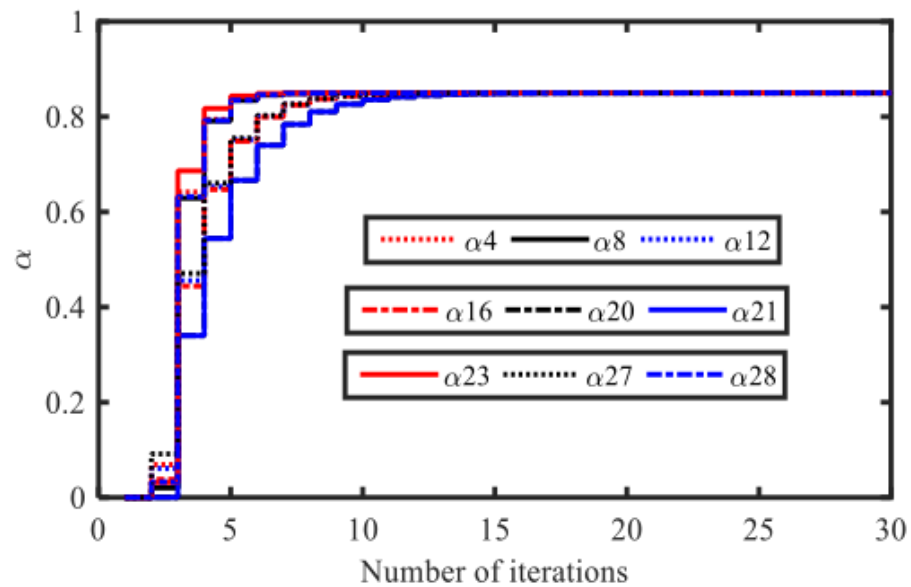
Figure 5.17: Uniform utilization ratio updates of 34-bus system

- It has been proved that making the approximation of $\cos(\delta_{ij}) = 1$ can provide comparable results to the one without approximation, which simplifies the calculation at the cost of only a few more iterations.

- Fair utilization ratio of reactive power generation is achieved for uniform utilization of all DGs.

- The proposed algorithm is scalable in the sense that, the iteration number does not increase exponentially as the size of the system increases, as validated in the 34-bus system.

Chapter 6

Conclusions and Future Research

This chapter presents the general conclusions drawn from the thesis, as well as possible directions for future work. The summary of the contributions are already mentioned at the end of each chapter and are therefore not repeated here.

6.1   Conclusions

Power systems are commonly controlled using hierarchical control schemes where three levels of control are performed to fully regulate the system. In this thesis, three algorithms are presented two for secondary control and one for tertiary control level of the power system. In the first two chapters existing literature related to control of power system is presented and then challenges associated with existing control schemes are described. Finally, in Chapters 3,4 and 5 new algorithms are presented to address the current challenges.

In the first algorithm presented in Chapter 3, a centralized secondary control algorithm is presented for the load frequency control application to minimze the frequency deviation in the system. In a centralized control scheme, a massive amount of data is needed to be transmitted to the central controller. To deal

with this challenge, SVD is utilized to decrease the data size of information being sent to the central controller. Compression ratio of the SVD is decided based on the tolerable information loss in the system. Simulation results show that the speed of LFC can be enhanced by decreasing the data size of the power system information.

In chapter 4, an algorithm for secondary voltage control is presented. To deal with the data size of the information being sent to the central controller, a compressive sensing based scheme is incorporated in the secondary voltage control. Secondary voltage control minimizes the voltage deviation of the load buses while CS deals with the problem of limited bandwidth capacity of the communication channel by reducing the size of the data to be transmitted. The proposed secondary control further incorporates the Morphological Median Filter (MMF) to reduce noise in the outputs of sensors in the power system. Furthermore, to keep the system secure and protected locally, Mathematical Singular Entropy based fault identification approach is utilized for fast discovery of faults in the control area. Simulation results with 27-bus and 486-bus power systems show that CS can reduce the data size up to 1/10th while the MSE based fault identification technique can accurately distinguish between fault and steady state conditions.

An algorithm for tertiary level of control is presented in chapter 5 where optimal reactive power generation is produced from generators in the system. A multi-objective function, which includes power loss, voltage deviation and cost of the reactive power generation of generators is minimized while generating optimal value of reactive power generation. It proposes a consensus-based distributed control algorithm and the formulated problem is shown to be convex. The proposed algorithm is tested on 6-bus and 34-bus systems to validate its effectiveness

and scalability. The proposed algorithm is also compared to the centralized Particle Swarm Optimization (PSO) technique, which demonstrates the effectiveness of the proposed distributed algorithm. In this work, a fully coupled distribution system is considered which means that power loss on the line is affected by both voltage magnitude and the voltage angle of both buses across the line. To address different DG capacities and realize equal contribution of reactive power generation, reactive power fair utilization ratio has been achieved.

6.2   Future Research

In this section, we present possible limitations of this work, which opens up avenues for future research.

1. **Non-linear Power Balance Constraints:** In Chapter 5 while dealing with tertiary control of ORPC, the two power balance equality constraints make the problem non-linear and non-convex. Although the ORPC problem is solved using a gradient based approach, better techniques may be developed to handle non-linear power balance constraints. For instance, they can be relaxed to a convex formulation and can be considered as a future work.

2. **Energy Storage Devices:** While optimizing the current control problems, effects of energy storage devices have not been considered. Optimal charging/discharging of the battery can be included in the optimal reactive power control algorithms. Optimal cost of battery charging/discharging subject to state of charge constraints may change the optimal reactive power control of the system.

In addition to it, charging and discharging efficiency depend on the battery degradation which is a highly non-linear function. Our future research aims to provide well behaved approximations of battery degradation and utilize it in the ORPC problem incorporating battery charging/discharging.

3. **Load Data Forecasting:** Optimal tertiary control of reactive power generation is obtained in Chapter 5 depends on real-time monitoring of real and reactive power load profiles. Monitoring of real-time loads, and then transmission of these load profiles to a central controller may slow down the optimal control. An alternative to the online monitoring of the system is forecasting of load demand profile based on existing large data sets using machine learning techniques. Forecasted load profiles will be provided to the controller before executing the optimization and it may make the algorithms fast. Forecasting of load profiles is another future research area.

4. **Optimal PMUs allocation:** In Chapter 4, secondary voltage control has been implemented without considering the effect of PMUs' locations. However, SVCON of load buses significantly depends on the locations of PMUs in the system. Thus, in the SVCON problem, it is important to incorporate optimal allocation of PMUs in the system. It will help control the secondary level voltage control more efficiently and reliability. Thus, one of the future research directions is to consider optimal allocation of PMUs in the SVCON problem.

5. **Building Energy Management and Demand Response:** In the frequency control in Chapter 3, load frequency of the generators has been controlled using SVD to compress the massive data size of information. Another way to control load frequency is by using local energy manage-

ment and demand response. Frequency of the generator heavily depends on the amount of the local load demand. By optimizing demand response, frequency of the system can be regulated. This is another future research direction, that is to optimize frequency deviation through demand response management.

Bibliography

[1] VK Mehta and Rohit Mehta. Principles of power system. *S. Chand, New Delhi*, 2004.

[2] Paula Ta-Shma, Adnan Akbar, Guy Gerson-Golan, Guy Hadash, Francois Carrez, and Klaus Moessner. An ingestion and analytics architecture for iot applied to smart city use cases. *IEEE Internet of Things Journal*, 5(2):765–774, 2018.

[3] Wei Zhang, Wenxin Liu, Xin Wang, Liming Liu, and Frank Ferrese. Distributed multiple agent system based online optimal reactive power control for smart grids. *IEEE Transactions on Smart Grid*, 5(5):2421–2431, 2014.

[4] Silvia Costa Ferreira, Robson Bauwlez Gonzatti, Rondineli Rodrigues Pereira, Carlos Henrique da Silva, LE Borges da Silva, and Germano Lambert-Torres. Finite control set model predictive control for dynamic reactive power compensation with hybrid active power filters. *IEEE Transactions on Industrial Electronics*, 65(3):2608–2617, 2018.

[5] Rahul Anilkumar, Griet Devriese, and Anurag K Srivastava. Voltage and reactive power control to maximize the energy savings in power distribution

system with wind energy. *IEEE Transactions on Industry Applications*, 54(1):656–664, 2018.

[6] MTL Gayatri, Alivelu M Parimi, and AV Pavan Kumar. A review of reactive power compensation techniques in microgrids. *Renewable and Sustainable Energy Reviews*, 81:1030–1036, 2018.

[7] Vikram Bhattacharjee and Irfan Khan. A non-linear convex cost model for economic dispatch in microgrids. *Applied Energy*, 222:637–648, 2018.

[8] Mashood Nasir, Saqib Iqbal, and Hassan A Khan. Optimal planning and design of low-voltage low-power solar dc microgrids. *IEEE Transactions on Power Systems*, 2017.

[9] S. Bahrami, M. H. Amini, M. Shafie-khah, and J. P. S. Catalao. A decentralized renewable generation management and demand response in power distribution networks. *IEEE Transactions on Sustainable Energy*, pages 1–1, 2018.

[10] Tarik Hrnjić and Tarik Donlagić. High-speed reliable data transfer for distribution smart grid applications. In *Telecommunications (BIHTEL), 2016 XI International Symposium on*, pages 1–6. IEEE, 2016.

[11] Kiran Siraj, Haris Siraj, and Mashood Nasir. Modeling and control of a doubly fed induction generator for grid integrated wind turbine. In *Power Electronics and Motion Control Conference and Exposition (PEMC), 2014 16th International*, pages 901–906. IEEE, 2014.

[12] H Hassan, Muhammad Nadeem, and Irfan Ahmad Khan. Evaluation of the transient overvoltage stresses on 132 kv power transmission network. *Evaluation*, 3(12), 2013.

[13] Mashood Nasir, Nauman Ahmad Zaffar, and Hassan Abbas Khan. Analysis on central and distributed architectures of solar powered dc microgrids. In *Power Systems Conference (PSC), 2016 Clemson University*, pages 1–6. IEEE, 2016.

[14] Irfan A Khan, Yinliang Xu, and Bilal Tahir. Design and manufacturing of digital mosfet based-avr for synchronous generator. In *Cyber Technology in Automation, Control, and Intelligent Systems (CYBER), 2015 IEEE International Conference on*, pages 217–222. IEEE, 2015.

[15] Fahad Zia, Mashood Nasir, and Abdul Aziz Bhatti. Optimization methods for constrained stochastic wind power economic dispatch. In *Power Engineering and Optimization Conference (PEOCO), 2013 IEEE 7th International*, pages 129–133. IEEE, 2013.

[16] Kianoosh G Boroojeni, M Hadi Amini, SS Iyengar, Mohsen Rahmani, and Panos M Pardalos. An economic dispatch algorithm for congestion management of smart power networks. *Energy Systems*, 8(3):643–667, 2017.

[17] M Hadi Amini, Rupamathi Jaddivada, Sakshi Mishra, and Orkun Karabasoglu. Distributed security constrained economic dispatch. In *Innovative Smart Grid Technologies-Asia (ISGT ASIA), 2015 IEEE*, pages 1–6. IEEE, 2015.

[18] Xiaoqiang Li, Pengfeng Lin, Yi Tang, and Kai Wang. Stability design of single-loop voltage control with enhanced dynamic for voltage-source converters with a low lc-resonant-frequency. *IEEE Transactions on Power Electronics*, 2018.

[19] Noman Bashir, Hira Shahzad Sardar, Mashood Nasir, Naveed Ul Hassan, and Hassan Abbas Khan. Lifetime maximization of lead-acid batteries in small scale ups and distributed generation systems. In *PowerTech, 2017 IEEE Manchester*, pages 1–6. IEEE, 2017.

[20] M Hadi Amini and Orkun Karabasoglu. Optimal operation of interdependent power systems and electrified transportation networks. *Energies*, 11(1):196, 2018.

[21] Bakhtyar Hoseinzadeh, M Hadi Amini, and Claus Leth Bak. Centralized load shedding based on thermal limit of transmission lines against cascading events. *arXiv preprint arXiv:1611.08891*, 2016.

[22] Jerry S Horton and LL Grigsby. Voltage optimization using combined linear programming & gradient techniques. *IEEE transactions on power apparatus and systems*, (7):1637–1643, 1984.

[23] O Alsac, J Bright, M Prais, and B Stott. Further developments in lp-based optimal power flow. *IEEE Transactions on Power Systems*, 5(3):697–711, 1990.

[24] MH Amini, Justin Frye, Marija D Ilić, and O Karabasoglu. Smart residential energy scheduling utilizing two stage mixed integer linear programming. In *North American Power Symposium (NAPS), 2015*, pages 1–6. IEEE, 2015.

[25] Rodrigo Palma-Behnke, Luis S Vargas, Alejandro Jofré, et al. A distribution company energy acquisition market model with integration of distributed generation and load curtailment options. *IEEE Transactions on Power Systems*, 20(4):1718–1727, 2005.

[26] Jesús Riquelme Santos, Alicia Troncoso Lora, Antonio Gómez Expósito, and José Luis Martínez Ramos. Finding improved local minima of power system optimization problems by interior-point methods. *IEEE transactions on power systems*, 18(1):238–244, 2003.

[27] Wei Yan, Juan Yu, DC Yu, and Kalu Bhattarai. A new optimal reactive power flow model in rectangular form and its solution by predictor corrector primal dual interior point method. *IEEE transactions on power systems*, 21(1):61–67, 2006.

[28] Himmat Singh and Laxmi Srivastava. Recurrent multi-objective differential evolution approach for reactive power management. *IET Generation, Transmission & Distribution*, 10(1):192–204, 2016.

[29] A Bhattacharya and PK Roy. Solution of multi-objective optimal power flow using gravitational search algorithm. *IET generation, transmission & distribution*, 6(8):751–763, 2012.

[30] Mala De and Swapan K Goswami. Optimal reactive power procurement with voltage stability consideration in deregulated power system. *IEEE transactions on power systems*, 29(5):2078–2086, 2014.

[31] Sattawat Burana, Panida Thararak, Peerapol Jirapong, and Kannathat Mansuwan. Optimal allocation of distributed generation with facts controller for electrical power loss reduction using genetic algorithm. In *Information Technology and Electrical Engineering (ICITEE), 2017 9th International Conference on*, pages 1–6. IEEE, 2017.

[32] Siddharth Deshmukh, Balasubramaniam Natarajan, and Anil Pahwa. Voltage/var control in distribution networks via reactive power injec-

tion through distributed generators. *IEEE Transactions on smart grid*, 3(3):1226–1234, 2012.

[33] Irfan Khan, Yinliang Xu, Soummya Kar, and Hongbin Sun. Compressive sensing-based optimal reactive power control of a multi-area power system. *IEEE Access*, 5:23576–23588, 2017.

[34] Ahad Abessi, Vahid Vahidinasab, and Mohammad Sadegh Ghazizadeh. Centralized support distributed voltage control by using end-users as reactive power support. *IEEE Transactions on Smart Grid*, 7(1):178–188, 2016.

[35] Martin S Lacher, Jörg Nonnenmacher, and Ernst W Biersack. Performance comparison of centralized versus distributed error recovery for reliable multicast. *IEEE/ACM Transactions on Networking (TON)*, 8(2):224–238, 2000.

[36] Qiang Wan, WenPing Zhang, Yinliang Xu, and Irfan Khan. Distributed control for energy management in a microgrid. In *Transmission and Distribution Conference and Exposition (T&D), 2016 IEEE/PES*, pages 1–5. IEEE, 2016.

[37] Nattawat Jumpasri, Kittapas Pinsuntia, Kaweepoj Woranetsuttikul, Taywin Nilsakorn, and Werachet Khan-ngern. Comparison of distributed and centralized control for partial shading in pv parallel based on particle swarm optimization algorithm. In *Electrical Engineering Congress (iEECON), 2014 International*, pages 1–4. IEEE, 2014.

[38] Mashood Nasir, Zheming Jin, Hassan Khan, Nauman Zaffar, Juan Vasquez, and Josep M Guerrero. A decentralized control architecture applied to

dc nanogrid clusters for rural electrification in developing regions. *IEEE Transactions on Power Electronics*, 2018.

[39] Prashant Kansal and Anjan Bose. Bandwidth and latency requirements for smart transmission grid applications. *IEEE Transactions on Smart Grid*, 3(3):1344–1352, 2012.

[40] Mashood Nasir, Hassan Abbas Khan, Arif Hussain, Laeeq Mateen, and Nauman Ahmad Zaffar. Solar pv-based scalable dc microgrid for rural electrification in developing regions. *IEEE Transactions on Sustainable Energy*, 9(1):390–399, 2018.

[41] Mohammad Hadi Amini, Behrouz Nabi, and Mahmoud-Reza Haghifam. Load management using multi-agent systems in smart distribution network. In *Power and Energy Society General Meeting (PES), 2013 IEEE*, pages 1–5. IEEE, 2013.

[42] Vijay Pratap Singh, Nand Kishor, and Paulson Samuel. Distributed multi-agent system-based load frequency control for multi-area power system in smart grid. *IEEE Transactions on Industrial Electronics*, 64(6):5151–5160, 2017.

[43] Mohammad Jawad Ghorbani, Muhammad Akram Choudhry, and Ali Feliachi. A multiagent design for power distribution systems automation. *IEEE Transactions on Smart Grid*, 7(1):329–339, 2016.

[44] Yamin Wang, Shouxiang Wang, and Lei Wu. Distributed optimization approaches for emerging power systems operation: A review. *Electric Power Systems Research*, 144:127–135, 2017.

[45] Changsun Ahn and Huei Peng. Decentralized voltage control to minimize distribution power loss of microgrids. *IEEE Transactions on Smart Grid*, 4(3):1297–1304, 2013.

[46] Anna Rita Di Fazio, Giuseppe Fusco, and Mario Russo. Smart der control for minimizing power losses in distribution feeders. *Electric Power Systems Research*, 109:71–79, 2014.

[47] Shahab Bahrami, M Hadi Amini, Miadreza Shafie-khah, and Joao PS Catalao. A decentralized electricity market scheme enabling demand response deployment. *IEEE Transactions on Power Systems*, 2017.

[48] Ali Maknouninejad and Zhihua Qu. Realizing unified microgrid voltage profile and loss minimization: A cooperative distributed optimization and control approach. *IEEE Transactions on Smart Grid*, 5(4):1621–1630, 2014.

[49] Muhammad Hamza, Muhammad Shehroz, Sana Fazal, Mashood Nasir, and Hassan Abbas Khan. Design and analysis of solar pv based low-power low-voltage dc microgrid architectures for rural electrification. In *Power & Energy Society General Meeting, 2017 IEEE*, pages 1–5. IEEE, 2017.

[50] Anna R Di Fazio, Giuseppe Fusco, and Mario Russo. Decentralized control of distributed generation for voltage profile optimization in smart feeders. *IEEE Transactions on Smart Grid*, 4(3):1586–1596, 2013.

[51] Ahsan Sarwar Rana, Mashood Nasir, and Hassan Abbas Khan. String level optimisation on grid-tied solar pv systems to reduce partial shading loss. *IET Renewable Power Generation*, 2017.

[52] Adnan Akbar, Francois Carrez, Klaus Moessner, and Ahmed Zoha. Pre-

dicting complex events for pro-active iot applications. In *Internet of Things (WF-IoT), 2015 IEEE 2nd World Forum on*, pages 327–332. IEEE, 2015.

[53] Julio Cesar Stacchini de Souza, Tatiana Mariano Lessa Assis, and Bikash Chandra Pal. Data compression in smart distribution systems via singular value decomposition. *IEEE Transactions on Smart Grid*, 8(1):275–284, 2017.

[54] Emmanuel J Candès and Michael B Wakin. An introduction to compressive sampling. *IEEE signal processing magazine*, 25(2):21–30, 2008.

[55] Jarvis Haupt, Waheed U Bajwa, Michael Rabbat, and Robert Nowak. Compressed sensing for networked data. *IEEE Signal Processing Magazine*, 25(2):92–101, 2008.

[56] Zilong Zou, Yuequan Bao, Hui Li, Billie F Spencer, and Jinping Ou. Embedding compressive sensing-based data loss recovery algorithm into wireless smart sensors for structural health monitoring. *IEEE Sensors Journal*, 15(2):797–808, 2015.

[57] Yan Yu, Feng Han, Yuequan Bao, and Jinping Ou. A study on data loss compensation of wifi-based wireless sensor networks for structural health monitoring. *IEEE Sensors Journal*, 16(10):3811–3818, 2016.

[58] Hamid Gharavi and Bin Hu. Scalable synchrophasors communication network design and implementation for real-time distributed generation grid. *IEEE Transactions on Smart Grid*, 6(5):2539–2550, 2015.

[59] Markus Leinonen, Marian Codreanu, and Markku Juntti. Sequential compressed sensing with progressive signal reconstruction in wireless sensor net-

works. *IEEE Transactions on Wireless Communications*, 14(3):1622–1635, 2015.

[60] Woohyun Kim and Srinivas Katipamula. A review of fault detection and diagnostics methods for building systems. *Science and Technology for the Built Environment*, 24(1):3–21, 2018.

[61] Yaojie Cai, Athula D Rajapakse, Naushath M Haleem, and Neethu Raju. A threshold free synchrophasor measurement based multi-terminal fault location algorithm. *International Journal of Electrical Power & Energy Systems*, 96:174–184, 2018.

[62] Sergio Silva, Pyramo Costa, Maury Gouvea, Alcyr Lacerda, Franciele Alves, and Daniel Leite. High impedance fault detection in power distribution systems using wavelet transform and evolving neural network. *Electric Power Systems Research*, 154:474–483, 2018.

[63] Georgios Anagnostou, Francesca Boem, Stefanie Kuenzel, Bikash C Pal, and Thomas Parisini. Observer-based anomaly detection of synchronous generators for power systems monitoring. *IEEE Transactions on Power Systems*, 2018.

[64] Adel Soheili, Javad Sadeh, and Reza Bakhshi. Modified fft based high impedance fault detection technique considering distribution non-linear loads: Simulation and experimental data analysis. *International Journal of Electrical Power & Energy Systems*, 94:124–140, 2018.

[65] Dubravko Miljković. Fault detection methods: A literature survey. In *MIPRO, 2011 proceedings of the 34th international convention*, pages 750–755. IEEE, 2011.

[66] Suresh Gautam and Sukumar M Brahma. Overview of mathematical morphology in power systemsa tutorial approach. In *Power & Energy Society General Meeting, 2009. PES'09. IEEE*, pages 1–7. IEEE, 2009.

[67] Lianfang Cai, Nina F Thornhill, and Bikash C Pal. Multivariate detection of power system disturbances based on fourth order moment and singular value decomposition. *IEEE Transactions on Power Systems*, 32(6):4289–4297, 2017.

[68] Markus P Müller and Michele Pastena. A generalization of majorization that characterizes shannon entropy. *IEEE Transactions on Information Theory*, 62(4):1711–1720, 2016.

[69] Carleton Coffrin and Pascal Van Hentenryck. A linear-programming approximation of ac power flows. *INFORMS Journal on Computing*, 26(4):718–734, 2014.

[70] Alberto Borghetti, Fabio Napolitano, and Carlo Alberto Nucci. Volt/var optimization of unbalanced distribution feeders via mixed integer linear programming. *International Journal of Electrical Power & Energy Systems*, 72:40–47, 2015.

[71] Amin Mohammadpour Shotorbani, Sajad Madadi, and Behnam Mohammadi-Ivatloo. Wide-area measurement, monitoring and control: Pmu-based distributed wide-area damping control design based on heuristic optimisation using digsilent powerfactory. In *Advanced Smart Grid Functionalities Based on PowerFactory*, pages 211–240. Springer, 2018.

[72] Štěpán Beneš and Jaroslav Kruis. Singular value decomposition used for

compression of results from the finite element method. *Advances in Engineering Software*, 117:8–17, 2018.

[73] Husheng Li, Aleksandar D Dimitrovski, Ju Bin Song, Zhu Han, and Lijun Qian. Communication infrastructure design in cyber physical systems with applications in smart grids: A hybrid system framework. *IEEE Communications Surveys and Tutorials*, 16(3):1689–1708, 2014.

[74] Wen Tan, Shuaibing Chang, and Rong Zhou. Load frequency control of power systems with non-linearities. *IET Generation, Transmission & Distribution*, 11(17):4307–4313, 2017.

[75] Pablo R Baldivieso Monasterios and Paul Trodden. Low-complexity distributed predictive automatic generation control with guaranteed properties. *IEEE Transactions on Smart Grid*, 8(6):3045–3054, 2017.

[76] Tapabrata Chakraborty, David Watson, and Marianne Rodgers. Automatic generation control using an energy storage system in a wind park. *IEEE Transactions on Power Systems*, 33(1):198–205, 2018.

[77] Feisheng Yang, Jing He, and Dianhui Wang. New stability criteria of delayed load frequency control systems via infinite-series-based inequality. *IEEE Transactions on Industrial Informatics*, 2017.

[78] Kab Seok Ko and Dan Keun Sung. The effect of ev aggregators with time-varying delays on the stability of a load frequency control system. *IEEE Transactions on Power Systems*, 33(1):669–680, 2018.

[79] Anjan Bose. Smart transmission grid applications and their supporting infrastructure. *IEEE Transactions on Smart Grid*, 1(1):11–19, 2010.

[80] Jinchun Zhan and Namrata Vaswani. Time invariant error bounds for modified-cs-based sparse signal sequence recovery. *IEEE Transactions on Information Theory*, 61(3):1389–1409, 2015.

[81] Yinliang Xu, Zaiyue Yang, Jingrui Zhang, Zhongyang Fei, and Wenxin Liu. Real-time compressive sensing based control strategy for a multi-area power system. *IEEE Transactions on Smart Grid*, 2017.

[82] Wei Dai and Olgica Milenkovic. Subspace pursuit for compressive sensing signal reconstruction. *IEEE transactions on Information Theory*, 55(5):2230–2249, 2009.

[83] Yi Wang, Qixin Chen, Chongqing Kang, Qing Xia, and Min Luo. Sparse and redundant representation-based smart meter data compression and pattern extraction. *IEEE Transactions on Power Systems*, 32(3):2142–2151, 2017.

[84] Ernane Antônio Alves Coelho, Dan Wu, Josep M Guerrero, Juan C Vasquez, Tomislav Dragičević, Čedomir Stefanović, and Petar Popovski. Small-signal analysis of the microgrid secondary control considering a communication time delay. *IEEE Transactions on Industrial Electronics*, 63(10):6257–6269, 2016.

[85] Kianoosh G Boroojeni, M Hadi Amini, and SS Iyengar. Reliability in smart grids. In *Smart Grids: Security and Privacy Issues*, pages 19–29. Springer, 2017.

[86] Kianoosh G Boroojeni, M Hadi Amini, Arash Nejadpak, SS Iyengar, Bakhtyar Hoseinzadeh, and Claus Leth Bak. A theoretical bilevel control scheme

for power networks with large-scale penetration of distributed renewable resources. In *Electro Information Technology (EIT), 2016 IEEE International Conference on*, pages 0510–0515. ieee, 2016.

[87] M Yang, Y Fu, C Wang, and P Wang. Decentralized sliding mode load frequency control for multi-area power system. *IEEE Transactions on Power System*, 28(4):4301–4309, 2013.

[88] Srivats Shukla and Lamine Mili. Hierarchical decentralized control for enhanced rotor angle and voltage stability of large-scale power systems. *IEEE Transactions on Power Systems*, 32(6):4783–4793, 2017.

[89] John W Simpson-Porco, Qobad Shafiee, Florian Dörfler, Juan C Vasquez, Josep M Guerrero, and Francesco Bullo. Secondary frequency and voltage control of islanded microgrids via distributed averaging. *IEEE Transactions on Industrial Electronics*, 62(11):7025–7038, 2015.

[90] MV Santos, AC Zambroni de Souza, BIL Lopes, and D Marujo. Secondary voltage control system based on fuzzy logic. *Electric Power Systems Research*, 119:377–384, 2015.

[91] Amir H Hajimiragha and Mohammad RD Zadeh. Research and development of a microgrid control and monitoring system for the remote community of bella coola: Challenges, solutions, achievements and lessons learned. In *Smart Energy Grid Engineering (SEGE), 2013 IEEE International Conference on*, pages 1–6. IEEE, 2013.

[92] Hongbin Sun, Qinglai Guo, Boming Zhang, Wenchuan Wu, and Bin Wang. An adaptive zone-division-based automatic voltage control system with ap-

plications in china. *IEEE Transactions on Power Systems*, 28(2):1816–1828, 2013.

[93] Wei Yan, Wei Cui, Wei-Jen Lee, Juan Yu, and Xia Zhao. Pilot-bus-centered automatic voltage control with high penetration level of wind generation. In *Industry Applications Society Annual Meeting, 2015 IEEE*, pages 1–8. IEEE, 2015.

[94] Wei Gu, Guannan Lou, Wen Tan, and Xiaodong Yuan. A nonlinear state estimator-based decentralized secondary voltage control scheme for autonomous microgrids. *IEEE Transactions on Power Systems*, 32(6):4794–4804, 2017.

[95] Hai Feng Wang, H Li, and H Chen. Coordinated secondary voltage control to eliminate voltage violations in power system contingencies. *IEEE transactions on Power Systems*, 18(2):588–595, 2003.

[96] Heng-Yi Su, Feng-Ming Kang, and Chih-Wen Liu. Transmission grid secondary voltage control method using pmu data. *IEEE Transactions on Smart Grid*, 2016.

[97] Juan Yu, Wei Dai, Wenyuan Li, Xuan Liu, and Juelin Liu. Optimal reactive power flow of interconnected power system based on static equivalent method using border pmu measurements. *IEEE Transactions on Power Systems*, 33(1):421–429, 2018.

[98] Emily R Fernandes, Scott G Ghiocel, Joe H Chow, Daniel E Ilse, De D Tran, Qiang Zhang, David B Bertagnolli, Xiaochuan Luo, George Stefopoulos, Bruce Fardanesh, et al. Application of a phasor-only state estimator to

a large power system using real pmu data. *IEEE Transactions on Power Systems*, 32(1):411–420, 2017.

[99] Mohammad Babakmehr, Marcelo G Simões, Michael B Wakin, and Farnaz Harirchi. Compressive sensing-based topology identification for smart grids. *IEEE Transactions on Industrial Informatics*, 12(2):532–543, 2016.

[100] Cheng-Yu Lu, Bing-Zhong Jing, Patrick PK Chan, Daoman Xiang, Wan-hua Xie, Jianxun Wang, and Daniel S Yeung. Vessel enhancement of low quality fundus image using mathematical morphology and combination of gabor and matched filter. In *Wavelet Analysis and Pattern Recognition (ICWAPR), 2016 International Conference on*, pages 168–173. IEEE, 2016.

[101] Musliyarakath Aneesa Farhan et al. Mathematical morphology-based is-landing detection for distributed generation. *IET Generation, Transmission & Distribution*, 11(14):3449–3457, 2017.

[102] LL Zhang, MS Li, TY Ji, QH Wu, L Jiang, and JP Zhan. Morphology singu-lar entropy-based phase selector using short data window for transmission lines. *IEEE Transactions on Power Delivery*, 29(5):2162–2171, 2014.

[103] Ma Jing, Wang Zengping, Xu Yan, and Ma Lei. Single-ended transient positional protection of transmission lines using mathematical morphology. In *Power Engineering Conference, 2005. IPEC 2005. The 7th International*, pages 1–603. IEEE, 2005.

[104] Pierre Soille. *Morphological image analysis: principles and applications*. Springer Science & Business Media, 2013.

[105] MH Amini, Marija D Ilić, and O Karabasoglu. Dc power flow estimation

utilizing bayesian-based lmmse estimator. In *Power & Energy Society General Meeting, 2015 IEEE*, pages 1–5. IEEE, 2015.

[106] Mingrui Yang and Frank de Hoog. Orthogonal matching pursuit with thresholding and its application in compressive sensing. *IEEE Transactions on Signal Processing*, 63(20):5479–5486, 2015.

[107] Dongqing Wang, Liwei Li, Yan Ji, and Yaru Yan. Model recovery for hammerstein systems using the auxiliary model based orthogonal matching pursuit method. *Applied Mathematical Modelling*, 54:537–550, 2018.

[108] I Dabbagchi and R Christie. Power systems test case archive. *University of Washington*, 1993.

[109] Jan Haase, Gerhard Zucker, and Mahmoud Alahmad. Energy efficient building automation: A survey paper on approaches and technologies for optimized building operation. In *Industrial Electronics Society, IECON 2014-40th Annual Conference of the IEEE*, pages 5350–5356. IEEE, 2014.

[110] Irfan Khan, Yinliang Xu, Hongbin Sun, and Vikram Bhattacharjee. Distributed optimal reactive power control of power systems. *IEEE Access*, 6:7100–7111, 2018.

[111] Yinliang Xu and Zhicheng Li. Distributed optimal resource management based on the consensus algorithm in a microgrid. *IEEE Transactions on Industrial Electronics*, 62(4):2584–2592, 2015.

[112] Tiago Sousa, Hugo Morais, Zita Vale, and Rui Castro. A multi-objective optimization of the active and reactive resource scheduling at a distribution level in a smart grid context. *Energy*, 85:236–250, 2015.

[113] Baosen Zhang, Albert YS Lam, Alejandro D Domínguez-García, and David Tse. An optimal and distributed method for voltage regulation in power distribution systems. *IEEE Transactions on Power Systems*, 30(4):1714–1726, 2015.

[114] Mojtaba Ghasemi, Sahand Ghavidel, Mohammad Mehdi Ghanbarian, Masihallah Gharibzadeh, and Ali Azizi Vahed. Multi-objective optimal power flow considering the cost, emission, voltage deviation and power losses using multi-objective modified imperialist competitive algorithm. *Energy*, 78:276–289, 2014.

[115] Mojtaba Ghasemi, Sahand Ghavidel, Ebrahim Akbari, and Ali Azizi Vahed. Solving non-linear, non-smooth and non-convex optimal power flow problems using chaotic invasive weed optimization algorithms based on chaos. *Energy*, 73:340–353, 2014.

[116] Konstantin Turitsyn, Petr Sulc, Scott Backhaus, and Michael Chertkov. Options for control of reactive power by distributed photovoltaic generators. *Proceedings of the IEEE*, 99(6):1063–1073, 2011.

[117] Benyamin Khorramdel and Mahdi Raoofat. Optimal stochastic reactive power scheduling in a microgrid considering voltage droop scheme of dgs and uncertainty of wind farms. *Energy*, 45(1):994–1006, 2012.

[118] Reza Taghavi, Ali Reza Seifi, and Haidar Samet. Stochastic reactive power dispatch in hybrid power system with intermittent wind power generation. *Energy*, 89:511–518, 2015.

[119] John W Simpson-Porco, Florian Dorfler, Francesco Bullo, Qobad Shafiee, and Josep M Guerrero. Stability, power sharing, & distributed secondary

control in droop-controlled microgrids. In *Smart Grid Communications (SmartGridComm), 2013 IEEE International Conference on*, pages 672–677. IEEE, 2013.

[120] Johannes Schiffer, Adolfo Anta, Truong Duc Trung, Jörg Raisch, and Tevfik Sezi. On power sharing and stability in autonomous inverter-based microgrids. In *Decision and Control (CDC), 2012 IEEE 51st Annual Conference on*, pages 1105–1110. IEEE, 2012.

[121] Johannes Schiffer, Thomas Seel, Jörg Raisch, and Tevfik Sezi. Voltage stability and reactive power sharing in inverter-based microgrids with consensus-based distributed voltage control. *IEEE Transactions on Control Systems Technology*, 24(1):96–109, 2016.

[122] Mashood Nasir and Hassan Abbas Khan. Solar photovoltaic integrated building scale hybrid ac/dc microgrid. 2016.

[123] Hua Han, Xiaochao Hou, Jian Yang, Jifa Wu, Mei Su, and Josep M Guerrero. Review of power sharing control strategies for islanding operation of ac microgrids. *IEEE Transactions on Smart Grid*, 7(1):200–215, 2016.

[124] M Mujahid, A Mohyuddin, AA Bhatti, and M Nasir. Energy sustainability: study on fuel efficiency and engine properties by using biodiesel and fossil diesel. In *Proceedings on International Conference on Energy and Sustainability*, 2013.

[125] Irfan Khan, Zhicheng Li, Yinliang Xu, and Wei Gu. Distributed control algorithm for optimal reactive power control in power grids. *International Journal of Electrical Power & Energy Systems*, 83:505–513, 2016.

[126] Jingrui Zhang, Shuang Lin, Houde Liu, Yalin Chen, Mingcheng Zhu, and Yinliang Xu. A small-population based parallel differential evolution algorithm for short-term hydrothermal scheduling problem considering power flow constraints. *Energy*, 123:538–554, 2017.

[127] Liming Liu, Hui Li, Yaosuo Xue, and Wenxin Liu. Decoupled active and reactive power control for large-scale grid-connected photovoltaic systems using cascaded modular multilevel converters. *IEEE Transactions on Power Electronics*, 30(1):176–187, 2015.

[128] Mohammad Nikkhah Mojdehi and Prasanta Ghosh. An on-demand compensation function for an ev as a reactive power service provider. *IEEE Transactions on Vehicular Technology*, 65(6):4572–4583, 2016.

[129] Hossein Nezamabadi and Mehrdad Setayesh Nazar. Arbitrage strategy of virtual power plants in energy, spinning reserve and reactive power markets. *IET Generation, Transmission & Distribution*, 10(3):750–763, 2016.

[130] Rajendra Kumar and Ashwani Kumar. Reactive power cost characteristics for synchronous generator in deregulated electricity markets. In *Power India International Conference (PIICON), 2014 6th IEEE*, pages 1–6. IEEE, 2014.

[131] Omid Homaee and Shahram Jadid. Investigation of synchronous generator in reactive power market–an accurate view. *IET Generation, Transmission & Distribution*, 8(11):1881–1890, 2014.

[132] Shangyou Hao. A reactive power management proposal for transmission operators. *IEEE Transactions on Power Systems*, 18(4):1374–1381, 2003.

[133] Steven H Low. Convex relaxation of optimal power flowpart i: Formulations and equivalence. *IEEE Transactions on Control of Network Systems*, 1(1):15–27, 2014.

[134] Changsen Feng, Zhiyi Li, Mohammad Shahidehpour, Fushuan Wen, Weijia Liu, and Xiaowei Wang. Decentralized short-term voltage control in active power distribution systems. *IEEE Transactions on Smart Grid*, 2017.

[135] Shaojun Huang, Qiuwei Wu, Jianhui Wang, and Haoran Zhao. A sufficient condition on convex relaxation of ac optimal power flow in distribution networks. *IEEE Transactions on Power Systems*, 32(2):1359–1368, 2017.

[136] Yinliang Xu and Wenxin Liu. Novel multiagent based load restoration algorithm for microgrids. *IEEE Transactions on Smart Grid*, 2(1):152–161, 2011.

[137] Wei Zhang, Ye Ma, Wenxin Liu, Satish J Ranade, and Yusheng Luo. Distributed optimal active power dispatch under constraints for smart grids. *IEEE Transactions on Industrial Electronics*, 64(6):5084–5094, 2017.

[138] Mashood Nasir and Muhammad Fahad Zia. Global maximum power point tracking algorithm for photovoltaic systems under partial shading conditions. In *Power Electronics and Motion Control Conference and Exposition (PEMC), 2014 16th International*, pages 667–672. IEEE, 2014.

[139] Bozju Zhao, CX Guo, and YJ Cao. A multiagent-based particle swarm optimization approach for optimal reactive power dispatch. *IEEE transactions on power systems*, 20(2):1070–1078, 2005.

[140] Irfan Khan and Vikram Bhattacharjee. Effect of the approximation of

voltage angle difference on the opf algorithms in the power network. *arXiv preprint arXiv:1806.07778*, 2018.

[141] William H Kersting. Radial distribution test feeders. *IEEE Transactions on Power Systems*, 6(3):975–985, 1991.